Hydropower's Contributions to Grid Resilience

October 2021

Abhishek Somani
Sohom Datta
Slaven Kincic
Vishvas Chalishazar
Bharat Vyakaranam
Nader Samaan
Alison Colotelo
Yichen Zhang
Vladimir Koritarov
Timothy McJunkin
Thomas Mosier
Joshua Novacheck
Michael Emmanuel
Marty Schwarz
Lawrence Markel
Christopher O'Reilley

PNNL-30554

PACIFIC NORTHWEST NATIONAL LABORATORY
operated by
BATTELLE
for the
UNITED STATES DEPARTMENT OF ENERGY
under Contract DE-AC05-76RL01830

Printed in the United States of America

Available to DOE and DOE contractors from the
Office of Scientific and Technical Information,
P.O. Box 62, Oak Ridge, TN 37831-0062;
ph: (865) 576-8401
fax: (865) 576-5728
email: mb-reports@osti.gov

Available to the public from the National Technical Information Service
5301 Shawnee Rd., Alexandria, VA 22312
ph: (800) 553-NTIS (6847)
email: orders@ntis.gov <https://www.ntis.gov/about>
Online ordering: http://www.ntis.gov

PNNL- 30554

Hydropower's Contributions to Grid Resilience

October 2021

Abhishek Somani[1]
Sohom Datta[1]
Slaven Kincic[1]
Vishvas Chalishazar[1]
Bharat Vyakaranam [1]
Nader Samaan[1]
Alison Colotelo[1]
Yichen Zhang[2]
Vladimir Koritarov[2]
Timothy McJunkin[3]
Thomas Mosier[3]
Joshua Novacheck[4]
Michael Emmanuel[4]
Marty Schwarz[4]
Lawrence Markel[5]
Christopher O'Reilley[5]

[1] Pacific Northwest National Laboratory
[2] Argonne National Laboratory
[3] Idaho National Laboratory
[4] National Renewable Energy Laboratory
[5] Oak Ridge National Laboratory

Acknowledgments

This work was authored by Pacific Northwest National Laboratory, operated for the U.S. Department of Energy (DOE) by Battelle under contract number DE-AC05-76RL01830; Argonne National Laboratory, operated by UChicago Argonne, LLC, for the DOE under award or contract number DE-AC02-06CH11357; National Renewable Energy Laboratory, operated for DOE by Alliance for Sustainable Energy, LLC, under Contract No. DE-AC36-08GO28308; Oak Ridge National Laboratory, operated for DOE by UT-Battelle, LLC under contract number DE-AC05-00OR22725,and supported by the HydroWIRES Initiative of the Energy Department's Water Power Technologies Office.

The authors are thankful to Dr. Samuel Bockenhauer, Hill Balliet, Alejandro Moreno, Timothy Welch, Jennifer Garson, and other staff of the DOE's Water Power Technologies Office for providing guidance and input on this project.

We would also like to recognize Marcelo Elizondo, Jason Fuller, Frank Tuffner, Erin McCann, Mark Freshley, TJ Heibel, and Rebecca O'Neil who have contributed to this report by reviewing draft versions and providing inputs and suggestions for improvements.

Context : HydroWIRES

In April 2019, the U.S. Department of Energy's (DOE's) Water Power Technologies Office launched the HydroWIRES Initiative to understand, enable, and improve hydropower and pumped storage hydropower (PSH) contributions to reliability, resilience, and integration in the rapidly evolving U.S. electricity system. The unique characteristics of hydropower, including PSH, make it well-suited to provide a range of storage, generation flexibility, and other grid services to support the cost-effective integration of variable renewable resources as well as reliability and resiliency enhancements.

The U.S. electricity system is rapidly evolving, bringing both opportunities and challenges for the hydropower sector. While increasing deployment of variable renewables such as wind and solar have enabled low-cost, clean energy in many regions in the United States, it also creates a need for resources that can store energy or quickly change their operations to ensure a reliable and resilient grid. Hydropower (including PSH) is not only a supplier of bulk, low-cost, renewable energy, but also a source of large-scale flexibility and a force multiplier for other renewable power-generation sources. Realizing this potential requires innovation in several areas: incorporating new operations into planning and licensing decisions; predicting new operations and management patterns and costs to prevent unplanned outages; and designing new turbines and control systems for fast response and frequent ramping while maintaining high efficiency.

HydroWIRES is distinguished in its close engagement with the DOE national laboratories. Argonne National Laboratory, Idaho National Laboratory, National Renewable Energy Laboratory, Oak Ridge National Laboratory, and Pacific Northwest National Laboratory work as a team to provide strategic insight and develop connections across the HydroWIRES portfolio as well as broader DOE and national laboratory efforts such as the Grid Modernization Initiative.

Research efforts under the HydroWIRES Initiative are designed to benefit hydropower owners and operators, independent system operators/regional transmission organizations, regulators, original equipment manufacturers, and environmental organizations by developing data, analysis, models, and technology research and development that can improve their capabilities and inform their decisions.

More information about HydroWIRES is available at https://energy.gov/hydrowires.

Executive Summary

The U.S. electricity system is critical infrastructure that supports the economy, public safety, and national security. Although the U.S. power grid is very reliable according to standard metrics, there is an increased interest in resilience—the grid's ability to respond to and recover from high-impact, low-probability events. These range from natural events, such as hurricanes, to human-related events, such as cyber and physical attacks. The impacts on system operations, and hence the responses needed by the system, can vary in magnitude, intensity, duration, and geography depending on characteristics of the extreme event. Hydropower facilities are often crucial in responding to these extreme grid events due to their agility and flexibility. They can quickly change both their real and reactive power outputs, and they are well-suited to provide voltage support, inertial response, primary frequency response, spinning, and operating reserves. Readily available conversion of stored energy—water stored behind dams—and low station power requirements make them ideal for black start restoration of the grid. Additionally, hydropower presently constitutes the power system's largest portion of long-duration energy storage, which can act as a buffer during extended-duration system outages. However, no standard practices presently exist to quantify the contributions of hydropower resources and their attributes and response characteristics, especially for non-market and non-monetized grid services such as voltage support and inertial and frequency responses.[1]

Given that the U.S. power system is continuing to evolve both in terms of system composition and the attributes related to reliability and resilience of operations, understanding hydropower's contributions will support appropriate valuation of resources and help justify investments in hydropower facilities to provide or increase reliability services. Hence, the study authors developed a framework to evaluate contributions to grid resilience that: a) classifies and categorizes the extreme events a power system may experience; b) describes hydropower's characteristics that enable resources to respond to system resilience needs; c) documents historical role and performance of hydropower based on literature survey and analysis of collected data; and d) identifies methods, tools, models, and datasets to carry out analyses across different timescales (spanning the continuum of seconds-hours-days-weeks). The methodologies were exercised to analyze the role of hydropower in maintaining system resilience using a set of scenarios representing events of different types. The framework and toolchain can be used by system operators, regulators, and policy analysts to assess the role of hydropower under different combinations of events and future grid states. This report follows the structure laid out in the framework.

The ability of the power system to withstand or recover from a severe disturbance, generally defined as grid resilience, covers four temporal stages of system performance. The stages are illustrated in the disturbance and impact resilience evaluation (DIRE) curve shown in Figure ES.1.[2]

[1] Hydropower's role in providing market-based and monetized reliability services, such as frequency regulation, spinning reserves¸ etc., have been analyzed in the recently published Hydropower Value Study and Hydropower Market Report for different regions of the country.
[2] C. G. Rieger. 2014. "Resilient control systems practical metrics basis for defining mission impact." 7th International Symposium on Resilient Control Systems, pp. 1–10.

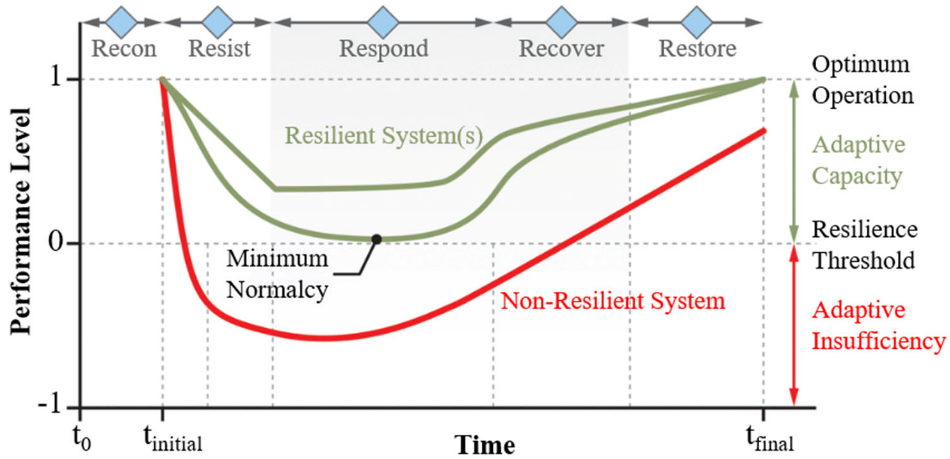

Figure ES.1. DIRE curve. More resilient systems result in less area enclosed by the curve.

The reconnaissance (Recon) phase is a continuous awareness of the system situation. The Resist phase generally corresponds to autonomous actions, such as inertial response, to slow the rate of performance degradation. The Respond phase returns the system to a stable operating point after the control system or operators have recognized and initiated mitigating actions. The Recover phase returns the system to the normal pre-contingency state and is required to regain capabilities that were expended in the response phase to be in position to absorb a future impact. The Restore phase accounts for the time needed to replace, repair, or maintain the system after it has been operated in an unusual or aggressive manner in response to a major event. Some grid attributes or operator actions that correspond to each of the phases of resilience are given in Table ES.1.

Table ES.1. Examples of attributes of grid components and operations for the phases of resilience.

Resilience Phase	Attributes for the Electric Grid
Recon	Contingency analysis, forecasting, positioning of operating points
Resist	Inertial response and frequency/voltage margins
Respond	Primary frequency response, voltage/volt-amperes reactive regulation, protection
Recover	Reserve dispatch and replenishing of expended energy reserves
Restore	Initiate black start cranking path, repair, and maintenance of generation, transmission, and distribution equipment

Hydropower resources can provide support during each of the resilience phases, but these capabilities depend on the type of resource. At least 40% of hydropower resources in the United States, by capacity, are comprised of pumped storage and “peaking” or reservoir hydropower plants that can store water to produce electricity at times of greatest need and value, and at least 18% are comprised of run-of-river (ROR) plants, which may have some operational flexibility but typically cannot impound and store additional water beyond inflows.[1] Within a given resource class, such as peaking or ROR plants, the capabilities depend on the site-specific electromechanical (physical) attributes and hydrological conditions. For a given plant, these capabilities will vary naturally over seasons and water years. Hence, the capabilities and limitations—based on plant design, available water resources, and institutional factors such as Federal Energy Regulatory Commission licenses and power purchase agreements—determine the response characteristics of a given resource at any given time. A summary of the three main categories of hydropower capabilities in the timeframe of system resilience is presented in ES.2.

[1] Oak Ridge National Laboratory. 2018. *HydroSource* web page. https://hydrosource.ornl.gov/.

Table ES.2. Resilience capabilities of run-of-river, reservoir, and pumped storage hydropower.

Resilience Phase	Run-of-River Hydropower	Reservoir Hydropower	Pumped Storage Hydropower
Recon	Power and spill setting	Storage and power setting	Storage and power setting
Resist	Inertia	Inertia	Inertia depends on type
Respond	Real and reactive power, spinning reserve	Real and reactive power, spinning and non-spinning reserve, with energy constraints	Real and reactive power, dependent on current direction, with energy constraints
Recover	N/A	Dispatch + response	Dispatch + response
Restore	Black start and sustained generation	Black start and sustained generation	Black start and sustained generation

In this study, the role of hydropower resources in supporting grid reliability and resilience was analyzed for a range of extreme events. These assessments were conducted using a combination of historical data and simulation-based analysis. The contributions of hydropower to grid resilience were quantified for two main categories of events, through specifically designed scenarios that will be introduced later:

- *Sudden loss of large generation assets (up to minutes to hours of duration)*: These event types result in short-duration disruptions, manifesting in a sudden increase or decrease in grid frequency, local voltages, etc., which if not corrected, can lead to cascading outages.
- *Changes in net load due to extreme weather (up to hours to days of duration), such as heat waves and cold snaps*: These types of events do not necessarily lead to short-term outages of power grid equipment. Rather, weather conditions that cause extreme heat or cold can also significantly decrease the power and energy production, especially from renewable energy resources, requiring redispatch of the entire online generation fleet.

The scenarios used to evaluate hydropower's role during extreme events were applied to the U.S. Western Interconnection (WI) system only[1], so specific results are only representative of the WI, but general capabilities and modes of operation should apply to other interconnections. The main findings from the study are the following:

1. **Hydropower is critical in stabilizing the Western Interconnection after events causing sudden large loss of generation.** The contributions of hydropower resources were observed to be consistent across different combinations of seasons, system loading, and water availability conditions. Hydropower's contributions also were consistent across different types of scenarios resulting from sudden loss of online generation capacity.
    - Analysis of historical data and simulation results shows that hydropower plants are a major resource for inertial and governor response during extreme events in the WI. Specifically, it was observed that hydropower facilities, collectively, contribute between 30–60% of governor response[2] to help stabilize system frequency after outage events. It should be noted that hydropower generation constitutes between 20–25% of generation capacity in the WI grid.

[1] The scenarios were designed for analysis of WI only due to availability of data and models. The modeling framework, including the tools, can be utilized for analysis of the Eastern Interconnections as well. The results, however, may vary requiring additional analysis.

[2] In a study conducted by American Governor Company, *The Impact of Hydroelectric Power and Other Forms of Generation on Grid Frequency Stability for the WECC Region*, the authors estimate that for the WI grid as a whole in 2008, hydropower generation contributed between 25–90% of the primary frequency control response in the first 10 seconds after an underfrequency event, before intervention from automatic generation control.

- Hydropower units have significant reactive power capability that helps maintain voltage stability during extreme events. Hydropower's ability to provide reactive power is similar to other conventional generation resources. However, conventional resources, especially baseload steam turbines (coal) and nuclear plants, operate close to their rated power capacities, which leaves little room to provide reactive power. Hydropower resources (and natural gas plants) generally operate at less than full capacity, which allows them to provide more reactive power support when needed. Simulation results for the WI show that hydropower units are a major source of reactive power support under all seasonal, loading, and water availability conditions.
- Other characteristics of hydropower units that can enhance a system's response and recovery attributes include a wide band of frequency ride-through ability and black start support. Analysis of past events and existing regulatory standards, such as North American Electric Reliability Corporation Protection and Control Standard 24, demonstrate that hydropower units can withstand a much wider range of frequency deviations compared to other conventional resources. This capability of hydropower resources can allow them to stay online longer than conventional resources after extreme events, which can help with quicker system recovery after those events.

2. Hydropower's storage capability and dispatch flexibility are critical to ensure system reliability during extreme weather events. Simulation results from extreme weather scenarios for the western United States showed significantly depressed wind and solar generation even though the impact on system load was not extreme. It was observed that hourly flexibility of hydropower resources was used to fill the resulting energy and capacity gaps. The cold wave scenario lasted over multiple days, and hence, hydropower resources' long-term storage capability was key in ameliorating the situation.

In the past and in simulated future event scenarios, this study demonstrated that hydropower resources contribute significantly to grid reliability and resilience during extreme events. The analyses in this study suggest that as the magnitude and frequency of extreme and stressful grid conditions increase, hydropower will continue to play a vital role in power system reliability and resilience. However, more work needs to be done to fully assess the role of hydropower under all potential combinations of future grid states and extreme events. The modeling framework developed in this project can be leveraged to assess some of these combinations, such as contingency events during extreme weather conditions with different water availability conditions. The toolchain established for this analysis also can be combined with capacity expansion models to determine hydropower's role in maintaining grid resilience under different realization of future grid states, such as those achieving 80-100% decarbonization by 2035.

Acronyms and Abbreviations

ADS	Anchor Dataset
AGC	automated generator control
BES	Bulk Electric System
COI	California-Oregon Intertie
DC	direct current
DCAT	Dynamic Contingency Analysis Tool
DIRE	disturbance and impact resilience evaluation
DOE	U.S. Department of Energy
FERC	Federal Energy Regulatory Commission
HS	heavy load, summer
HW	heavy load, winter
HWR	hydropower with reservoir
IID	Imperial Irrigation District
ISO	independent system operator
LS	light load, summer
LW	light load, winter
NERC	North American Electric Reliability Corporation
PCM	production cost modeling
PDCI	Pacific DC Intertie
PG&E	Pacific Gas & Electric Company
Pgen	Actual real-power generated
Pmax	Maximum power generation
PMU	phasor measurement unit
PSH	pumped storage hydropower
PSLF	Positive Sequence Load Flow
PSPS	Public Safety Power Shutoff
PV	photovoltaics
RAS	Remedial Action Scheme
ROR	run-of-the-river
SCADA	supervisory control and data acquisition
SDG&E	San Diego Gas & Electric
SONGS	San Onofre Nuclear Generating Station
SPS	Special Protection System
UFLS	Underfrequency load shedding
USACE	US Army Corps of Engineers
VAR	volt-amperes reactive

WALC	Western Area Power Administration—Lower Colorado
WECC	Western Electricity Coordinating Council
WI	Western Interconnection

Contents

Figures

Tables

1.0 Introduction

The U.S. electricity system is critical infrastructure that supports the economy, public safety, and national security. Although the U.S. power grid is very reliable, the recent increased interest in resilience is based on the grid's ability to respond to and recover from high-impact, low-probability events. These range from natural events, such as hurricanes, to human-related events, such as cyber and physical attacks. The impacts on system operations and the responses needed by the system can vary in magnitude, intensity, duration, and geography depending on characteristics of the extreme event. Hydropower facilities are often crucial in responding to these extreme grid events due to their agility and flexibility. They can quickly change both their real and reactive power outputs, and are well-suited to provide voltage support, inertial response, primary frequency response, spinning, and operating reserves. Readily available fuel such as water and low station power requirements make them ideal for black start restoration of the grid. Additionally, hydropower presently constitutes the power system's largest portion of long-duration energy storage, which can act as a buffer during extended-duration system outages.

In order to evaluate hydropower resources' contribution to grid resilience, the study authors developed a framework to evaluate contributions to grid resilience that: a) classifies and categorizes the extreme events a power system may experience; b) describes hydropower's characteristics that enable resources to respond to system resilience needs; c) documents historical role and performance of hydropower based on literature survey and analysis of collected data; and d) identifies methods, tools, models, and datasets to carry out analyses across different timescales (spanning the continuum of seconds-hours-days-weeks). The methodologies were exercised to analyze the role of hydropower in maintaining system resilience using a set of scenarios representing events of different types. The remainder of this section covers the general concept of power system resilience and how to improve grid resilience.

The rest of this report is structured as follows:

- Section 2.0 presents a hazardous grid events taxonomy. Quantitative evaluation, prediction, anticipation, and preparedness for these events and their impacts on the electricity system play crucial roles in national safety, productivity, comfort, and convenience. The results from a literature survey of different types of historical events and the resultant impacts on grid operations are presented in Sections 2.1 and 2.2. The findings have informed the development of a taxonomy structure to classify and describe grid conditions, event impacts, and responses needed. Section 2.3 discusses the different types of grid responses and services needed at different timescales to maintain grid reliability and resilience during a grid disturbance. The impacts to system operations dictate the types of responses needed from resources, which forms the basis to evaluate the characteristics of different resources, including hydropower, that support a system's resilience requirements. Section 2.4 presents a high-level classification of these impacts, which motivates the scenarios, analyzed and presented in Section 3.
- Section 0 presents a hydropower resilience assessment framework to assess the contribution of hydropower toward minimizing the impacts on the bulk-power system from extreme events. The stages during an extreme event—preparedness (reconnaissance), responses (intrinsic resistance and response), recovery, and restoration—require the grid to have several essential capabilities, such as high flexibility, fast ramping rate, and black start. Hydropower offers a cost-competitive and low-carbon energy source that provides the full range of services required by the electrical bulk-power system under normal, fault, and emergency conditions. This section describes the role of hydropower in all stages and presents results from historical case studies and future grid scenarios (modeled) to determine the potential role of hydropower in response to extreme events. Two types of extreme events are evaluated: Section 3.1 explores events triggered by sudden outage of large generators, and Section 3.2 looks at extreme weather events, such as heat waves and cold snaps, that require alternate

dispatch schedules for hydro generators. The two types of events require different responses and thus different methodologies to quantify hydropower's contributions. An overview of the methodologies, models, tools, and datasets is also provided in this section.

- Section 4 summarizes all the findings from the study and presents topics for future research.
- Appendices A through G provided supplemental information.

1.1 Power System Resilience

Power system resilience does not have a single broadly accepted definition.[1] Presidential Policy Directive 21 characterizes resilience as "the ability to prepare for and adapt to changing conditions and withstand and recover rapidly from disruptions."[2] The severe events described in Sections 0and 2.2 have resulted in large disruptions of critical infrastructure and motivated stakeholders to look at system resilience. Power system resilience embodies the qualities of being able to withstand threats and disruptive events, limiting damages and/or outages from disruptive events, and restoring service and service quality to customers in a timely manner after a system outage. System-level reliability metrics, including from the U.S. Department of Energy (DOE)-sponsored Grid Modernization Laboratory Consortium Foundational Metrics project,[3] tend to look historically at power system availability over time and to estimate the availability of the bulk electric system (BES) if it were to face the same conditions and experience the same types of events in the future as it has in the past. Resilience is more concerned with the performance of the grid during and after specific (even hypothetical) extreme events and the consequences of that performance for power system customers and society.

A more resilient system also may be more reliable in the long run, but that is not always the case. A utility may take actions to improve a resilience posture that could adversely impact reliability statistics in the short run but position the system to reduce the risk of wider spread calamity.[4] Examples include instituting rolling blackouts during a disturbance, siting spare equipment (such as large power transformers) in secure locations that better protect them from threats but require longer times to transport and replace damaged equipment, and keeping more generating reserves offline to insulate them from a possible cyberattack. In the long run, a more resilient system should be more reliable as improved performance during extreme events will probably offset any short-term decreases in reliability during normal operations. While the methods to quantify power system reliability in terms of various metrics are fairly mature, the definition and characterization of a power system's resilience is still a topic of research and debate. The National Academy of Sciences has stated that better understanding of measures of resilience is needed and suggests formulating metrics for use in the operation of critical infrastructure[5] to predict resilience and provide improved situational awareness to operators.

The goal outcomes for a more resilient system include being better prepared for the event, capable of remaining as operational as possible during the event and restoring to the pre-event state expeditiously. From a resilience perspective, the ability of the power system to withstand or recover from a severe disturbance covers four temporal stages of the system performance level. The

[1] NARUC. 2020. "Advancing Electric System Resilience with Distributed Energy Resources: A Review of State Policies." National Association of Regulatory Utility Commissioners, Washington, D.C.
[2] Presidential Policy Directive 21. 2013. Critical Infrastructure Security and Resilience, Washington, D.C.
[3] Petit F and V Vargas. 2020. Grid Modernization: Metrics Analysis (GMLC 1.1) – Resilience. Volume 3. https://gmlc.doe.gov/sites/default/files/resources/GMLC1.1_Vol3_Resilience.pdf
[4] Clark-Ginsberg A. 2016. What's the difference between reliability and resilience? Rand Corporation. DOI: 10.13140\RG.2.2.20571.46885.
[5] National Academies of Sciences, Engineering, and Medicine. 2017. "Enhancing the resilience of the nation's electricity system." National Academies Press, Washington, D.C. https://doi.org/10.17226/24836.

stages are illustrated in the disturbance and impact resilience evaluation (DIRE) curve shown in Figure 1.[1] DIRE curves represent attributes of the system that can intrinsically resist or slow the rate of performance degradation followed by the response to a disturbance after the control system or operators have recognized and initiated mitigating action. To return the system to a normal state, a recovery phase (Recover) is required to regain capabilities that were expended in the response phase (Respond) and to be in position to absorb a future impact. The restore period accounts for the time needed to replace, repair, or maintain the system after it has been operated in an unusual or aggressive manner in response to a major event. The restoration phase (Restore) may also refer to the period during which a system that does not ride through the event requires to be "boot-strapped" back to functionality. The reconnaissance phase (Recon) is a continuous awareness of the system situation. A recon phase is critical to identify appropriate resources and provide them to the system in order for it to withstand given contingencies or forecastable events. Some grid attributes or operator actions that correspond to each of the phases of resilience are given in Table 1.

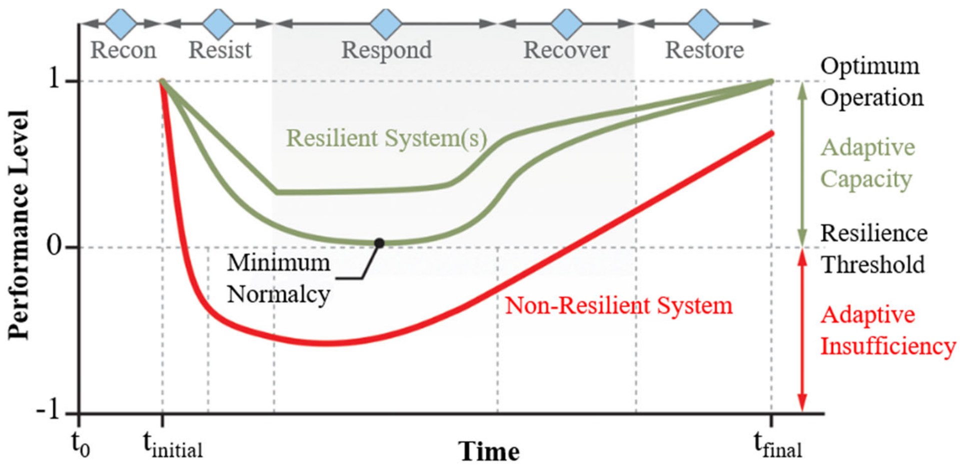

Figure 1. DIRE curves illustrate performance of a power system before, during, and after a grid disturbance event. More resilient systems result in less area enclosed by the DIRE curve.

Table 1. Attributes of the five phases of resilience. The attributes for the grid that correspond to each of the five phases of resilience of resilience includes all different types of data and grid responses needed.

Resilience Phase	Attributes for the Electric Grid
Recon	Contingency analysis, forecasting, positioning of operating points
Resist	Inertial response and frequency/voltage margins
Response	Primary frequency response, voltage/volt-amperes reactive (VAR) regulation, protection
Recovery	Reserve dispatch and replenishing of expended energy reserves
Restore	Initiate black start cranking path, repair and maintenance of generation, transmission, and distribution equipment

[1] Rieger CG. 2014. "Resilient control systems practical metrics basis for defining mission impact." 7th International Symposium on Resilient Control Systems (ISRCS), 1–10.

Evaluating the capabilities of a given set of resources against the anticipated outcomes of a specific natural or man-made threat requires modeling the grid network in greater detail[1 2] and developing useful metrics to assess the resilience of the system as well as identify the contributions of particular resources (e.g., hydropower) to improving those metrics. Some examples of the system-level resilience metrics (e.g., time and cost to recover, cumulative critical load not served, recovery rate, vulnerability to additional events or threats, performance degradation, and restoration efficiency indices) are given in Cicilio et al.,[3] Chalishazar et al.,[4] Johnson et al.,[5] and Chalishazar.[6] To identify ways to improve resilience, there must be a way to connect these system-level metrics to asset-level resilience response capabilities, such as those defined in Phillips et al.,[7] which describes the assets in terms of real-power production, reactive power management, energy constraints, control latency, and flexibility of responses. These resilience response capabilities were mapped to hydroelectric generation for this project.[8] Ways to improve power system resilience include:

- Increase redundancy by adding generation reserves or additional transmission paths, adding transmission or transformer capacity, energy reserves (i.e., energy storage), redundancy in support systems (e.g., communications, components and equipment, computers, and databases), and more work crews. [Recon, Resist, Respond, Recover]
- Harden systems and equipment by using more durable materials and designs to better withstand specific threats and enhancing cybersecurity. [Resist]
- Increase operational flexibility and responsiveness by switching transmission or distribution and enhancing the ability to vary generator output (real and reactive power) in timeframes from sub-seconds to hours. [Respond, Recover]
- Improve capability to recover quickly from a grid outage through black start, microgrids, facilitating delivery, and installing spare or replacement equipment. [Recover, Restore]

Power systems have been designed with resources and operating procedures to be available to serve the demand for electricity despite events, both natural and human-caused, detailed in Sections 2.1 and 2.2. Reliability standards address what power availability is acceptable; reliability metrics primarily address expected availability or observed historical availability. However, extreme events, though not frequently

---

[1] Chalishazar V, B Johnson, E Cotilla-Sanchez, and TKA Brekken. 2018. "Augmenting the Traditional Bus-Branch Model for Seismic Resilience Analysis." *2018 IEEE Energy Conversion Congress and Exposition (ECCE)*, Portland, Oregon, pp. 1133-1137. DOI: 10.1109/ECCE.2018.8557820.
[2] Chalishazar V, C Huo, I Fox, T Hagan, E Cotilla-Sanchez, A Von Jouanne, J Zhang, T Brekken, and R Bass. 2017. "Modeling power system buses using performance-based earthquake engineering methods," *2017 IEEE Power & Energy Society General Meeting*, Chicago, Illinois, pp. 1-5. DOI: 10.1109/PESGM.2017.8274307.
[3] Cicilio P, D Glennon, A Mate, A Barnes, V Chalishazar, E Cotilla-Sanchez, B Vaagensmith, J Gentle, C Rieger, R Wies, and M Kapourchali. 2021. "Resilience in an Evolving Electrical Grid." *Energies* 14, no. 3: 694. https://doi.org/10.3390/en14030694.
[4] Chalishazar VH, TKA Brekken, D Johnson, K Yu, J Newell, K Chin, R Weik, E Dierickx, M Craven, M Sauter, A Olennikov, J Galaway, and A Radil. 2020. “Connecting Risk and Resilience for a Power System Using the Portland Hills Fault Case Study.” *Processes 8*, 1200.
[5] Johnson B, V Chalishazar, E Cotilla-Sanchez, and TKA Brekken. 2020. "A Monte Carlo methodology for earthquake impact analysis on the electrical grid." *Electric Power Systems Research* 184: 106332.
[6] Chalishazar VH. 2019. “Evaluating the Seismic Risk and Resilience of an Electrical Power System,” Oregon State University, Corvallis, Oregon.
[7] Phillips T, T McJunkin, C Rieger, J Gardner, and H Mehrpouyan. 2020. “An operational resilience metric for modern power distribution systems.” *2020 IEEE International Conference on Software Quality, Reliability and Security Companion*, Requirements.
[8] Phillips T, V Chalishazar, T McJunkin, M Maharjan, SM Alam, T Mosier, and A Somani. 2020. “A Metric Framework for Evaluating the Resilience Contribution of Hydropower to the Grid.” *Resilience Week 2020*, Salt Lake City, Utah.

occurring, have resulted in extended and widespread power outages with severe economic and safety effects. The threat vector to the BES has changed with the increasing incidence of severe natural events (e.g., strong hurricanes), appreciation of the feasibility of rare but potentially catastrophic natural events (geomagnetic storms), and human threats (sabotage or cyber-, physical, and electromagnetic attacks). These high-impact low-frequency events and threats are characterized by failures or destruction of multiple types and locations of grid assets. Preparing for them goes beyond traditional reliability-based planning methods and standards.[1]

1.2 Hydropower in the United States

In 2019, hydropower capacity (80.25 GW) accounted for 6.7% of installed electricity generation capacity in the United States, and its generation (274 TWh) represented 6.6% of all electricity generated and 38% of electricity from renewable resources produced in the U.S. The U.S. hydropower fleet generated 274 TWh of electricity. Hydropower in the U.S. is largely concentrated in the Pacific Northwest; the western interconnect has 55% of the country's hydropower capacity and Texas interconnect, by contrast, has almost no hydropower. Roughly half of all U.S. hydropower capacity is concentrated in three states on the Pacific coast: Washington, Oregon, and California. For Washington and Oregon, hydropower accounts for more than 50% of the electricity generated in those states.

Hydropower facilities are often crucial in responding to extreme grid events due to their agility and flexibility. The U.S. has approximately 21 GW of pumped storage (~25% of U.S. hydropower capacity) with an estimated capacity of 550 GWh, which represents 99% of grid-scale (long-duration) storage in the nation, presently. Additionally, at least 40% of the hydropower capacity is composed of reservoir hydropower plants that can store water to produce electricity at times of greatest need and value. This allows the resources to quickly change both real and reactive power outputs, making them well-suited to provide voltage support, primary frequency response, and spinning and operating reserves. Online hydropower resources are synchronously connected to the grid, allowing them to provide inertial response to help stabilize the grid frequency after outage events. Readily available conversion of stored energy and low station power requirements make them well-suited for black start restoration of the grid. Hydropower represents less than 6.7% of U.S. electricity generation capacity but provides approximately 40% of black start resources. At least 18% of the U.S. hydropower fleet is composed of run-of-river (ROR) plants that can produce electricity only at times when water is flowing, and hence, that power is considered non-dispatchable.

The attributes of the hydropower resources, and hence, the capability to provide grid services are often based on site-specific design criteria, governed by hydrological and geological conditions, environmental regulations, and multi-use benefits of water at the location. Table 2 presents a mapping of potential relationships between various hydrological, mechanical, and other site-specific constraints on the response capabilities of hydropower resources.

Hydropower plants are custom built to suit the geography, hydrology, and ecology of a specific location so it is difficult to come up with general theories to describe the operations/capabilities of the fleet. (and, therefore, their contributions to resilience.)

---

[1] For example, if historically a city has experienced hurricanes whose magnitude on average is 2.5, it is not sufficient to design the power system to withstand up to Category 3 hurricanes if Category 4 or 5 storms, though infrequent, have occurred.

Table 2. Constraints on hydropower capabilities from multipurpose benefits.

		Constraints Involved				
		Water Use Priorities	**Min Pool Elevation**	**Max Pool Elevation**	**Min Flow**	**Flow Max Ramp Rate**
Multipurpose Benefits Drive Constraints	M&I water supply	✓✓✓	✓✓✓			
	Irrigation	✓✓✓	✓✓✓		✓	
	Reservoir recreation	✓✓✓	✓✓✓	✓✓✓		
	Stream reach recreation					✓✓✓
	Seasonal flood control		✓✓✓	✓✓✓		
	Navigation		✓✓✓	✓✓✓	✓✓✓	✓✓✓
	Fish and wildlife				✓✓✓	✓✓✓
Constraints Restrict Grid Capabilities	Inertial constant					
	Reactive power control					
	Synchronous condensing mode					
	Cold start-up	✓✓✓				
	Flexible power dispatch	✓✓✓	✓✓✓	✓✓✓	✓✓	✓✓
	Ramp rates		✓✓		✓✓	✓✓✓
	Isolated unit start-up					✓✓✓

✓✓✓ Well-understood relationship; ✓✓ relationship exists but is not well understood; ✓possible relationship.

2.0 Different Extreme Events and Effects on the Power Grid

There are many types of extreme events that cause disturbances and each results in different conditions on the grid. Depending on the severity, type, and frequency, these events require different mitigation services to prevent loss of load. Sections 2.1 and 2.2 provide a taxonomy of these extreme events, describing both the theoretical and historical effects of each event type. Section 2.3 then describes the types of ancillary services that are required to mitigate the effects of extreme events. Finally, Section 2.4 presents a high-level classification of the events in the taxonomy, which is then used to select representative events for simulating hydropower's contributions to grid resilience.

2.1 Natural Events

A statistical analysis[1] of North American Electric Reliability Corporation (NERC) data on grid outages, carried out by the University of Vermont showed that nearly 44% of the events (out of a total 933 events that caused outages between 1984 and 2006) were weather related. The analysis also revealed that some of the reported events have multiple initiating causes because some events (such as lightning) can trigger other outages or operator errors. Examples of key natural events that resulted in damage to the electric grid are presented in grey within each section below.

2.1.1 Wind Events, Hurricanes, Tornadoes, Thunderstorms

High-speed winds and lightning occur due to different types of meteorological phenomena, such as hurricanes, tornadoes, derechos, and thunderstorms. High-speed winds can damage the power grid both indirectly and directly. This is due primarily to knocking over trees, especially when the ground is already saturated with water from rainfall or flooding. Fallen trees can damage or down distribution power lines, resulting in power outages. Winds may directly knock over utility poles and damage electrical wires. This damage triggers protection devices, causing widespread outages. High winds can also damage components at the transmission level of the electric power system, denying service to distribution substations. Tornadoes generally create a narrow path of destruction and do not cause widespread power outages, but if a tornado passes close to a major transmission substation or transmission corridor, the localized damage to the system could lead to widespread power outages. Lightning usually comes with thunderstorms and can cause arcs. Undesired or unintended electric arcing can have detrimental effects on electric power transmission, distribution systems, and electronic equipment.

- Due to hurricane Maria in September 2017, 80,000 homes were without electricity in the north of Dominica and nearly half of Puerto Rico's residents were still without power by the end of 2017.[2] (Both direct and indirect impacts to regional hydroelectric generation).
- On August 27 and 28, 2011, Hurricane Irene caused over 4.3 million people on the east coast of the United States to lose power, from North Carolina to Massachusetts.[3] (Both direct and indirect impacts to regional hydroelectric generation)

[1] N. Komendantova, D. Kroos, D. Schweitzer, C. Leroy, E. Andreini, B. Baltasar, T. Boston, M. Keršnik, K. Botbaev, J. Cohen, and C. Eismann. 2016. "Protecting Electricity Networks from Natural Hazards." Organization for Security and Cooperation in Europe (OSCE).
[2] Pasch RJ, AB Penny, and R Berg. 2019. *National Hurricane Center Tropical Cyclone Report: Hurricane Maria*. Tropical Cyclone Report AL152017, National Oceanic and Atmospheric Administration and the National Weather Service. https://www.nhc.noaa.gov/data/tcr/AL152017_Maria.pdf.
[3] National Weather Service. 2012. "Hurricane Irene August 26-27, 2011." https://www.weather.gov/mhx/Aug272011EventReview.

2.1.2 Inland and Coastal Flooding, Tsunami

Flooding is often the outcome of landfall hurricanes and tsunamis. In the transmission and distribution system, substations are the elements most vulnerable. Flooding can damage ground-level substation control equipment and low-voltage switchgear. High-voltage components, including insulators, circuit breakers, air-break switches, transformers, dead-end towers, lightning arrestors, and metering transformers, are situated high above ground to use air space for insulation from surrounding ground faults; therefore, flooding is less directly threatening to high-voltage power system components. As a rule of thumb, facilities located in areas with more than 4 feet of floodwater will likely be out of service and could sustain damage to transformers and circuit breakers.[1] If floodwaters do not damage the transmission and distribution systems, crews can restore these systems shortly after the floodwaters recede. If other infrastructures are also damaged, co-restorations will be needed. The restoration time for damaged transmission-level components, specifically high-voltage transformers at individual substations, could be months.[1] Floods can also damage generation sites, crippling their cooling systems and reducing available generation capacity. Subsequent landslides may occur and destroy or damage overhead and underground infrastructure, transformer stations, customer connections, and metering equipment.

- When Hurricane Katrina came ashore on August 29, 2005, more than 2.7 million people in Louisiana and Mississippi lost power due to combined wind and flooding.[2] This was in addition to the 1.3 million people who had lost power in southeastern Florida when the hurricane made landfall there several days earlier. (Both direct and indirect impacts to regional hydroelectric generation)

2.1.3 Winter Storms, Ice Storms, Freezing Rain, Extreme Cold, Polar Vortex

During an extreme cold weather event, the demand for natural gas increases and may exceed the capacity of natural gas pipelines. If the gas pipeline is physically unable to deliver gas required by firm contracts held by electric power generators, these generators are derated or shut down. The stress on the electrical grid created by the loss of generation may be compounded by high electrical demand for heating due to the extreme cold. Other impacts on generators include frozen coal piles, interrupted fuel-oil delivery or sluggish flow, and malfunctions of generator protection devices due to cold temperature.[3] Besides the generating units, transmission systems can also be impaired. Ice accumulation adds weight to power lines and increases the cross-sectional area for wind drag on the lines, leading to increased mechanical stress and breakage of power lines and support structures.[4] In addition to increased weight, wind blowing against ice-laden transmission lines can cause low-frequency (1 Hz) high-amplitude (1 m) oscillations (called conductor gallop) that further stress towers and insulators.[5] Ice accumulation on nearby trees can cause branches to fall on lines or bring vegetation close enough to allow arcing current to cause a short.[1]

---

[1] National Infrastructure Simulation and Analysis Center. 2011. *Analysis of Population, Infrastructure, and Economic Impacts Resulting from Morganza Spillway Flooding*. Sandia National Laboratory, Albuquerque, New Mexico.
[2] DOE. 2005. "Hurricane Katrina Situation Report #42." Office of Electricity Delivery and Energy Reliability, Washington, D.C. https://www.oe.netl.doe.gov/docs/katrina/katrina_092305%20_1500.pdf.
[3] NERC. 2013. *Assessment of Previous Severe Winter Weather Reports 1983–2011*. Atlanta, Georgia. www.nerc.com/pa/rrm/ea/February%202011%20Southwest%20Cold%20Weather%20Event/Final_Draft_Assessment_of_Previous_Severe_Winter_Weather_Report.pdf.
[4] Merrill HM and J Feltes. 2006. "Transmission icing: A physical risk with a physical hedge." *2006 Power Engineering Society General Meeting*. www.merrillenergy.com/Icing31.pdf.
[5] National Academies of Sciences, Engineering, and Medicine. 2017. *Enhancing the resilience of the Nation's electricity system*. National Academies Press, Washington, D.C. https://www.naesb.org/misc/nas_report.pdf.

- During the polar vortex of January 2014, extreme cold weather had a major impact on generator equipment. Of the approximately 19,500 MW of capacity lost due to cold weather conditions, over 17,700 MW was due to frozen equipment. Many outages, including a number of those in the southeastern United States, were the result of temperatures that fell below plant design bases for cold weather. At the height of generation outages (January 7 at 0800), the southeastern United States accounted for approximately 9,800 MW of the outages attributed to cold weather.[1] (Both direct and indirect impacts to regional hydroelectric generation)
- From January 4–10, 1998, a series of storms generated along a stationary weather front brought warm Gulf of Mexico precipitation events across a stationary cold air mass. The tremendous weight of accumulated ice resulted in the collapse of 770 electric transmission towers and required replacement of more than 26,000 distribution poles and 4,000 pole-mounted transformers and restringing of 1,800 miles of transmission and distribution circuits. At its peak, more than 5.2 million customers in the interconnected areas of eastern Canada, New York, and New England were without power. Three weeks after the storm, hundreds of thousands of customers still had no power; some customers did not have power restored until more than a month later. Storm damage was estimated at about $4 billion. [2] In Canada alone, the utility company Hydro-Québec had to repair or rebuild 1,864 miles of their network, including approximately 1,000 steel pylons, 24,000 poles, and 4,000 transformers.[3] Two weeks after the storm, 400,000 customers were still without power; two weeks after that complete restoration was achieved.[4]

2.1.4 Drought

Production of all types of energy, including electricity, requires water. Because the energy sector is dependent on water availability, drought can severely impact energy systems, particularly on hydroelectric power generation and other generations through infrastructure interdependency.[5]

Hydroelectric and pumped storage hydropower (PSH) resources can be affected by low rainfall, low snowpack volume, changing melt patterns, and groundwater depletion. Some of these effects are short and midterm, such as low rainfall, and can impact availability and productivity, and further affect the power system operations in these timeframes. Hydropower plays essential roles in power system operations to provide all types of grid services such as regulation and frequency response, load following, spinning reserve, supplemental reserve, as well as unique capability in extreme grid events, such as black start. The absence of these services and capabilities could jeopardize power delivery. Other effects are induced due to long-term climate changes.

The West and Pacific Northwest of the United States are expected to see annually increased temperatures, resulting in less precipitation in the summer months and more precipitation in the form of rain and snow in the winter months. Increased temperatures are already causing snowpack to melt earlier in the year and this trend is expected to continue. More winter precipitation, earlier snowmelts, and less summer precipitation combine to yield an earlier powerful peak flow which can flood out smaller dams, followed by drought conditions in the summer when hydroelectricity is needed most to power air-conditioning

---

[1] NERC. 2014. *Polar Vortex Review*. Atlanta, Georgia. https://www.nerc.com/pa/rrm/January%202014%20Polar%20Vortex%20Review/Polar_Vortex_Review_29_Sept_2014_Final.pdf.
[2] National Academies of Sciences, Engineering, and Medicine. 2017. *Enhancing the resilience of the Nation's electricity system*. National Academies Press, Washington, D.C. https://www.naesb.org/misc/nas_report.pdf.
[3] Risk Management Solutions. 2008. *The 1998 Ice Storm: 10-year Retrospective*. Newark, California.
[4] Cigre Working Group B2.06. 2008. *Big storm events: what we have learned.*
[5] National Oceanic and Atmospheric Administration. 2021. *National Integrated Drought Information System*: *Energy* web site. https://www.drought.gov/sectors/energy.

units across the region.[1] These long-term changes impose challenges on power system planning and water resource management. Fortunately, most of these drought-induced events can be predicted with good accuracy.

Drought can also decrease the productivity of thermoelectric electricity generation. These plants use steam turbines to generate electricity from a variety of fuel sources. Large amounts of water are needed to generate steam and for cooling. Drought conditions can result in reduced plant efficiency and generation capacity. They will also increase the power demand for pumping and treatment. Based on historical events, the shortage of cooling water usually will not impact the power generation severely as the power plants were flexible enough at the plant level to adapt by switching to less water-intensive technologies. Furthermore, reduced water availability affects the production and refining of petroleum and natural gas, introducing fuel starvations for thermoelectric generators.

- In 2014, California experienced its worst drought in 119 years.[2] Consequently, hydroelectric generation for June 2014 was only 58% of the 10-year average.

2.1.5 Extreme Heat and Heatwaves

Extreme heat and heatwaves can impose adverse effects on demand side, supply side, and transmission systems simultaneously, driving the power grid closer to the point of collapse. On the demand side, a severe heat wave can increase air-conditioning load significantly. This can drive up the entire system load, with the largest increases during the mid- to late-afternoon peak hours.[3] Cooling degree days have already increased in the United States by roughly 20% over the last few decades and this trend is projected to continue in the future. On the supply side, high ambient-temperature conditions have an impact on combustion turbines because of the reduced density of the air at higher temperatures. Unless inlet cooling technologies are used, the output capacity of a combustion turbine decreases because the efficiency of converting fuel to power also decreases.[4] As for transmission systems, extreme heat can lower the carrying capacity of transmission lines and transformers, resulting in transmission line overloading.[5]

- On August 10, 1996, power surges due to high summer loads led to heavy loading conditions for the 500 kV Northwest transmission lines in the Western Electricity Coordinating Council (WECC) system. Then a ground fault caused a series of equipment trips, which eventually opened the COI,

[1] Blackshear B, T Crocker, E Drucker, J Filoon, J Knelman, and M Skiles. 2011. *Hydropower Vulnerability and Climate Change*. Middlebury College, Vermont. http://www.middlebury.edu/media/view/352071/original/globalhydro_final_dm.pdf.
[2] U.S. Geological Society. 2021. *California Drought* web page. http://ca.water.usgs.gov/data/drought/.
[3] Dirks JA, WJ Gorrissen, JE Hathaway, DC Skorski, MJ Scott, TC Pulsipher, M Huang, Y Liu, and JS Rice. 2015. "Impacts of Climate Change on Energy Consumption and Peak Demand in Buildings: A Detailed Regional Approach." *Energy* 79(1): 20-32.
[4] Bastianen M. 2013. "Multi-Stage Turbine Inlet Cooling for Increased Efficiency." *Turbine Inlet Cooling Association Meeting*, Naperville, Illinois.
[5] Vine E. 2008. *Adaptation of California's Electricity Sector to Climate Change*. San Francisco: Public Policy Institute of California. www.ppic.org/content/pubs/report/R_1108EVR.pdf.

the main power artery between the Pacific Northwest and California.[1] This blackout affected more than 4 million people in nine states.[2]

2.1.6 Earthquakes, Landslides

Ground shaking can affect the structural integrity of electric power assets through various modes of permanent ground deformation: soil liquefaction, lateral spreading, and/or vertical displacement. Records indicate that overhead electrical transmission lines are not particularly vulnerable to significant earthquake damage, but distribution systems, distribution poles, and substation components located in areas with unstable soil are at risk of damage. Earthquake-related damage includes broken porcelain components, toppled equipment, line failures because of inadequate slack or in underground lines, and leaking gaskets. Distribution line damage can occur if trees fall onto wires or poles, platform-mounted transformers topple, or wires tangle.[3] In severe cases, both systems can be damaged by landslides and rock falls.

- As a result of the Tohoku earthquake of March 11, 2011, in Japan, the Tohoku Electric Company immediately lost about 55% of the gross fossil-fired and geothermal capacity, which amounted to 4.926 GW. In addition, the Tokyo Electric Power Company lost 13 out of 63 fossil-fired generating stations—another 8.475 GW capacity (about 30%). As a result, around 4.4 million customers lost power. Approximately 90–95% of them were restored within 10 days.4 (Indirect impacts to regional hydroelectric generation)

2.1.7 Volcanic Activity

Volcanic ash consists of fine, jagged pieces of rock and glass. Ash is hard, abrasive, and mildly corrosive; conducts electricity when wet; does not dissolve in water; and is spread over broad areas by wind. Volcanic ashfall can quickly lead to widespread loss of electricity. The generation, transmission, and distribution, and substation components of a modern power system are vulnerable to different and specific ash-induced impacts, depending on the equipment at each phase of power delivery. The most commonly reported problems are supply outages from insulator flashover caused by ash contamination, disruption of generation facilities, controlled outages during ash cleaning, abrasion and corrosion of exposed equipment, and line (conductor) breakage due to ash loading. Electrical networks are vulnerable to a number of impacts from ashfall. Flashover may occur with <3 mm of ashfall, provided a significant portion of the insulator creepage distance ($>50\%$) is covered in wet ash. This is the most common and widespread impact. Ash accumulation may overload lines, weak poles, and light structures, and cause additional treefall onto lines.[5]

- On September 25, 1995, volcanic ash from Mt. Ruapaehu volcano in New Zealand caused shorting of high-voltage electrical power lines at the base of the volcano. Mt. Ruapaehu is located in the Taupo

---

[1] Golden T.1996. "Blackout May Be Caution Sign on Road to Utility Deregulation." *New York Times*. http://www.nytimes.com/1996/08/19/us/blackout-may-be-caution-sign-on-road-to-utilityderegulation.html?pagewanted=1.

[2] NERC. 2002. *1996 System Disturbances - Review of Selected 1996 Electric System Disturbances in North America*. Princeton, New Jersey. https://www.nerc.com/pa/rrm/ea/System%20Disturbance%20Reports%20DL/1996SystemDisturbance.pdf.

[3] Federal Emergency Management Agency. 1990. *Earthquake Resistant Construction of Electric Transmission and Telecommunication Facilities Serving the Federal Government Report*. Washington, D.C. www.fema.gov/media-library-data/20130726-1505-20490-2834/fema-202.pdf.

[4] Kazama M and T Noda. 2012. "Damage statistics (Summary of the 2011 off the Pacific Coast of Tohoku Earthquake damage)." *Soils and Foundations* 52(5):780–792. DOI:10.1016/j.sandf.2012.11.003.

[5] Volcanic Ashfall Impacts Working Group. 2015. *Volcanic Ash Impacts & Mitigation* web site. https://volcanoes.usgs.gov/volcanic_ash/ruapehu_1995.html.

Volcanic Zone, central North Island of New Zealand. This caused voltage fluctuations and problems for electrical equipment throughout the North Island.[1] Ash washed into the upper stream river and had a major impact at a hydroelectric power plant with a 120 MW rate as the ash entered the intake structure, causing considerable abrasion damage to the station's turbine. The total value of loss of generation was estimated in excess of $12 million New Zealand dollars. The blade was replaced at a cost of $12 million New Zealand dollars. On June 17, 1996, electricity supplies were disrupted in parts of the city of Rotorua, located on North Island of New Zealand, after an explosion at a local substation. The explosion was caused by ash and water settling on a transformer when a resident hosed ash from the roof of a neighboring building.[1]

2.1.8 Sea-Level Rise

Sea-level rise poses a potential threat to energy infrastructure in the coastal zone in two possible ways. First, a sustained increase in sea level could potentially result in the permanent inundation of coastal land, some of which supports electricity infrastructure.[1] Second, sea-level rise could threaten electricity assets through interactions with storm-surge events associated with tropical cyclones, hurricanes, and nor'easters. Sea-level rise is projected to increase the depth of inundation associated with storm surges, as well as their inland penetration. This may increase the frequency at which electricity assets are exposed to inundation as well as the severity of inundation during storm events. The effects of sea-level rise are most significant for low-intensity hurricanes because the change in sea level is relatively large compared to the typical storm surge. For major hurricanes, sea-level rise has comparatively little additional impact on the anticipated inundation of existing infrastructure.[2]

2.1.9 Wildfires

Wildfires pose a threat to the electricity system, particularly because they impact high-voltage transmission lines. These events can trigger emergency line derating or shutdowns to prevent line damage. Smoke from wildfires can induce a line fault, resulting in loss of service.[3] If wildfires penetrate into residential and/or commercial areas, they can also affect electricity distribution systems and substations, and disrupt generation facilities.[4]

- The October 2017 Northern California wildfires coincidently occurred with strong downslope winds and burned a majority of the area within 12 hours of ignition. By contrast, the December 2017 Southern California wildfires occurred during the longest Santa Ana wind event on record, resulting in the largest wildfire in California's modern history.[5] In 2019, California Public Utility Commission approved the Public Safety Power Shutoff (PSPS)[6] program, which requires the state's largest investor-owned utilities to monitor territories prone to wildfires and de-energize transmission lines in the

---

[1] DOE. 2014. *Effect of Sea Level Rise on Energy Infrastructure in Four Major Metropolitan Areas*. Office of Electricity Delivery and Energy Reliability, Washington, D.C. http://energy.gov/sites/prod/files/2014/10/f18/DOE-OE_SLR%20Public%20Report_Final%20_2014-10-10.pdf.

[2] Maloney MC and BL Preston. 2014. "A geospatial dataset for US hurricane storm surge and sea-level rise vulnerability: Development and case study applications," *Climate Risk Management*, 2: 26–41.

[3] Sathaye J, L Dale, P Larsen, and G Fitts. 2011. *Estimating Risk to California Energy Infrastructure from Projected Climate Change*. Lawrence Berkeley National Laboratory, Berkeley, California. http://www.osti.gov/scitech/servlets/purl/1026811.

[4] Dale L, M. Carnall, M Wei, G Fitts, and S Lewis MacDonald. 2018. *Assessing the Impact of Wildfires on the California Electricity Grid*. California Energy Commission.

[5] Nauslar N, J Abatzoglou, and P Marsh. 2018. "The 2017 North Bay and Southern California fires: a case study." *Fire* 1(1):18. https://www.spc.noaa.gov/publications/nauslar/2017cali.pdf.

[6] *Public Safety Power Shutoff* web site. 2021. https://prepareforpowerdown.com/.

interest of public safety. That year, around 2.2 million customers were affected by de-energization of transmission lines.[1,2] (Both direct and indirect impacts to regional hydroelectric generation)

2.1.10 Geomagnetic Disturbances

During geomagnetic disturbances, the magnetic fields at the Earth's surface produce geoelectric fields that can drive geomagnetically induced currents through grounded transformers and transmission lines. This quasi-direct current (DC) can saturate transformer cores leading to voltage collapse and/or excessive heating and failure of a significant number of high-voltage transformers. The damage to large transformers could result in long-term, widespread blackouts and lead to lengthy (from weeks to months) repairs or replacements.[3,4] A power system is more vulnerable to geomagnetic disturbances when the system is heavily loaded. Increasing power demand and industry deregulation have led to power systems being operated closer to their limits, making them more vulnerable to outside disturbances. A distinctive feature of geomagnetically induced current effects on power systems is that problems occur simultaneously on many pieces of equipment. This is different from other types of power system problems such as lighting strikes or equipment failures, which are more localized and independent of each other. The interconnections of modern power systems are designed to provide safeguards against localized failures but may contribute to an increased vulnerability to geomagnetically induced currents.

- On March 13, 1989, a geomagnetic storm caused the entire Hydro-Québec power system to collapse in just over 90 seconds. The predominance of hydropower generation in the system allowed 83% of the total load to be restored within 11 hours.[5] The reported events are listed in Table 3.

Table 3. Reported North American power system impacts, March 13, 1989, 16:00–17:23 EST. Note that a geomagnetic storm caused the entire Hydro-Québec power system to collapse in just over 90 seconds.

Time (EST)	Area	Event	Time (EST)	Area	Event
1600	Atl. Elec.	MVAR	1658	WAPA	Line
1602	Va. Pwr.	Capacitor	1658	WKPL	Alarm
1610	PJM	Noise	1658	BPA	Capacitor
1615	PJM	Generator	1658	BPA	Transformer
1625	PJM	Oscillograph	1700	UPA	Voltage
1626	PJM	Oscillograph	1700	LILCO	Voltage
1630	SC Edison	Current	1700	IIGE	Voltage
1630	SC Edison	Current	1700	WEP	Noise
1630	SC Edison	Noise	1701	PJM	Capacitor
1640	PJM	Voltage	1701	NIMO	Capacitor
1644	PJM	Alarm	1701	Va. Pwr.	Capacitor
1644	PJM	Capacitor	1701	Va. Pwr.	Capacitor

[1] California Public Utilities Commission. 2021."De-Energization (PSPS)." https://www.cpuc.ca.gov/deenergization/.
[2] California Public Utilities Commission. 2021. "De-Energization (PSPS)." Available at https://www.cpuc.ca.gov/uploadedFiles/CPUCWebsite/Content/News_Room/NewsUpdates/2020/De-energization%20Event%20History%20Thru%20Dec%2031%202019%20(as%20of%20Jan%2010%202020).xlsx.
[3] Space Studies Board. 2008. *Severe Space Weather Events--Understanding Societal and Economic Impacts: A Workshop Report*. National Academies Press, Washington, D.C. www.nap.edu/openbook.php?record_id=12507&page=R1.
[4] Maynard T. 2003. "Solar Storm Risk to the North American Electric Grid." Lloyds, London, United Kingdom. www.lloyds.com/~/media/lloyds/reports/emerging%20risk%20reports/solar%20storm%20risk%20to%20the%20north%20american%20electric%20grid.pdf.
[5] Kappenman J. 2010. *Geomagnetic Storms and Their Impacts on the U.S. Power Grid.* Meta-R-319. Metatech Corporation, Goleta, California.

Time (EST)	Area	Event	Time (EST)	Area	Event
1645	WPL	Voltage	1701	OH	Voltage
1649	PJM	Recorder	1701	OH	Oscillograph
1651	NIMO	Capacitor	1703	Va. Pwr.	Capacitor
1653	NIMO	Capacitor	1708	UPA	Capacitor
1654	PJM	Alarm	1709	WAPA	Converter
1655	Minn. Power	Voltage	1709	WAPA	Transformer
1655	Atl. Elec.	Voltage	1709	WAPA-Fargo	Voltage
1665	Atl. Elec.	MVAR	1709	WAPA	Line
1658	BC Hydro	Voltage	1709	WAPA	Relay
1658	OH	Demand	1711	NIMO	Capacitor
1658	WAPA	Converter	1720	UPA	Voltage
1658	BPA	Noise	1723	Va. Pwr.	Capacitor

2.1.11 Wildlife and Vegetation

Wildlife can affect transmission, distribution, and substations. Animal intrusions into substations are particularly problematic, resulting in faults that can cause outages over larger areas. Animal waste, if it falls on devices, will impact insulation characteristics and flashover may happen. This is especially dangerous for high-voltage devices. Vegetation can also pose a threat, particularly to distribution systems. The effects of vegetation are often indirect, through their association with weather events (e.g., wind or ice), which can lead to falling branches, trees, or other debris. Fortunately, utilities have vegetation-management programs that can significantly reduce the risks and impacts of related outages.

- A 2015 survey of energy utilities indicated that wildlife-related outages associated with the distribution system exceeded those associated with severe weather.[1] In the average customer-weighted occurrence rates per 1,000 customers, the occurrence rate of the wildlife is 2.37, followed by overhead equipment failure, which is 2.02, and weather, which is 1.38. In 2005, the annual costs of wildlife-caused power outages for California alone were estimated between $32 million and $317 million.[2] Although there were multiple causes of the 2003 Northeast blackout, including software malfunctions and operation errors in First Utility's control center, the direct cause was that a 345 kV overhead transmission line in northeast Ohio failed due to contact with a tree in Walton Hills, Ohio.[1] The tree contact was caused by conductor sag due to hot weather.

2.2 Human-Related Events

According to the statistical analysis of grid outages, performed by Komendantova (2016),[3] more than 50% of the events were human related. The table also revealed that some of the reported events have multiple initiating causes because some events (such as lightning) can trigger other outages or operator errors. Examples of key natural events that resulted in damage to the electric grid are presented in boxes within each section below.

---

[1] American Public Power Association. 2016. *Evaluation of Data Submitted in APPA's 2015 Distribution System Reliability & Operations Survey*. Arlington, Virginia. http://www.publicpower.org/files/PDFs/2015DSReliabilityAndOperationsReport_FINAL.pdf.

[2] Energy and Environmental Economics, Inc. 2005. *The Costs of Wildlife-Caused Power Outages to California's Economy*. CEC-500-2005-030. California Energy Commission, Public Interest Energy Research Program, San Francisco, California. http://www.energy.ca.gov/2005publications/CEC-500-2005-030/CEC-500-2005-030.PDF.

[3] N. Komendantova, D. Kroos, D. Schweitzer, C. Leroy, E. Andreini, B. Baltasar, T. Boston, M. Keršnik, K. Botbaev, J. Cohen, and C. Eismann. "Protecting Electricity Networks from Natural Hazards." Organization for Security and Cooperation in Europe (OSCE); 2016 May 25

2.2.1 Technical and Human—Unintentional

Unintentional human-related events include pandemics, software or computer errors, and operations errors and have been responsible for approximately 40% of blackouts. Of those, equipment failure was the most frequently observed cause of blackouts. Specific impacts to the grid due to unintentional human-related events are described below.

2.2.1.1 Pandemics

Power system operations rely on critical personnel. Medical or biological events, such as pandemics, may cause critical personnel to be unavailable to operate the electric power system. Without these personnel, operational issues would increase as less-trained or less-experienced individuals work to operate generation plants, address mechanical failures, restore power following outages caused by weather and other natural events, and operate the system.[1] Furthermore, large-scale, long-duration pandemics may alter the load pattern, thus making it more difficult to have accurate load forecasts and posing challenges for system operators.

This type of event differs from most other threats for several reasons. First, unlike many threats that are localized, a pandemic has the potential to impact operations simultaneously across North America and around the world. It would affect all employees and the availability of resources and services upon which the electric sector depends. Second, a pandemic could severely disrupt operations through multiple waves that could last longer than 6 to 8 weeks and span several seasons or even years. Different magnitudes and times of the wave peaks can significantly impact demands of power and interdependent sectors, such as gas and water. Decreasing predictability of electric power demand and operation patterns of other critical utilities will compromise the resilience of the power grid.

- As nearly 20 million New Yorkers adjusted their lives in response to the COVID-19 crisis in 2020, the changing patterns of behavior reduced and shifted electricity consumption. By the middle of March 2020, energy use on the grid had declined by roughly 2–3%, with daily peak energy use (the highest amount of energy used at any point during the day) about 2% below peak for the time of year. During the week of March 27, energy use declined even further with a total reduction of 4–5%. By the week of April 3, that decline was 7–8%. The load forecast at the ISO New England admitted larger errors during the beginning of the pandemic, then the artificial-intelligent-based algorithms and models were able to learn the new pattern and provide good forecasting. The combined effects of low demand caused by the pandemic and large-scale solar power penetration made the residual load drop remarkably. This required the system to have faster ramping resources to handle the evening peak when the solar power was no longer available. Thanks to all the regional transmission organizations and independent system operator (ISOs), the BES continued to operate reliably across the United States and North America during the pandemic despite the stress placed on all system operators. (Both direct and indirect impacts to regional hydroelectric generation)

2.2.1.2 Software/Computer Errors

Software and computer systems deliver key functions to power system operations, such as state estimation, fault alarms and responses, and substation automation. Software bugs may not be noticed until they are triggered by a particular set of events. These errors, once triggered, can send incorrect fault information and switch commands, leading to loss of components and incorrect operation actions.

[1] NERC and DOE. 2010. *High-Impact, Low-Frequency Event Risk to the North American Bulk Power System*. Washington, D.C. https://www.energy.gov/sites/prod/files/High-Impact%20Low-Frequency%20Event%20Risk%20to%20the%20North%20American%20Bulk%20Power%20System%20-%202010.pdf.

- The 2003 Northeast blackout was triggered by a simple fault—a tree caused a transmission line to short circuit—but within hours it became the largest blackout in U.S. history, owing to, among other reasons, two computer/software errors that caused a lack of situational awareness for grid operators.[1] (Indirect impacts to regional hydroelectric generation)
- On November 9, 1965, a major disruption in the power supply for the Northeast left more than 30 million people without power. A few days before the incident, a protective relay on a transmission line was set too low near Sir Adam Beck Station No. 2, the Niagara generation station in Queenston, Ontario. On November 9, the weather was cold, which put a large strain on the system. A tiny surge in power, originating from the Robert Moses generating plant in Lewiston, New York, tripped the relay which deactivated a major power line that was headed for northern Ontario. The rest of the power flowing to the tripped line was diverted, causing other lines to overload. Each of their relays tripped. With nowhere else to go, the power headed east into New York state, overloading those lines.[2] (Indirect impacts to regional hydroelectric generation)

2.2.1.3 Operations Errors

Operations errors may result in key components being shut off in transmission corridors or with incorrect commands pushing systems into insecure operating conditions. These errors can happen in both control rooms and in the field, such as at a substation. Depending on system conditions and the nature of faults, operator errors can unfold over periods of minutes to hours.

- The 2011 Southwest blackout took place on September 8, 2011. Due to a mistake by a technician, a 500 kV line was accidentally shut down between Tonopah and Yuma, Arizona. Most of the power to the San Diego area was then rerouted through Southern California Edison's system. This caused several key transformers to be overloaded and disconnect, causing another transmission line to trip off, leading to the formation of several small grid islands that were completely separated from the Western Interconnection (WI). These islands had insufficient generation and rapidly spun down. Load shedding was implemented throughout the system, but some generation was still lost. The outage caused significant financial losses to restaurants and grocery stores, which had to discard large quantities of spoiled food. Perishable food losses were estimated at $12 million to $18 million.[3] (Indirect impacts to regional hydroelectric generation)

2.2.2 Human—Intentional

One of the principal types of high-impact, low-probability events the BES faces is a concerted, well-planned cyber, physical, or blended attack conducted by an active adversary against multiple points on the system. Such an attack, although never experienced in North America, could damage or destroy key system components, significantly degrade system operating conditions, and in extreme cases result in prolonged outages to large parts of the system. The attacks are targeted at the physical systems, measuring and communication systems, and control systems. Examples of physical systems that can be attacked are generators, substation, transmission lines, switches, relays, transformers, and distributed energy resources. Among measuring and communication systems, smart meters, corporate networks, and supervisory

---

[1] U.S.-Canada Power System Outage Task Force. 2004. *Final Report on the August 14, 2003, Blackout in the United States and Canada: Causes and Recommendations.* https://www.energy.gov/sites/prod/files/oeprod/DocumentsandMedia/BlackoutFinal-Web.pdf.
[2] Vassell GS. 1991. "Northeast Blackout of 1965." *IEEE Power Engineering Review*, vol. 11, no. 1.
[3] FERC/NERC. 2012. *Arizona-Southern California Outages on September 8, 2011*. Washington D.C. https://www.nerc.com/pa/rrm/ea/September%202011%20Southwest%20Blackout%20Event%20Document%20L/AZOutage_Report_01MAY12.pdf.

control and data acquisition (SCADA) are vulnerable to be attacked. As for the control systems, control room computers and power plant distributed controllers can be the common targets.

2.2.2.1 Cyberattack

As the U.S. power system has evolved into an industrial control system-enabled industry that increasingly relies on intelligent electronic devices using bidirectional communication to execute operations, new cybersecurity concerns have arisen. As a modern system, the power grid can be regarded as a composition of physical, measurement and communication, and control systems. Cyberattack can have different forms. In a distributed denial-of-service attack, attackers flood network resources to render physical systems unavailable or less than fully responsive for a period of time. Rogue unauthorized devices can be replaced to access the system, manipulating it or providing incorrect data to system operators. Reconnaissance attacks are where attackers probe a system to gather information on capabilities, vulnerabilities, and operation. Eavesdropping attacks can break the confidentiality of communication within a network. Unauthorized access attacks are an adversary exercising a degree of control over the system and accessing and manipulating assets without authorization. An authorized user can use assets, resources, or information in an unauthorized manner,[1] which can result in system operators getting inaccurate information from a "trusted" source and being misled into making decisions that impact the system. Cyber-attackers can inject malicious code or malware such as viruses, worms, and Trojan horses, to interrupt the normal functions of control software.

Generation-control loops primarily include an automatic voltage regulator, governor control, and automatic generator control (AGC). The modern digital automatic voltage regulator and governor-control modules use Modbus protocol to communicate with computers in the control center via Ethernet. The regulator and governor control are local control loops. They do not depend on SCADA telemetry infrastructure for their operations, so the attack surface for these control loops is limited. However, these applications are still vulnerable to malware that could enter the substation local area network through other entry points such as Universal Serial Bus keys. In addition, the digital control modules in both control schemes possess communication links to the plant control center. Once this intrusion is achieved, an adversary can disrupt normal operation by corrupting the logic or settings in the digital control boards.[2] On the other hand, the AGC relies on tie-line and frequency measurements provided by the SCADA telemetry system. An attack on the AGC could have direct impacts on system frequency, stability, and economic operation. Denial-of-service type attacks might not have a significant impact on AGC operation unless supplemented with another attack that requires AGC operation.[3]

The major transmission components that are vulnerable to cyberattacks include state estimation, flexible alternate current transmission systems, high-voltage DC systems, renewable generators, and wide-area network monitoring and control systems. The major threat to the state estimation function is false-data-injection attacks that escape detection by using existing bad measurement identification algorithms, provided they had knowledge of the system configuration. Upon attack, the system will lose observability and maintaining normal operation will become difficult. The attacks involving inverter-interfaced devices include denial-of-cooperative operation, desynchronization, and data-injection attacks. The performance of compromised inverter-interfaced devices will degrade, leading to inadequate active and reactive power support; they could even destabilize the grid by injecting power in a coordinated adversary fashion.

---

[1] Weiss J. 2009. *Control System Cyber Vulnerabilities and Potential Mitigation of Risk for Utilities*. Juniper Networks, Inc. Sunnyvale, California.
[2] Sridhar S, A Hahn, and M Govindarasu. 2011. "Cyber–physical system security for the electric power grid." *Proceedings of the IEEE 100*, no. 1: 210-224.
[3] Lee RM. 2016. "ICS Cross-Industry Learning: Cyber-Attacks on Electric Transmission and Distribution (Part One)" *SANS ICS Security Blog*. www.ics.sans.org/blog.

Cyberattacks on phasor measurement units (PMUs) could affect applications using wide-area measurements such as wide-area-network-based damping control and protection systems.

In distribution systems, protection systems, advanced metering infrastructures, and demand-side management are imposed to counter cyberthreats. Modern relays are Internet Protocol ready and support communication protocols such as the International Electrotechnical Commission's Standard 61850. An attack on relay communication infrastructure or a malicious change to control logic could result in unscheduled tripping of distribution feeders, leaving load segments unserved. Control over whether the meter is enabled or disabled and the ability to remotely disable devices through load-control switching provide potential vulnerabilities to attackers. A malicious meter-disabling command can likely be prevented through the use of time-wait periods.

- In a recent, well-publicized cyberattack, approximately 225,000 people were left without power for approximately 6 hours on December 23, 2015, in Ukraine. Attackers gained access to internal networks of three utilities through spear-phishing schemes, malware, and manipulation of long-known Microsoft Office macro vulnerabilities. Rather than try to engineer breaches through the firewall, the attackers patiently harvested the credentials needed to gain access to the SCADA system and learned how to operate the software. These actions prevented operators from accessing the SCADA system, left control centers without power, and rendered cyber monitoring and control systems inoperable. Service was restored by shutting off the SCADA system and resorting to manual operation. Although power was restored relatively quickly, control centers were not fully operational for months after the attack. (Indirect impacts to regional hydroelectric generation)

2.2.2.2 Physical Attack

In a physical attack, the attacker targets the physical components and devices in a power network. Unlike the cyberattack cases, where many detection algorithms have been developed and deployed, a physical attack could occur with limited warning. Since the physical power system spreads over a wide area, the forms of physical threats are numerous and less predictable compared with a cyberattack. A few critical scenarios are illustrated. Threat actors armed with explosive devices have the potential to physically damage or destroy substations, transmission lines, distribution lines, control centers, or generation components. An individual can drive a vehicle rigged with explosives through a substation, distribution poles, or a generation facility fence. The attacker can commit sabotage of equipment using standoff weapons, long-range rifles, or shoulder-launched weapons. Hijacking a control center and forcing individuals to cause damage or disruption to the system at gunpoint can also happen.

Globally, transmission and distribution systems have been a focus of physical attacks, bombings, and terrorist activity—for example in Afghanistan, Colombia, Iraq, Peru, and Thailand. In the United States, there have been relatively few well-planned attacks on the electricity system. Recovery could easily require many days or weeks. Generation facilities tend to have greater physical security and thus are less vulnerable to physical attack than substations and transmission facilities.

- In April 2013, the Pacific Gas & Electric (PG&E) Company-owned Metcalf Transmission Substation outside of San Jose, California, was attacked by one or more gunmen. When the first law enforcement officers arrived, 17 transformers had been seriously damaged as oil leaked from bullet holes, allowing electric components to overheat. No major outages occurred because operators were able to reconfigure the system and engage nearby generators to provide necessary power, but the attack caused more than $15 million in damage.[1]

2.2.2.3 Man-made Electromagnetic Pulse

Two important reports by the Congressional Electromagnetic Pulse Commission were published, one in 2004[2] and the other in 2008.[3] Both clearly indicate that U.S. infrastructure is vulnerable to a single high-altitude nuclear burst. A man-made electromagnetic pulse is one that originates from a nuclear detonation or a directed-energy weapon. Energy fields resulting from a nuclear detonation at altitudes above 25 miles are referred to as high-altitude electromagnetic pulse, denoted as the E1 environment. Following the E1 environment, a more slowly varying and less intense electromagnetic field is observed on the ground, denoted as the intermediate-time E2 environment. E1 and E2 waveform components are followed by E3, a low-amplitude, late-time signal on the order of tens of volts per kilometer. The early-time E1 effects appear as flashovers and voltage-stress damage to power delivery equipment and to communications electronics. E2 effects fall within the normal criteria for frequently occurring natural incidents (e.g., lightning) and expected man-made incidents, such as switching transients. An exception would be the case in which the E1 pulse has destroyed some surge protection devices, thus making systems more vulnerable to E2 as well. As stated previously, E3 manifests on long power lines as a quasi-DC that flows through transformers and shunt reactors.[1]

2.3 Multi-Timescale Grid Responses and Services

To maintain normal power system operation and make the BES robust against faults and extreme events, the Federal Energy Regulatory Commission (FERC) has defined six types of resources and/or capabilities, designated as ancillary services, that are "necessary to support the transmission of electric power from seller to purchaser given the obligations of control areas and transmitting utilities within those control areas to maintain reliable operations of the interconnected transmission system."[4] FERC defines the following ancillary services:

- Scheduling, system control, and dispatch service
- Reactive supply and voltage control from generation sources service
- Regulation and frequency response service
- Energy imbalance service
- Operating reserve—spinning reserve service
- Operating reserve—supplemental reserve service.

[1] Smith R. 2014. "Assault on California Power Station Raises Alarm on Potential for Terrorism." Wall Street Journal, New York, New York. https://www.wsj.com/articles/assault-on-california-power-station-raises-alarm-on-potential-for-terrorism-1391570879.
[2] EMP Commission. 2004. *Report of the Commission to Assess the Threat to the United States from Electromagnetic Pulse (EMP) Attack*, Vol. I: Executive Report. http://www.empcommission.org.
[3] House of Representatives Committee on Armed Services. 2008. *Report of the Commission to Assess the Threat to the United States from Electromagnetic Pulse (EMP) Attack: Critical National Infrastructures*. Washington D.C.
[4] FERC. 2016. *Guide to Market Oversight—Glossary* web page. http://www.ferc.gov/market-oversight/guide/glossary.asp

These ancillary services are necessary to maintain acceptable operation of the BES. Another service contributing to resilience is black start capability, which addresses the BES's ability to recover from a severe event. Black start is the process of restarting operation of a power plant from a completely unenergized operating state to power up other generating plants and reenergize loads, thus restoring power to the electric grid. Planning for extreme events requires evaluation and improvement of the power system's resilience. A resilient system—one that can withstand and recover from extreme events–requires flexible operating capability and redundant assets sufficient to counter infrequent but feasible threats and contingencies. FERC-defined ancillary services (to resist and respond resiliently) and black start capability (to recover in a timely manner) are hallmarks of a resilient power system. Hydropower has historically been a major provider of all these services.

These six services aim to maintain system-wide and local balance of power generation and consumption on timescales ranging from sub-seconds to hours. A common aspect of these services is that they constitute flexibility of the power system and its assets, particularly generators, to adapt power production (real and reactive) to changes in demand or in the amount of system capacity or energy that is available to serve demand. This flexibility in power production needed during extreme events can be provided by different grid responses at different timescales as shown in Table 4. These range from exciter response (up to 1/3 second) to inertial response (1/3 to 10 seconds) to governor control or primary frequency response (2 to 20 seconds) to AGC changes in generator fuel input for conversion to electricity (8 seconds to 15 minutes) to operator-adjusted generator dispatch and steady-state output (5 to 30 minutes) to rescheduling the system generation depending on resource adequacy for different types of generation (hours to weeks or longer as unit commitment is re-optimized).

Table 4. Timescales, energy sources, and drivers to support grid responses during extreme events.

Time	Energy Source	Drivers
Immediate to 1/3 sec.	Magnetic field inside generator	• Electrical distance to lost generator • Strength/speed of excitation system
1/3 to ~10 sec.	Rotational energy in rotating machines (inertia)	• Equipment mass (~2,000 tons for steam or hydro) and rotational speed
~2 to ~20 sec.	Frequency-responsive generators (governor control) and loads: primary frequency response	• Droop settings • Headroom • Generator capacity • Amount of synchronous motor load
~8 sec. to ~15 min.	AGC-responsive generators	• Economic dispatch settings • Ramp rate
~5 to 30 min.	System operator dispatch of generators	• Ramp rate • Generator capacity
Hours to weeks	System schedulers and operators	• Plant capacity • Adequate resource • Environmental constraints

Section 3 associates the specific capabilities of hydroelectric power to the temporal stages of resilience and the characteristics of a resilient system. As detailed in Section 3.1, by providing grid services such as inertia, governor response, energy storage, and power dispatch (real and reactive) flexibility, hydroelectricity can provide substantial support to the resilience posture of the electric grid. With an accumulative set of BES assets, operational flexibility, and energy reserves, hydroelectricity is demonstrably a key contributor to the response to major and catastrophic events such as those described in Sections 2.1 and 2.2. Sections 3.2 and 3.3 presents detailed case studies analyzing hydropower's contribution to BES resilience for specific severe weather events where hydropower is needed to provide long-term response.

2.4 Selection of Representative Events

In terms of the responses required to maintain a resilient grid, the extreme events, detailed in this section, can be grouped into different categories (this is shown in Table 5). Each event type can then be mapped to a particular mode of operations for hydropower to help stabilize and restore system operations. In some cases, one event can lead to impacts associated with multiple event types. For instance, a localized generation outage (Event Type 1) can sometimes result in cascading outages throughout the grid (Event Type 2), requiring different types of responses from the available generation resources to help restore operations. The interaction graph in Appendix D, can be used to map the impact(s) that an event can cause.

While this is certainly a simplified perspective on resilience, and certainly not a standardized taxonomy, it allows for the selection of a few, representative grid conditions (scenarios) that can be simulated and analyzed. This is done in Section 3, where Scenario 1 is represented by the largest, credible contingency in the WI (Event Type 1), Scenario 2 is represented by cascading failure of a significant portion of natural gas generation (Event Type 2), and Scenario 3 and 4 are represented by a cold and heat (respectively) wave that cause extremely high net-load (Event Type 3). The scenarios for this study were designed primarily for the WI because hydropower is a much larger fraction of the total generation capacity (>50% of all U.S. hydropower exists in the WI). The tools and methodologies, however, can be applied to other regions too, contingent on availability of data and models.

Table 5. Categories of Extreme Events.

Event Type 1: **Sudden, localized loss of generation**	**Event Type 2:** **Widespread Outages of Natural Gas Plants**	**Event Type 3:** **Sustained, gradual change to net load or supply**
Wind events, hurricanes, tornadoes, thunderstorms	Winter storms, ice storms, freezing rain, extreme cold, polar vortex	Drought
Inland and coastal flooding, tsunami	Wildfires	Extreme heat and heatwaves
Earthquakes, landslides	Wildlife and vegetation	Wildfires
Volcanic activity	Software/computer errors	Cyberattack
Sea-level rise	Cyberattack	Winter storms, ice storms, freezing rain, extreme cold, polar vortex
Geomagnetic disturbances	Physical attack	Pandemics
Software/computer errors	Wind events, hurricanes, tornadoes, thunderstorms	
Operations errors	Earthquakes, landslides	
Cyberattack		
Physical attack		
Man-made electromagnetic pulse		

There are many types of extreme events that cause disturbances, and each impose different conditions on the grid. Depending on the severity, type, and frequency, these events require different mitigation services to prevent loss of load. Sections 2.1 and 2.2 provide a taxonomy of these extreme events, describing both the theoretical and historical effects of each event type. Section 2.3 then describes the types of ancillary services that are required to mitigate the effects of extreme events. Finally, Section 2.4 presents a high-level classification of the events in the taxonomy, which is then used to select representative events for simulating hydropower's contributions to grid resilience.

3.0 Hydropower's Contributions to Grid Resilience

Extreme grid events have multifaceted negative impacts from security to social welfare. The stages during an extreme event (mapped to the DIRE curve)— preparedness (reconnaissance), responses (resistance and response), recovery, and restoration—require the grid to have several essential capabilities, such as high flexibility, fast ramping rate, and black start. This section describes the role of hydropower in all stages from both positive and negative perspectives.

Hydropower is a cost-competitive and low-carbon energy source that provides the full range of services required by the BES under normal and fault conditions (in other words, *N-k* contingencies) as well as critical supports during extreme grid events. Although the role of hydropower under catastrophic scenarios is the central scope of this report, a brief introduction on its capability for full ranges of ancillary grid services would be beneficial because many of these services will also be required under extreme conditions.

All types of grid services are provided by hydropower in varying degrees across the United States.[1] The timescales at which hydropower can provide grid services range from sub-seconds, as in the case of frequency regulation, to days for services such as scheduling. In addition, adjustable speed PSH or advanced PSH with multiple configurations (e.g., binary, ternary, and quaternary sets) could provide more flexible dynamic support because it employs a doubly fed induction machine configuration.[2] The U.S. hydropower fleet contributes to grid resilience through significant ramping capabilities and the provision of a host of grid services, including frequency regulation, operation reserves, and black start.[3] The extreme condition of a power network can be categorized into totally de-energized and fully/partially energized, where hydropower plays different and essential roles. The following sections discuss in detail the framework to assess hydropower's contribution towards grid resilience (Section 3.1) and assess hydropower's ability to provide support during events where sudden loss of large generation occurs (Section 3.2) and during extreme weather events not resulting in sudden loss of large generation (Section 3.3).

3.1 Framework to Assess Hydropower Contribution to Grid Resilience

Preparing the power system with a robust state that can withstand extreme weather, which is denoted as preventive scheduling, can significantly reduce the negative impacts of natural disasters as well as cost and duration of system restoration. Such a state should contain considerable flexibility to generate and absorb power energy to eliminate imbalance due to outages of large thermal units and load zones and to reroute power flow to mitigate congestion due to transmission line tripping. Hydropower can largely contribute to such a flexibility requirement as it can rapidly ramp generation up and down in response to power imbalance. In an update to the Energy Information Administration's Form 860, more than 80% of reporting hydropower capacity (inclusive of PSH) is listed as capable of ramping from cold shutdown to full power within 10 minutes.

---

[1] Muller N Z, R Mendelsohn, and W Nordhaus. 2011. "Environmental Accounting for Pollution in the United States Economy." *American Economic Review*. (101:5). 1649–1675. DOI: 10.1257/aer.101.5.1649. https://www.aeaweb.org/ articles?id=10.1257/aer.101.5.1649.

[2] Koritarov V, TD Veselka, J Gasper, BM Bethke, A Botterud, J Wang, M Mahalik, Z Zhou, and C Milostan. 2014. *Modeling and Analysis of Value of Advanced PSH in the United States*. ANL/DIS-14/7. Argonne National Laboratory, Argonne, Illinois.

[3] Uria-Martinez R, M Johnson, P O'Connor, NM Samu, AM Witt, H Battey, T Welch, M Bonnet, and S Wagoner. 2018. *2017 Hydropower market report*. Oak Ridge National Laboratory, Oak Ridge, Tennessee. https://www.osti.gov/servlets/purl/1513459.

Figure 2 describes the hydropower resilience assessment framework, which identifies the general factors that influence the application of hydropower to major events. Influences on hydropower's ability are shown as policy constraints on water availability and designated uses that connect to flow into the hydro system. The framework identifies contributions of hydropower asset in different epochs of the DIRE curve. Numerous factors considered in this framework for assessing hydropower's contribution to resilience are adaptive capacity, storage flexibility, plant-level constraints, and regulatory policies for different types of resources. The framework also considers the health of the power delivery network as an important factor in the usefulness of any asset's contribution to overall grid resilience; whereas, the plant's location and network architecture are connected with the efficacy of real and reactive power capabilities under this framework.

Storage constraints are dependent on the type of hydroelectric facility and determine the long-term flexibility available from these resources. For example, each of the three types of hydro facilities—PSH, run of the river (ROR), hydropower with reservoir (HWR)—have different storage constraints, with ROR having no appreciable storage flexibility. The limitations based on the plant design, predicated by the available water resource, then determine the temporal flexibility or the adaptive capacity of a given resource. Adaptive capacity is the primary response characteristics in terms of real and reactive power available at the time of a disturbance. PSH and HWR both have energy constraints determined by the state of storage that provide a temporal limit to flexibility, whereas ROR is constrained by the flow into the system. The availability and integrity of the network determines its ability to deliver the resource to the needed location. Each resource's deliverable-response capability will be determined by how the transmission and/or distribution systems, connecting generation to load, have been affected by an event. A summary of these types of capabilities towards overall grid resilience is detailed in Table 6

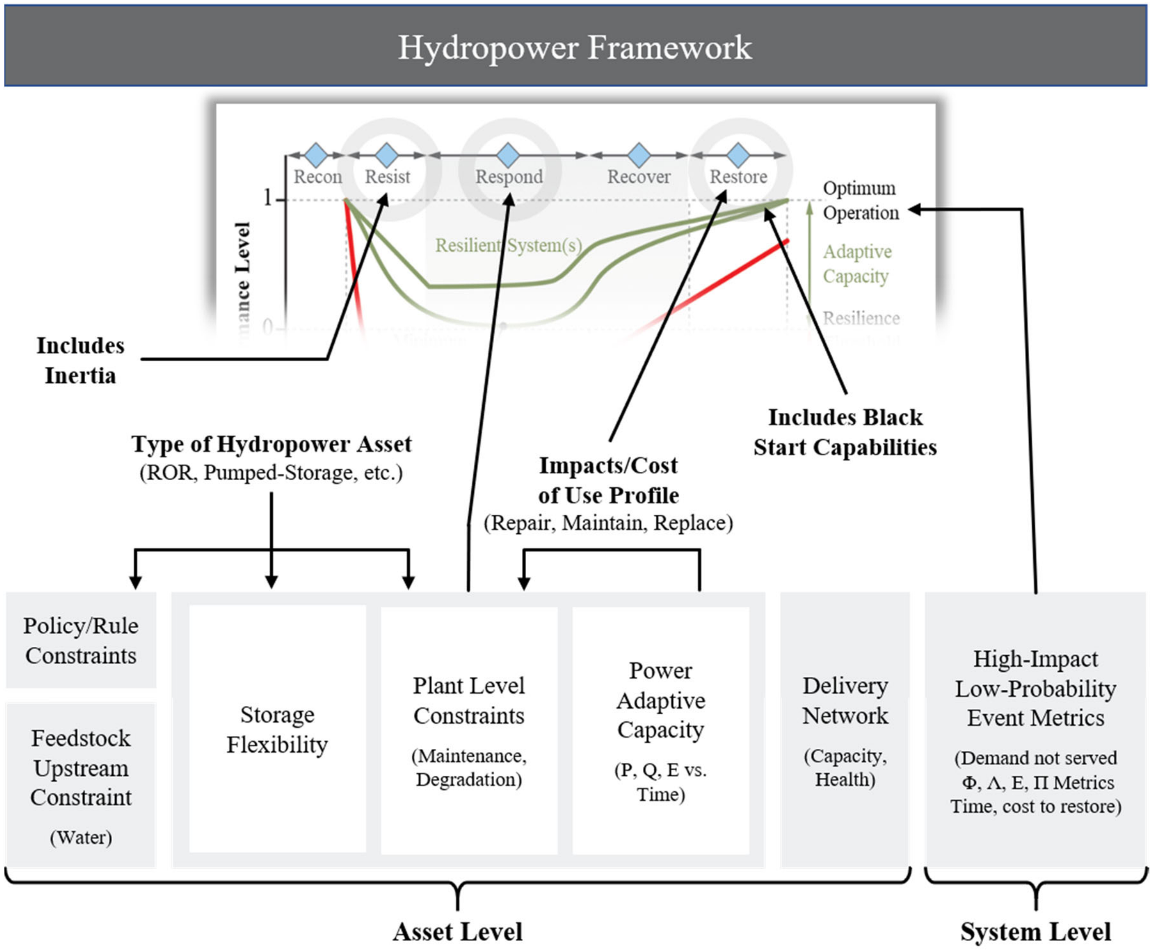

Figure 2. Mapping hydropower resilience assessment framework characteristics like policy, water, flexibility, and storage constraints along with plant- and system-level capabilities to different epochs of the DIRE curve.[1] The system-level metric examples used are demand not served,[2] the "FLEP" resilience metric system (Φ, Λ, E, Π), where Φ is how fast and Λ is how low the resilience level drops, E is for how extensive the post-event degraded state, and Π is how promptly the network recovers to its pre-event resilient state[3] and the time and cost to restore the system.[4]

---

[1] Phillips T, V Chalishazar, T McJunkin, M Maharjan, SM Shafiul Alam, T Mosier, A Somani. 2020. "A Metric Framework for Evaluating the Resilience Contribution of Hydropower to the Grid." *2020 Resilience Week*, Salt Lake City, Utah, pp. 78-85, DOI: 10.1109/RWS50334.2020.9241249.

[2] Johnson B, V Chalishazar, E Cotilla-Sanchez, and TK Brekken. 2020. "A monte carlo methodology for earthquake impact analysis on the electrical grid." *Electric Power Systems Research*, vol. 184, p. 106332.

[3] Panteli M, P Mancarella, D Trakas, E Kyriakides, and N Hatziargyriou. 2017. "Metrics and quantification of operational and infrastructure resilience in power systems," *IEEE Transactions on Power Systems*, vol. 32, no. 6, pp. 4732–4742.

[4] Chalishazar V. 2019. *Evaluating the seismic risk and resilience of an electrical power system*. PhD Dissertation, Oregon State University, Corvallis, Oregon.

Table 6. Summary of resilience capabilities of the three types of hydropower during the phases of resilience.

Resilience Phase	ROR	HWR	PSH
Recon	Power and spill setting	Storage and power setting	Storage and power setting
Resist	Inertia	Inertia	Inertia depends on type
Respond	Real and reactive power, spinning reserve, with energy constraints	Real and reactive power, spinning and non-spinning reserve, with energy constraints	Real and reactive power, dependent on current direction, with energy constraints
Recover	N/A	Dispatch + response	Dispatch + response
Restore	Black start and sustained generation	Black start and sustained generation	Black start and sustained generation

The recon phase requires decisions about operating point not only for all generating units, but also for how much storage would be optimal. The state of the system is obviously dependent on prior use. The planning for optimal use of the resource would necessarily require factoring in a desired adaptive capacity for response to unpredicted events. ROR and HWR have inertia as a property to slow frequency change, where PSH depends on the technology applied to the system. All types are capable of providing a response in real and reactive power, with HWR and PSH requiring consideration of energy constraints. The ability to store energy and the need to restore depleted energy reserves put HWR and PSH in position to provide or possibly need resources to set the system back to a pre-event state to be in position for a subsequent event. All hydropower resources can provide black start and sustained generation. Of course, the ability to deliver restoration is dependent on the condition of the connective network.

This framework and the phases of resilience tie directly Section 3.2, hydropower responses to events where sudden loss of large generation occurs lasting minutes to hours, and Section 3.3, hydropower responses to extreme weather events not resulting in sudden loss of large generation, lasting hours to days. The two types of events require different responses, and hence different methodologies to quantify hydropower's contributions. Additionally, the framework captures the need for the connected network and potential maintenance and repair due to the event that is covered in subsections on direct impacts to hydropower assets and the limitations of hydropower in supporting the grid.

3.2 Responses to Events Leading to Sudden Loss of Large Generation

During an extreme event, it is likely that multiple generating units would be tripped. Under such a circumstance, inertial and primary frequency response are critical to limit the rate of change of frequency and the range of frequency deviation within permissible ranges. The underlying physical process of the inertial responses is that kinetic energy stored in the rotating mass of synchronous generators is released and converted into electric energy due to the electromagnetic coupling between synchronous generators and the electric grid. In turn, the energy conversion leads to the decline of generator rotational speed and consequently system frequency. If the converted electric energy is not adequate to eliminate the power imbalance, the rate of change of frequency (RoCoF) will not be arrested and primary frequency response controls will be activated. The primary frequency control measures frequency deviation and sends a proportional signal to the turbine to increase mechanical-power input and finally arrest the frequency. Frequency response (in some literature it is called primary frequency response) from generation resources, through inertial and governor responses, is needed to arrest the drop in frequency after a major event, such as loss of a large generator. Secondary frequency response comes to play when generators in AGC respond to change in area control error, estimated as a function of change in interchange flow and frequency, to make sure the area interchange flows are set to nominal values. At a later stage, system operators manually or economically dispatch generation at an optimal setting. Figure 3 presents a stylized example of frequency drop after the loss of a large generator, followed by periods of recovery through inertial, primary, secondary, and tertiary frequency response provided by various system resources.

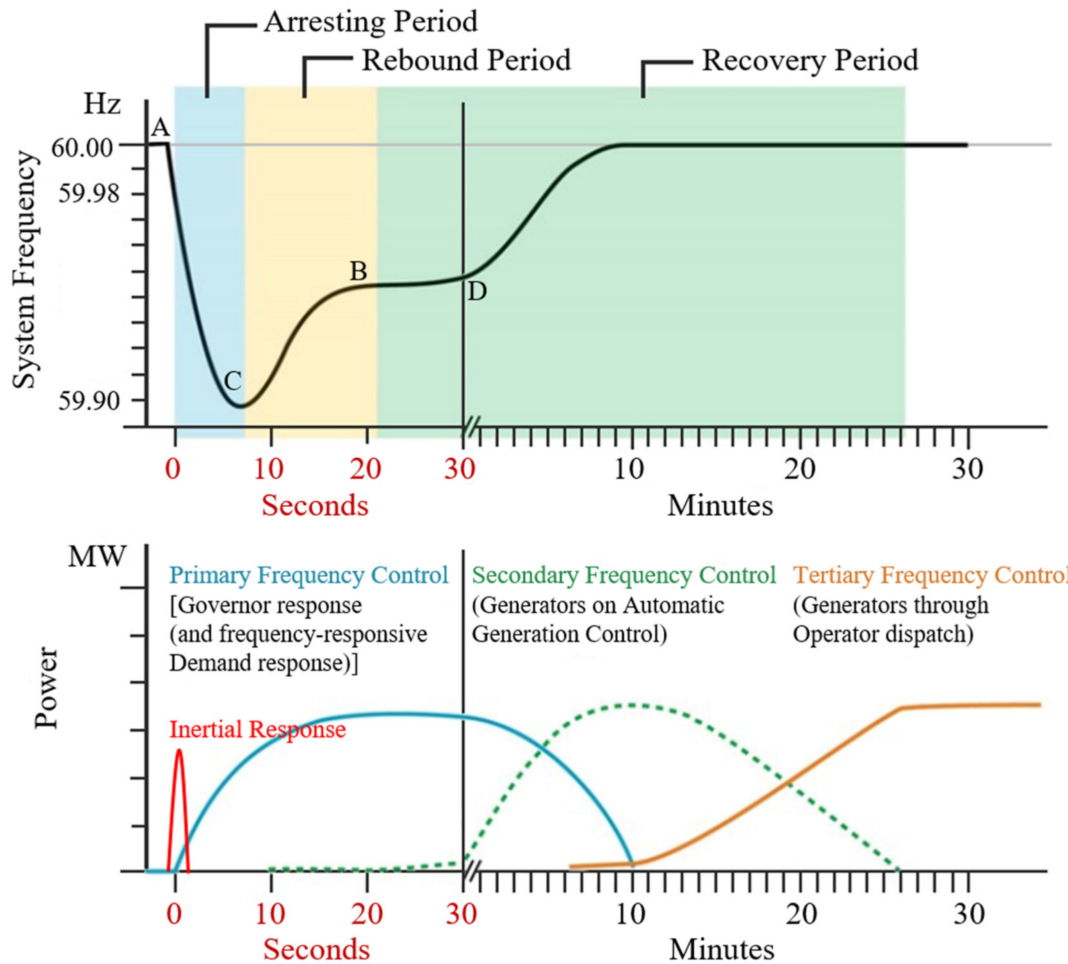

Figure 3. Frequency response characteristics.[1]

Hydropower is one major source of power system inertia and a key provider of primary frequency response, supplying a majority of primary response in the WI.[2] In the Nordic grid, especially in Norway and Sweden, hydropower penetration is high and the frequency control is mainly carried out by hydropower plants, which can be regulated faster with less loss of efficiency when compared to thermal generating units.[3]

[1] Eto JH, J Undrill, C Roberts, P Mackin, and J Ellis. 2018. *Frequency Control Requirements for Reliable Interconnection Frequency Response*. LBNL-2001103. Lawrence Berkeley National Laboratory. Berkeley, California.

[2] Aswani D, R Clarke-Johnson, and G Runyan. 2011. *The Impact of Hydroelectric Power and Other Forms of Generation on Grid Frequency Stability for the WECC Region*. American Governor Company, Warminster, Pennsylvania. https://www.americangovernor.com/wp-content/uploads/2013/04/Impact-of-Hydropower-on-Grid-StabilityHV2011.pdf.

[3] Saarinen L. 2014. *A hydropower perspective on flexibility demand and grid frequency control.* Doctoral dissertation, Uppsala universitet, Sweden.

3.2.1 Frequency Response from Hydropower and Other Conventional Resources

3.2.1.1 Inertial Response

Inertial capacity of the conventional generator turbine set is measured by the inertia constant *H*. The inertia constant *H* [MWs/MVA] is defined as the kinetic energy in the rotational masses at the rated speed per-unit VAR of the generator turbine set and expressed as

$$H = \frac{1}{2}\frac{J\omega_{0m}^2}{\mathrm{VA}_{base}}$$

where *J* [kgm^2] is the moment of inertia and ω_{0m} is the rated angular velocity in mechanical radians per second. Hence, the inertia of a generator turbine set depends on both the total mass (reflected by *J*) and the mechanical rotational speed. Hydro turbines and generators are heavier than steam and gas-based turbines, but they rotate at a much slower rate. Table 7 gives normal range within which the inertia constant lies for thermal and hydro generating units.

Table 7. Range of inertia constant H for thermal and hydro generating units.[1]

Type of generating unit	H [MWs/MVA]
Thermal unit	
3600 r/min (2 poles)	2.5–6
1800 r/min (4 poles)	4–10
Hydro unit	2–4

H of a typical hydro unit, when normalized per-unit rating, is generally smaller than that of a thermal unit. However, the total online inertia and energy stored in rotational masses depends on the number and sizes of generator units that are online at a given time. Hence, to compare the inertial response capabilities of hydro and thermal turbine generator sets, the total stored energies in the rotational masses are compared.

Stored energy in the rotational masses of generators can be estimated as

$$Stored\ energy\ in\ rotational\ masses\ (MJ) = \sum_{i=1}^{\#\ of\ units} MVA_i \times Inertia\ Constant\ H_i\ (s)$$

Figure 4 summarizes a total amount of energy that is stored in rotational masses at rated frequency, providing that all units in the plant are dispatched. For large hydroplants with multiple units, the total stored energy in the rotational masses can be higher than large nuclear/thermal facilities.

[1] Kundur P. 1994. *Power System Stability and Control*. McGraw-Hill, New York, New York.

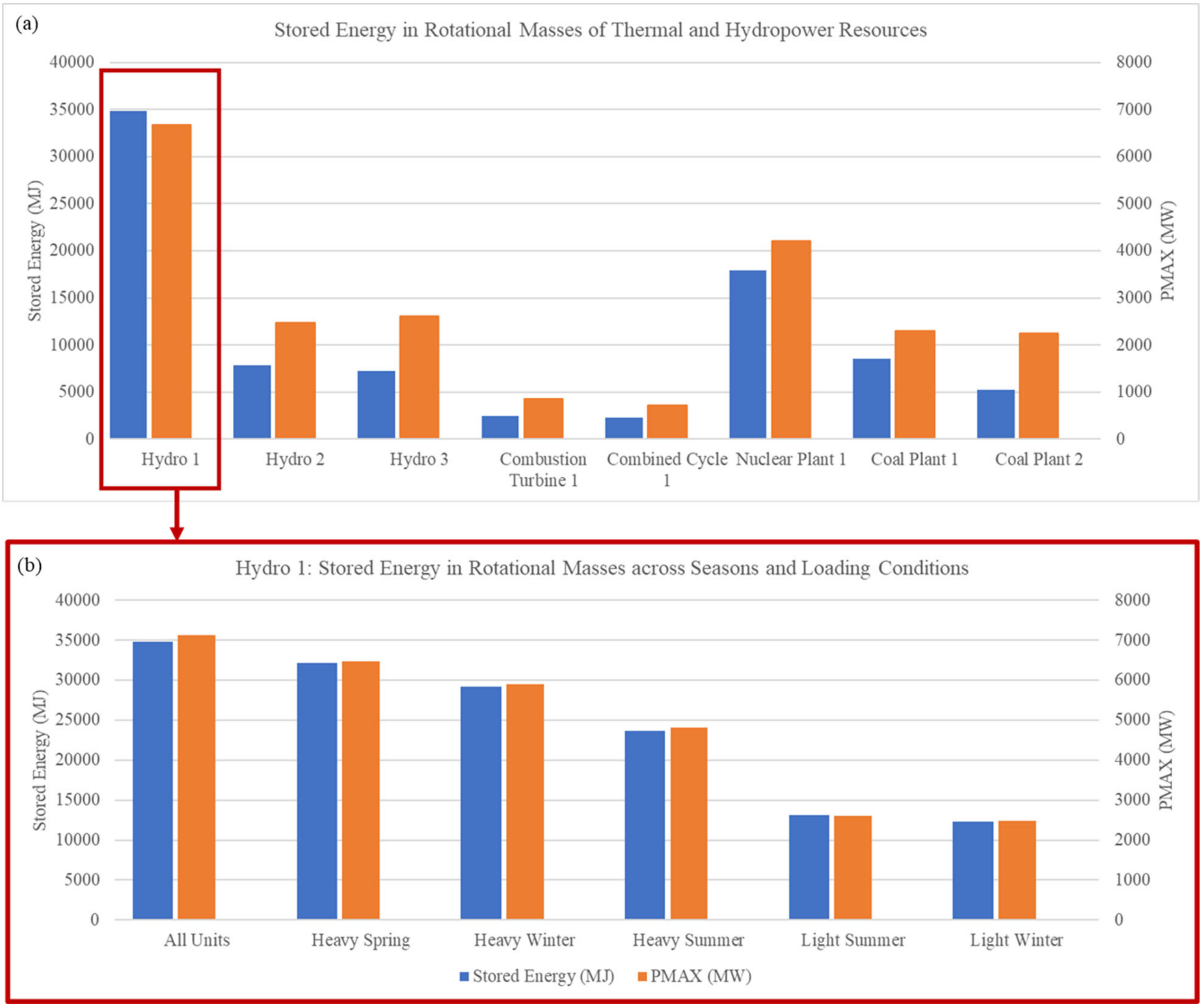

Figure 4. (Top) Stored energy in rotational masses of thermal and hydropower resources in the WI. (Bottom) Hydro 1 hydropower resources available energy from inertia across seasons and loading conditions.

However, especially for hydropower resources, not all units are committed across various seasons and loading conditions. Figure 4 (bottom) shows how much energy is stored in rotational masses of a single large hydro project at rated frequency. The amount of stored energy is significantly lower in light load conditions when multiple units are offline and varies based on water availability across seasons. The coal plants on the other hand are usually run as baseload generators and their equivalent inertia remains consistent across seasons and loading scenarios.

3.2.1.2 Governor Response

The primary frequency response or governor response is the ability of the turbine generator set to measure change in frequency and in the mechanical-power output of the turbine generator set. The accurate modeling of the various governors in power system studies is essential to understand the response of various resource types following a large loss of generation.[1] Fossil fuel plants typically burn coal/crude oil and nuclear plants use nuclear energy to heat a boiler that produces high-temperature, high-pressure steam that is passed through the turbine to produce mechanical energy. The operation of steam turbines is challenging as main steam temperature and pressure need to be maintained and governor response is provided by opening the main steam control valves. The process involves significant time delay resulting in the governor action being slower. Gas turbines, on the other hand, can provide fast governor response and are considered an important resource to provide flexible generation and ramping capability. However, gas turbines are dependent on ambient temperature and their efficiency is affected by the temperature of the compressed air intake required to generate power.

For hydro turbines, the governor action results in changing the wicket gate position to change the flow of water, and consequently the real-power output of the generator. Because hydroplant dynamics are non-minimum phase, power output will drop before rising when power is commanded to increase and vice versa. Because of this, hydro governor response is rate limited to improve system stability. There may not be a large initial delay due to water time constant, but the hydro governor response is overall slow to arrest frequency drops. Hydro generators are temperature independent devices, making the efficiency of primary frequency response only affected by water availability.

3.2.2 Hydropower's Contribution to Frequency Support for Past Events

Several historical events from 2018 were analyzed to quantify the percentage contribution of hydropower resources toward frequency response, using available PMU data. The study team had access to limited data, which included PMU data for certain resources in the Pacific Northwest, as well as the flow in the COI interface. Based on available data, the contribution of hydro governor toward frequency response was estimated as follows:

$$Northwest\ hydropower\ contribution\ = \frac{Change\ in\ flow\ (MW)\ on\ COI}{Generator\ outage\ MW} \times Online\ Northwest\ hydro$$

To estimate the total hydropower capacity in the northwest that could contribute toward frequency response, the 2018 WECC planning base case was used to establish the set of online generation (only hydropower generators with "base load" flag, i.e., frequency response enabled were selected).

<u>Event 1 – Generation outage in the Southwest:</u> Figure 5 shows the frequency response and interface flow change following a generator trip, carrying 1,340 MW, in the Southwest. Immediately following the event, the COI line flow increased by 600 MW indicating at least 600 MW of governor response from generators in the Pacific Northwest. Hence, it can be concluded that at least 600/1340 × 88% = 39% of the governor response was supplied by generators in the Pacific Northwest, which came predominantly from hydropower (online hydropower resource in the Northwest was approximately 88%, and large thermal plants typically have their governors blocked). Figure 6 shows response of various resource types following the event and it is quite evident that hydropower is the only resource providing the governor response, while co-gen and nuclear plants only provide inertial response.

Note: After governor response, the system enters a new steady state (Point B on the frequency graph) at a lower frequency. Speed governors respond to frequency deviation based on their droop setting and arrest the frequency drop. Governors reach equilibrium after the frequency drop is arrested, and hence, the system frequency does not recover back to the precontingency level. As the total system load at the time

[1] IEEE Power System Dynamic Performance Committee. 2013. *Dynamic Models for Turbine-Governors in Power System Studies*. IEEE Power System Stability Subcommittee, IEEE PES Task Force on Turbine-Governor Modeling. Piscataway, New Jersey.

of the event is unknown, accurate estimation of the change in the load at the new steady state at Point B is not possible. However, knowing that the system loading decreased because load decreases with frequency (typically 1% change in frequency leads to 1–2% change in load), we know that the contribution of hydro would have been even higher.

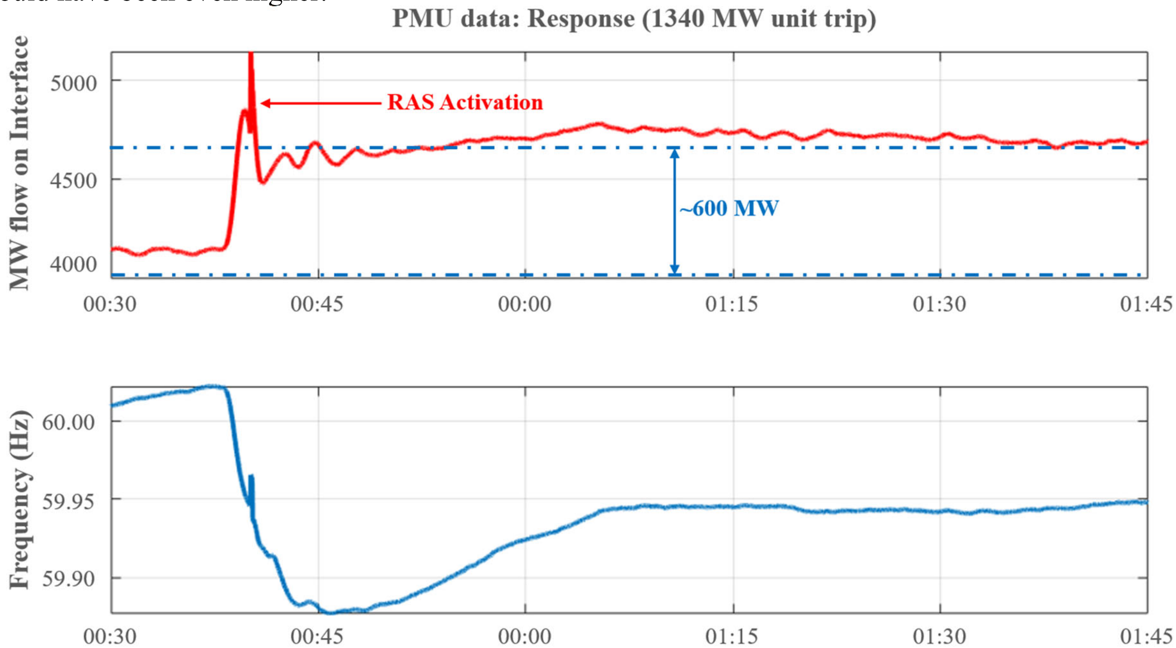

Figure 5. COI power flow and system frequency response for Event 1

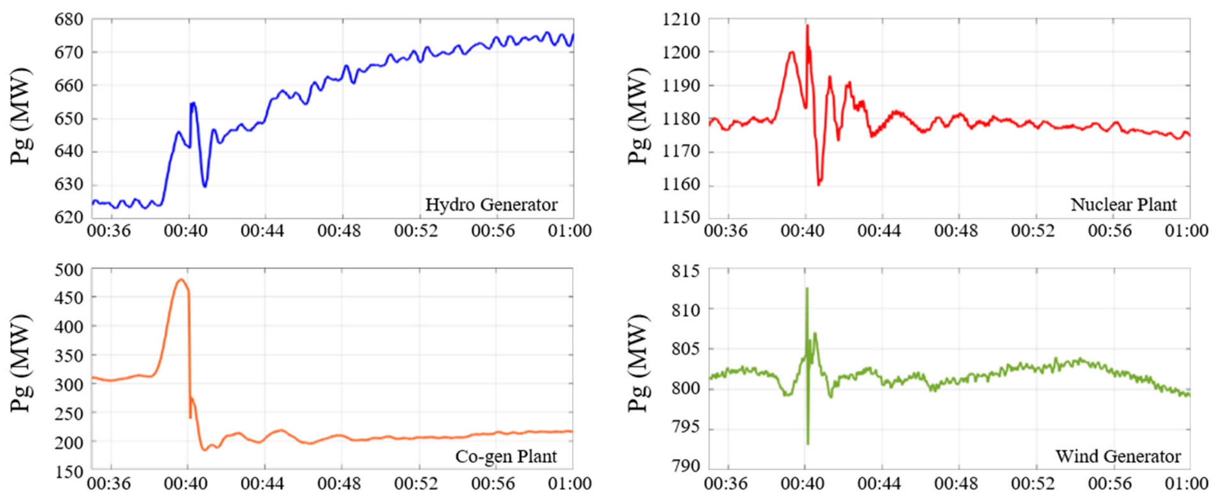

Figure 6. Response at individual facilities of various generation types following Event 1.

<u>Event 2 – PV plant outage in California:</u> This event is characterized by loss of photovoltaic generation in California[1] in 2018. The COI flow and frequency output from the PMU data are illustrated in Figure 7 and the response of a hydropower generator is shown in Figure 8.

[1] NERC. 2018. *Solar PV Disturbance Report.* https://www.nerc.com/pa/rrm/ea/April_May_2018_Fault_Induced_Solar_PV_Resource_Int/April_May_2018_Solar_PV_Disturbance_Report.pdf

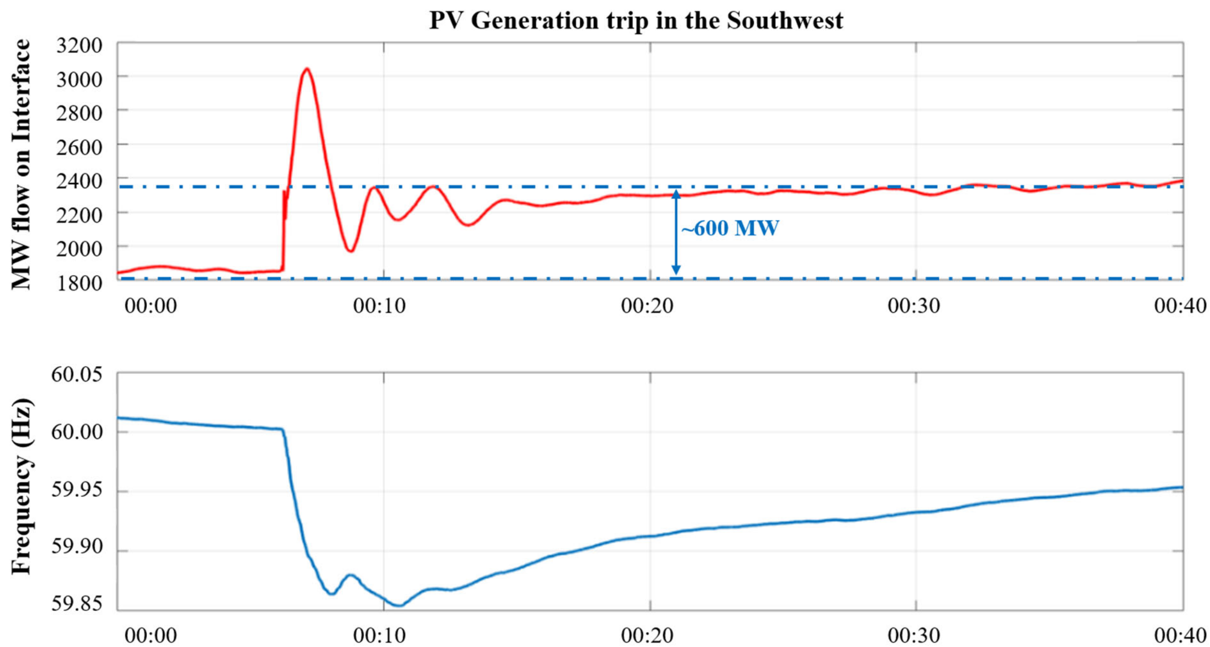

Figure 7. COI power flow and system frequency response for Event 2.

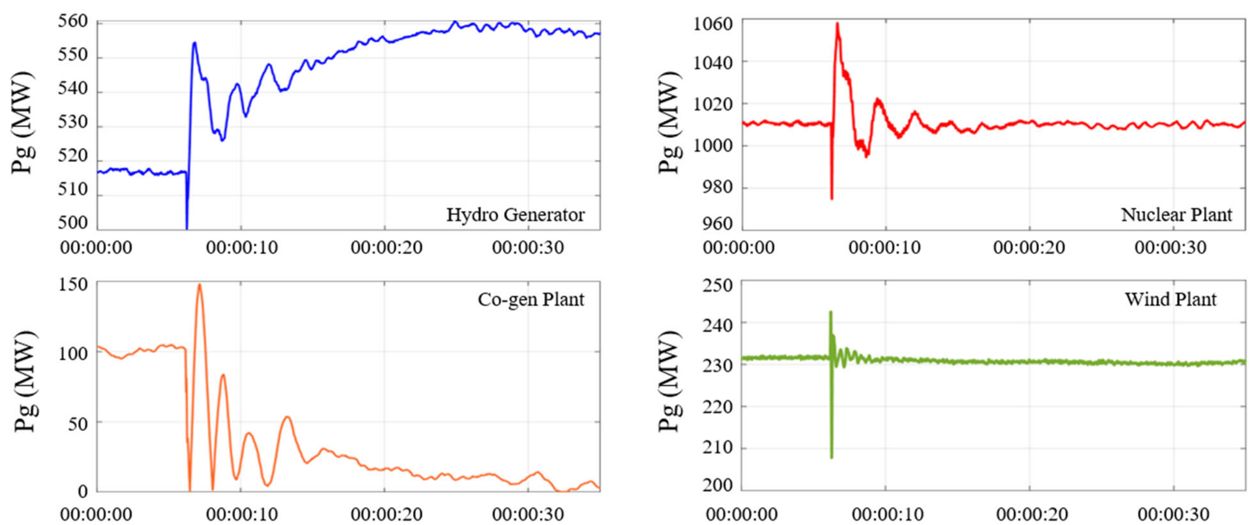

Figure 8. Response at individual facilities of various generation types following Event 2.

Consistent with Event 1, it was observed that contribution of hydropower generator toward frequency response is significant, relative to other resources. The frequency response contribution from the Pacific Northwest is translated to percentage contribution from hydropower generators and shown in Table 8 for various disturbances, as captured by historical PMU data.

Table 8. Hydropower's historical contribution towards primary frequency response.

Event Timeline	Event Description	Increase in COI Flow	Northwest Online Hydropower Capacity	Northwest Hydropower Contribution to Primary Frequency Response
Feb 2018, (Winter)	1,340 MW generation trip in Southwest	**600 MW**	>88%	$\geq \mathbf{39\%}$
Apr 2018, (Spring)	700 MW solar plant trip in Southwest	**480 MW**	>89%	$>\frac{\mathbf{480}}{\mathbf{700}} \times \mathbf{89\%} = \mathbf{61\%}$
Jul 2017 (Summer)	925 MW generation trip in Southwest	**320 MW**	>88%	$>\frac{\mathbf{320}}{\mathbf{925}} \times \mathbf{88\%} = \mathbf{30\%}$
Mar 2017 (Spring)	680 MW generation trip in Southwest	**330 MW**	>89%	$>\frac{\mathbf{330}}{\mathbf{680}} \times \mathbf{89\%} = \mathbf{43\%}$

3.2.3 Hydropower's Contribution to Frequency Support using Simulations

In the following sections, short-term extreme events (Scenarios 1 and 2) are simulated using power system modeling tools. Sudden outage of a large power plant due to mechanical failure or sudden loss of a transmission line due to a wildfire can manifest in sudden increase or decrease in grid frequency, local voltages, and other system conditions that, if not corrected in a matter of seconds, can lead to cascading outages. Such grid events require immediate responses to prevent frequency excursions, bring voltages back to normal limits, and return the system to a stable operating state post-contingency. The ability of grid resources to provide these responses depend on the electrical and mechanical characteristics of the different resources. In this analysis, these dynamic electromechanical interactions of various grid equipment are modeled using industry-wide state-of-the-art software to accurately estimate grid response following such extreme events.

The primary objectives of the analysis were to ascertain:

1. System-level impacts from an extreme event, such as sudden loss of a large generator(s)
2. Resource-level responses required to restore system operations to acceptable performance
3. Role of hydropower in providing those needed responses
4. Conditions or circumstances affecting the grid's ability to survive the extreme event
5. Gaps in data, models, and simulation tools.

3.2.3.1 Scenario 1: Largest Credible Contingency Event in the WI

In this section, we will present the impact of the single largest credible contingency event in the WI: the loss of two generating units at Palo Verde nuclear power plant. To analyze the impacts of losing a large generator in the WI, dynamic simulations were preformed to enumerate the grid response as seen in the analysis of historical data in the previous section. These simulations also help ascertain the contributions of hydropower (and other resource types) in keeping the system stabile and recovering after the event.

Scenario Details

The tripping of the Palo Verde units is considered by the industry as the largest credible contingency in the WECC and is often used as a benchmark event to analyze system performance. In this simulation, two Palo Verde units are tripped at the steady-state precontingency operating point and the dynamic response of the event is simulated for 30-60 s. The event is modeled under five different seasonal and loading conditions of 2018 WECC planning cases (Figure 9): 1) light load, summer (LS), 2) heavy load, summer (HS), 3) light load, winter (LW), 4) heavy load, winter (HW), and 5) heavy load, spring.

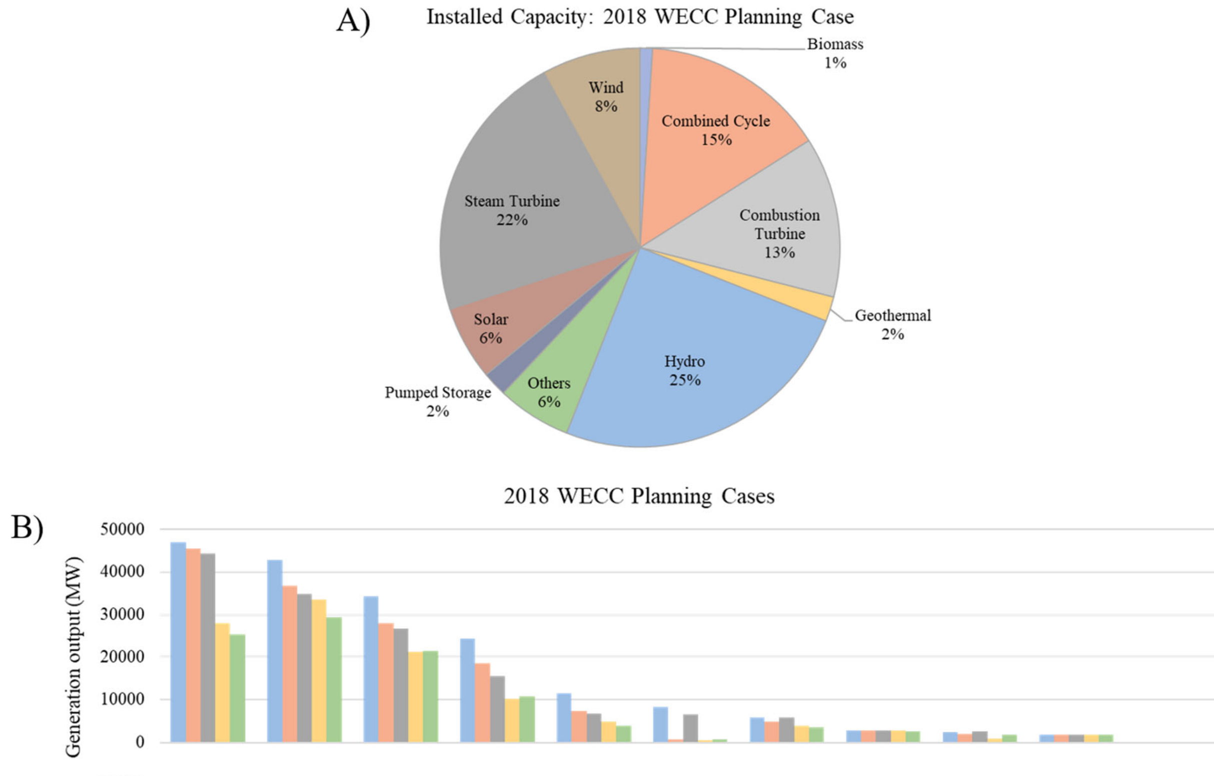

	Hydro	Steam Turbine	Combined Cycle	Combustion Turbine	Others	Solar	Wind	Geothermal	Pumped Storage	Biomass	Battery Storage
2018HS	46999	42866	34368	24258	11538	8316	5713	2686	2340	1738	103
2018HW	45550	36842	28102	18537	7302	701	4880	2733	1981	1792	44
2018HSP	44307	34929	26697	15491	6801	6579	5781	2706	2662	1733	-13
2018LS	28048	33471	21270	10213	4832	421	3885	2770	884	1744	-1
2018LW	25319	29406	21321	10808	3871	704	3616	2657	1765	1782	44

Figure 9. (A) Installed capacity in the base WECC 2018 planning case. (B) Comparison of online generation capacity for variants of 2018 WECC planning cases.

Figure 10 presents the frequency response at the COI substation for the contingency event resulting from sudden tripping of two Palo Verde generating units. Under light-load conditions, with multiple synchronous machine units offline, the equivalent inertia (stored energy in rotational masses) in the system is less, which results in increased drop in frequency (right after the event). Even though heavy-load conditions are considered operationally challenging and vulnerable to generation outages, the light-load case shows worse inertial and primary frequency response than in heavy loading conditions because there is overall less synchronous generation (both hydro and thermal) online.

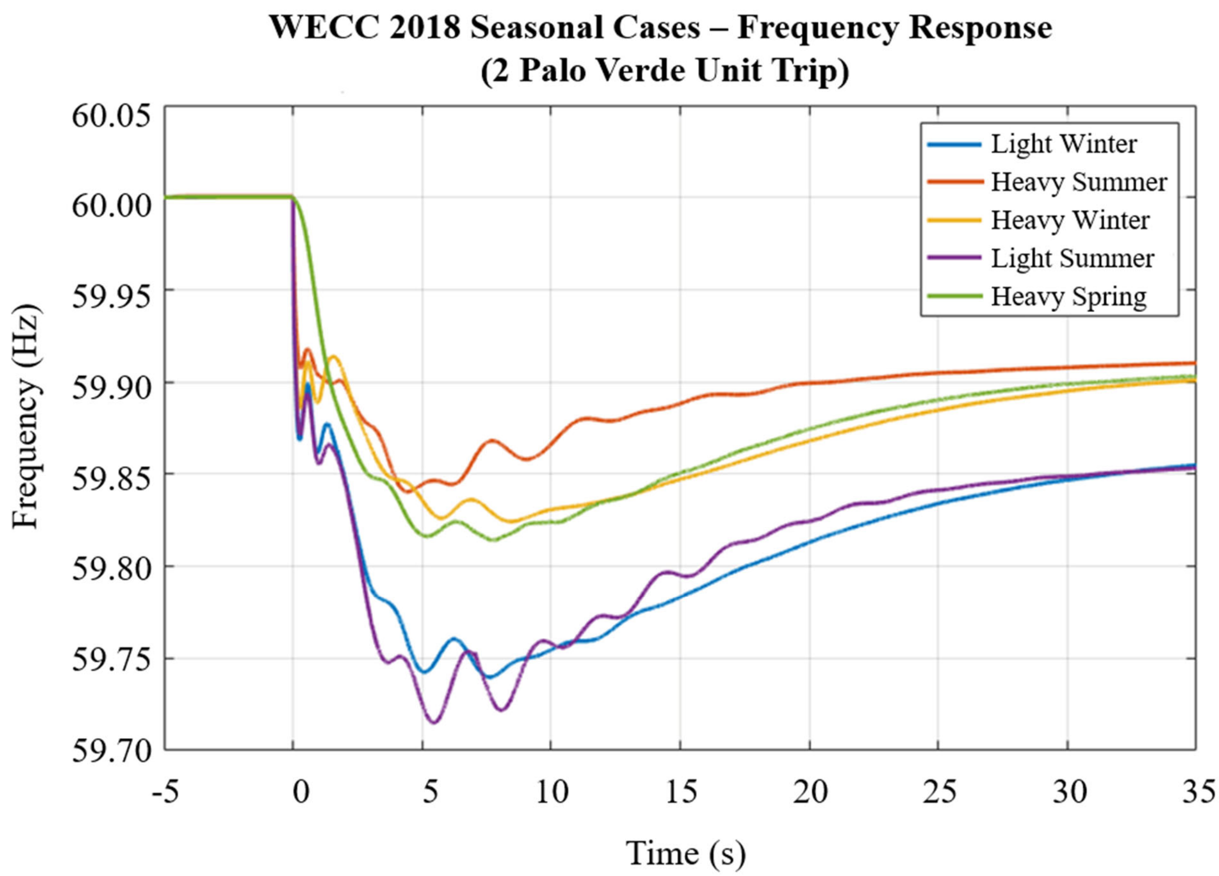

Figure 10. Frequency response comparison of Palo Verde unit trip contingency for 2018 WECC planning cases.

Simulation Results: Hydropower's Response to the Contingency Event

During system disturbances, the power grid resources must be able to change active and reactive power generation to meet current operating conditions. Real power is used to maintain frequency stability following a loss-of-generation event through automatic governor response. Reactive power helps in maintaining voltage stability through the excitation system of a generator and other system resources. Thus, to quantify the contribution of hydropower resources in the recovery process, real and reactive power variation metrics were analyzed. The results on frequency response are presented next.

Evaluation Criteria 1: Frequency Response—Inertial and Governor Response

Figure 11 shows the summary of real-power variation from a precontingency operating point to the post-contingency stable operating point following the contingency event for various 2018 WECC planning cases. The variation of generation captures the total frequency response of the generator types due to governor action by different types of resources. Table 9 presents the details of frequency response provided by hydropower resources, specifically. Simulation results show that hydropower is a major contributor to frequency response in the WI. In fact, hydropower is the single largest source of frequency response, followed by natural gas plants (combined cycle and combustion turbine generators). The simulation results are in line with the observations from data on historical events (Section 3.2.3). Furthermore, hydropower's contribution is relatively constant across different seasonal, loading, and water availability conditions.

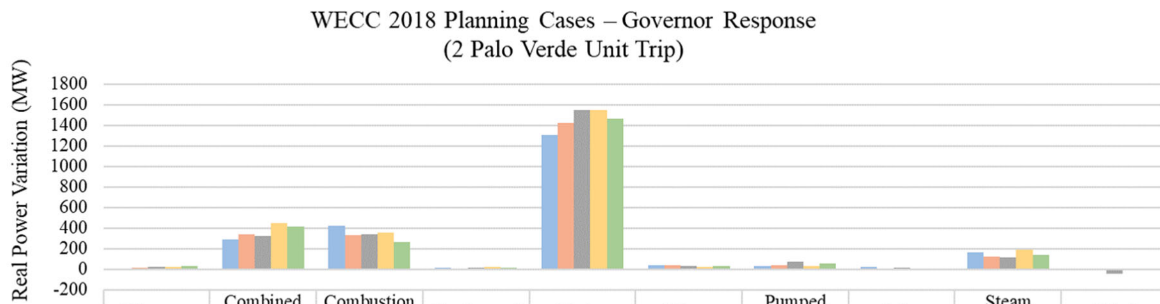

	Biomass	Combined Cycle	Combustion Turbine	Geothermal	Hydro	Others	Pumped Storage	Solar	Steam Turbine	Wind
High Summer	10	296	422	15	1305	43	33	25	171	-2
Heavy Winter	18	341	337	13	1423	41	39	4	127	-7
High Spring	22	325	343	14	1548	38	75	20	121	-42
Light Summer	23	448	359	23	1549	28	31	0	193	6
Light Winter	31	421	270	16	1463	35	57	11	143	2

Figure 11. Governor response comparison from various generation types following two Palo Verde unit trip contingency for 2018 WECC planning cases.

Table 9. Hydropower contribution toward primary frequency response after single largest contingency event in the WI.

Scenario	Contingency (MW)	Hydro Governor Response (MW)	Hydro Contribution (%)
Heavy Summer	2755	1305	$= \frac{1305}{2755} = 47\%$
Heavy Winter	2755	1423	$= \frac{1423}{2755} = 52\%$
Heavy Spring	2755	1548	$= \frac{1548}{2755} = 56\%$
Light Summer	2755	1549	$= \frac{1549}{2755} = 56\%$
Light Winter	2755	1463	$= \frac{1463}{2755} = 53\%$

The total response for stabilizing system frequency after an extreme event requires a combination of inertial and primary frequency. Figure 12 shows the total response of hydro, combined cycle, combustion turbine, and steam turbine resources following the trip of two Palo Verde generation units for the 2018 HW planning case. It shows that inertial response from combined cycle, combustion turbine, and steam turbine is significantly more and quicker than other resources 2–3 s after the event; however, the governor/primary frequency response from hydro resources are significantly high from 5–35 s. Scenario 2 will analyze the role of hydropower when the system faces a widespread outage of natural gas power plants (combined cycles and combustion turbines).

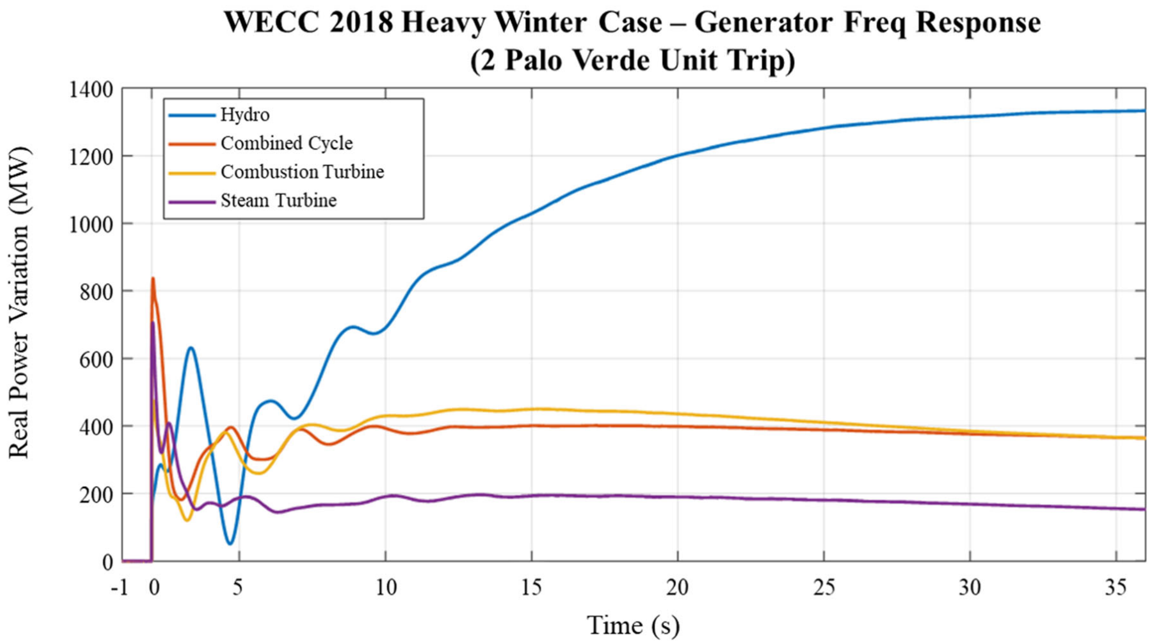

Figure 12. Dynamic response of various generation types following two Palo Verde Trip: 2018 WECC HW case.

Evaluation Criteria 2: Reactive Power Contributions

Along with frequency stability, system voltages must be held within predefined limits.1 Voltage control is supported by reactive power management. Reactive power is a critical component of operating an alternating current electricity system and is required to control system voltage within appropriate ranges for efficient and reliable operation of the transmission system. Reactive power can be provided by a variety of resources. Generators can operate within a range of leading and lagging power factors with continuously variable reactive power output to meet the voltage schedule set by the transmission provider. Reactive power sources are generally categorized as static or dynamic based on the speed and continuity at which they can produce or absorb reactive power in response to changes in system conditions.[2]

In the case of a contingency, such as the outage of a large generator, hydropower resources (and other resources) provide increased active power to help restore system frequency, which increases the requirement for reactive power support to ensure that voltage does not sag at the point of interconnection. Hence, additional voltage support is needed along transmission lines that deliver increased power to load centers that have lost a generator. Hydropower resources are a significant source of reactive power in the WI because hydroplants typically have many units within a single facility, and some units are designed to operate with lower power factor than the typical +/-0.95 power factor of non-hydroplants. Contributions of reactive power from hydropower can be of great significance during grid disturbances because baseload units (large thermal coal and nuclear plants) in the WI typically operate near or at nameplate MW output, so there is often not enough capacity left for additional reactive power support.

[1] One of the root causes of the 1996 blackouts was tripping of the McNary generation plant without which the local voltage support dwindled. NERC Report on 1996 Blackout.

[2] FERC. 2014. *Payment for Reactive Power*. Washington, D.C. https://cms.ferc.gov/sites/default/files/2020-05/04-11-14-reactive-power.pdf.

Figure 13 shows that the additional reactive power supplied by hydropower, post-contingency, was observed to be consistently greater than other resources for all combinations of seasonal and system loading conditions that were modeled, and for the characteristics and location of the contingency under study. Figure 14 shows the dynamic reactive power response from different resources over the entire duration of the contingency event for the HW case. For the contingency under study, hydropower resources in aggregate contributed more dynamic and post-contingency static reactive power than all other resource types combined.

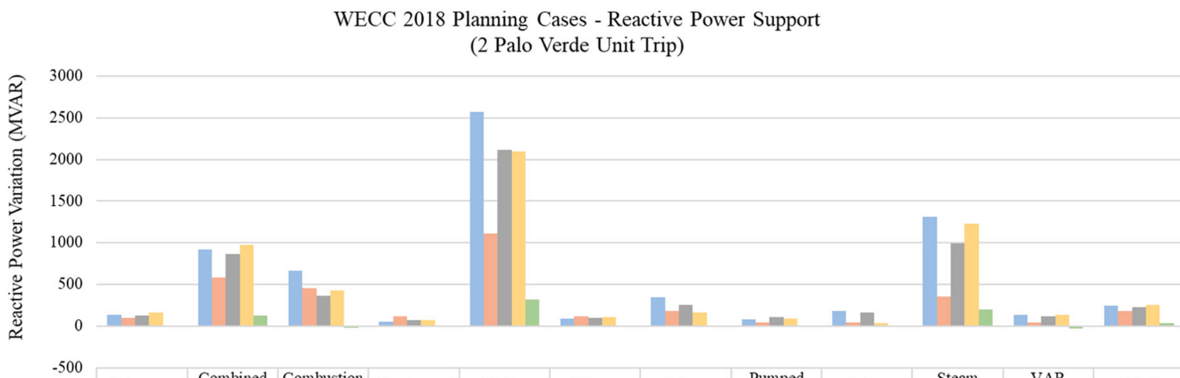

	Biomass	Combined Cycle	Combustion Turbine	Geothermal	Hydro	Motor	Others	Pumped Storage	Solar	Steam Turbine	VAR Devices	Wind
High Summer	134	921	660	53	2572	89	344	78	180	1313	133	243
Heavy Winter	100	586	452	115	1113	118	180	39	45	351	46	182
High Spring	122	868	360	74	2114	101	251	104	160	996	118	226
Light Summer	161	978	426	71	2093	109	165	91	38	1232	139	251
Light Winter	1	127	-19	1	319	-14	-8	-10	5	198	-26	31

Figure 13. Additional reactive power supplied from various generation types following two Palo Verde Unit Trip contingency for 2018 WECC planning cases.

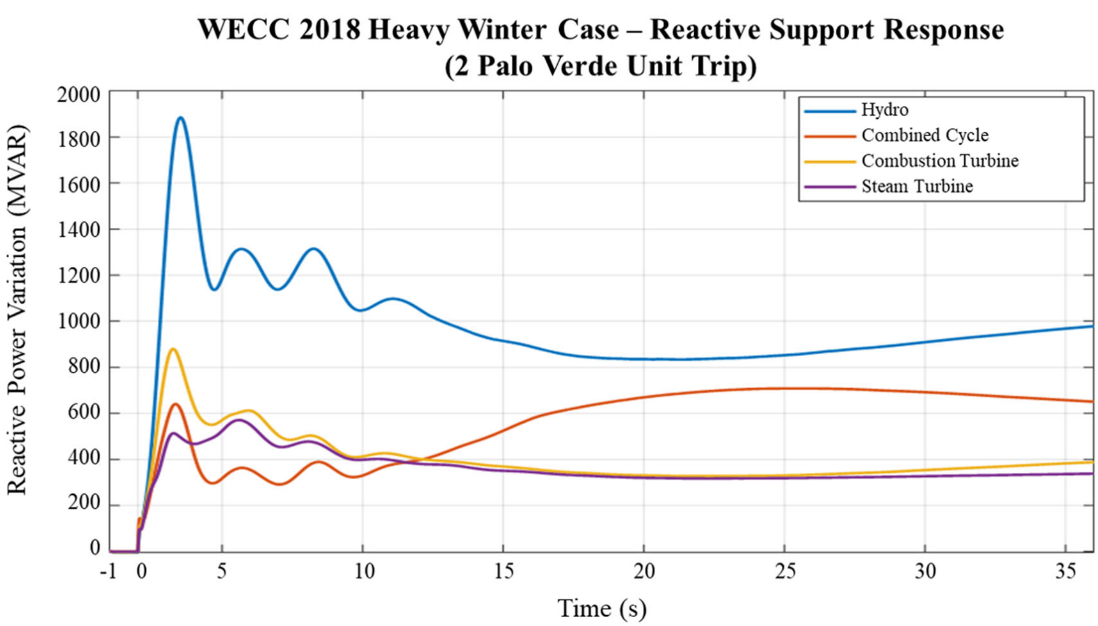

Figure 14. Voltage ride-through of various resources by providing dynamic reactive power response following two Palo Verde Trip 2018 WECC HW case.

3.2.3.2 Scenario 2: Widespread Outages of Natural Gas Plants

Natural gas power plants play a crucial role in meeting reliability needs of the power system. Like hydropower units, natural gas power plants can quickly respond to extreme events by changing their outputs of real and reactive power. As seen in Sections 3.2.1, 3.2.2, and 3.2.4, natural gas plants are major contributors of inertial and primary frequency response as well as reactive power in the WI. Any event that causes widespread outage of natural gas generators is likely to result in severe stress to the power grid and potentially impact its ability to respond to and recover from extreme events. In such a scenario, other online generation including hydropower will be required to provide the necessary responses. Hence, to assess the role of hydropower in contributing to grid resilience, a scenario was designed consisting of widespread outage of natural gas-fired plants in the WI. The outage scenarios were modeled and simulated to occur at different times of the year and under different assumptions of system loading and water availability conditions. The main objectives were to: 1) analyze and quantify the impact of outages on grid operations; 2) quantify the responses needed to ensure system stability; and 3) quantify and analyze the role of hydropower. The details of the natural gas plants' outage scenario are presented next, followed by a brief overview of simulation methodology and details of the system conditions prior to and after the event occurred.

Scenario Details

The scenario postulates a hypothetical severe event[1] in the WI resulting in outages of numerous natural gas-fired generators over a period of approximately one hour. The impacts of the large-scale generation outage on the WI power grid were analyzed and quantified using the WECC 2018 planning case as the base system model.

It should be noted that composition of available generation, including hydropower, differs based on the combination of seasonal and load conditions; HW conditions have more generators online, both generating power and providing reserves, than LS conditions. Hence, to fully analyze the role of hydropower in responding to the grid events after the outage of natural gas generators, three seasonal and load conditions were selected:

1. HW with average hydro, labeled as "Heavy Winter"
2. LS with normal hydro, labeled as "Light Summer"
3. LS with dry hydro, labeled as "Light Summer (dry)"

To further analyze the role of hydropower under different conditions, the grid model was subjected to the same outage scenarios by assuming different hydrological scenarios (varying degrees of water availability). Specifically, the LS case was examined for a normal hydro year and a dry-hydro year. Dry conditions were obtained from historical dry-year conditions, for which the 2018 WECC planning case was modified by adjusting the available head room for hydropower resources in the Northwest region. The methodology to model changes in system conditions during a dry hydrological season for the 2018 WECC planning models is provided in Appendix B.

System State Prior to Outages of Natural Gas Generators

The installed capacity and online generation mixes of the 2018 WECC planning models for various seasonal and loading conditions are presented Figure 15 (A) and (B), respectively. The total amount of online generation capacity, including hydropower, is the lowest under LS conditions. The composition of

---

[1] In WECC 2018, the authors present results from detailed modeling of various gas pipeline disruption scenarios and the resulting outages of natural gas power plants in the WI. The various disruption scenarios resulted in outage of 8-24 generators.

available generation impacts the system's ability to respond to extreme grid events due to differences in available inertial and primary frequency response, reactive power, and other reserves. Inertial response, specifically, is determined by the number and types of resources connected to the electric grid. Figure 16 shows the comparison of stored energy for inertial response from various fuel mixes for the LS and HW cases. Under light-load conditions, multiple units are offline, mostly hydropower and other non-baseload resources such as gas-fired generators, resulting in reduced inertial and primary frequency response capability, and hence delayed recovery of system frequency to the steady-state value.

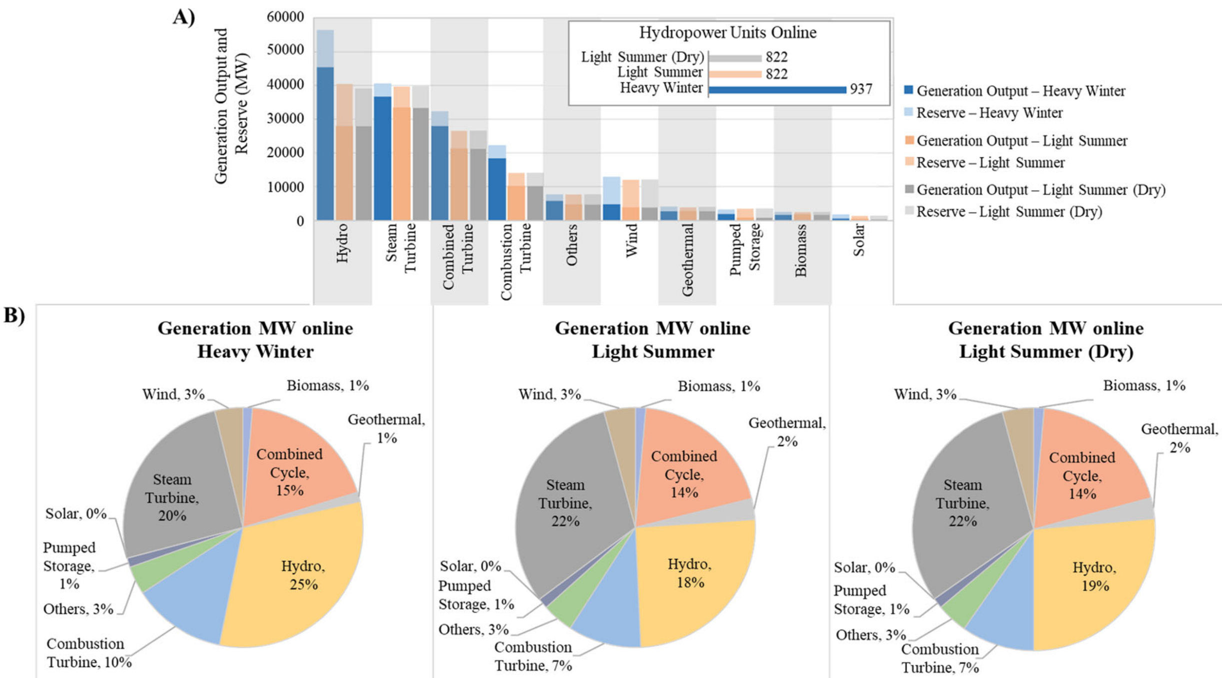

Figure 15. (A) Online generation mix for various 2018 WECC planning cases. (B) Percentage of generation online and available reserves for the 2018 WECC planning cases.

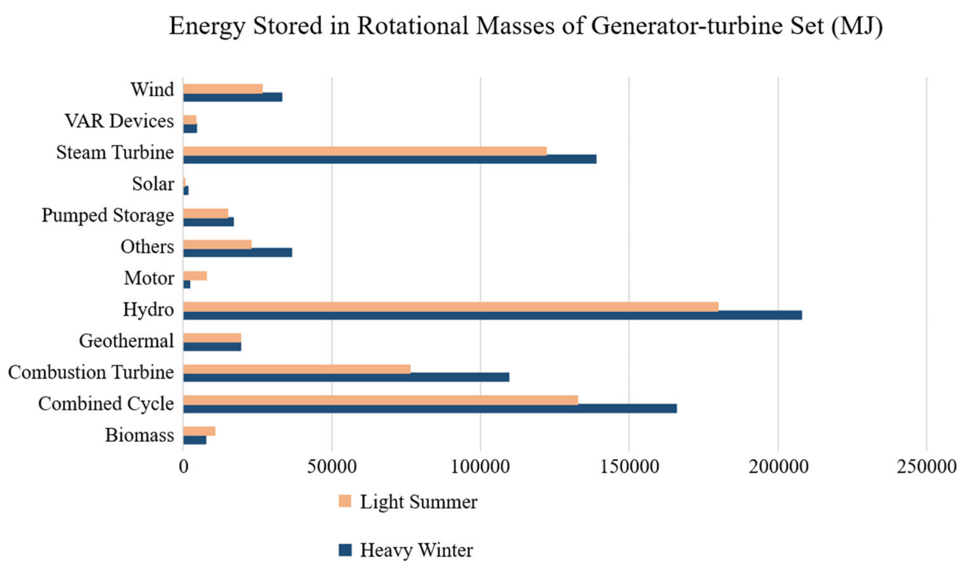

Figure 16. Total energy stored in rotational masses (MJ) for LS and HW 2018 WECC planning cases.

The outages of natural gas plants were assumed to occur in a sequence of events, called contingencies. Each contingency consisted of outages of multiple natural gas plants. Figure 17 shows the incremental amount of natural gas generation lost in the WI for LS and HW cases, respectively. In the HW scenario, approximately 9,000 MW (~6.3 % of total load) of generation was assumed to be lost over a course of 18 different contingency events, while in the case of LS, approximately 6,000 (~5.9 % of total load) MW of generation was assumed to be lost over the course of 15 different contingency events. To assess the impact of outages of natural gas plants, the process of dynamic stability analysis was used.

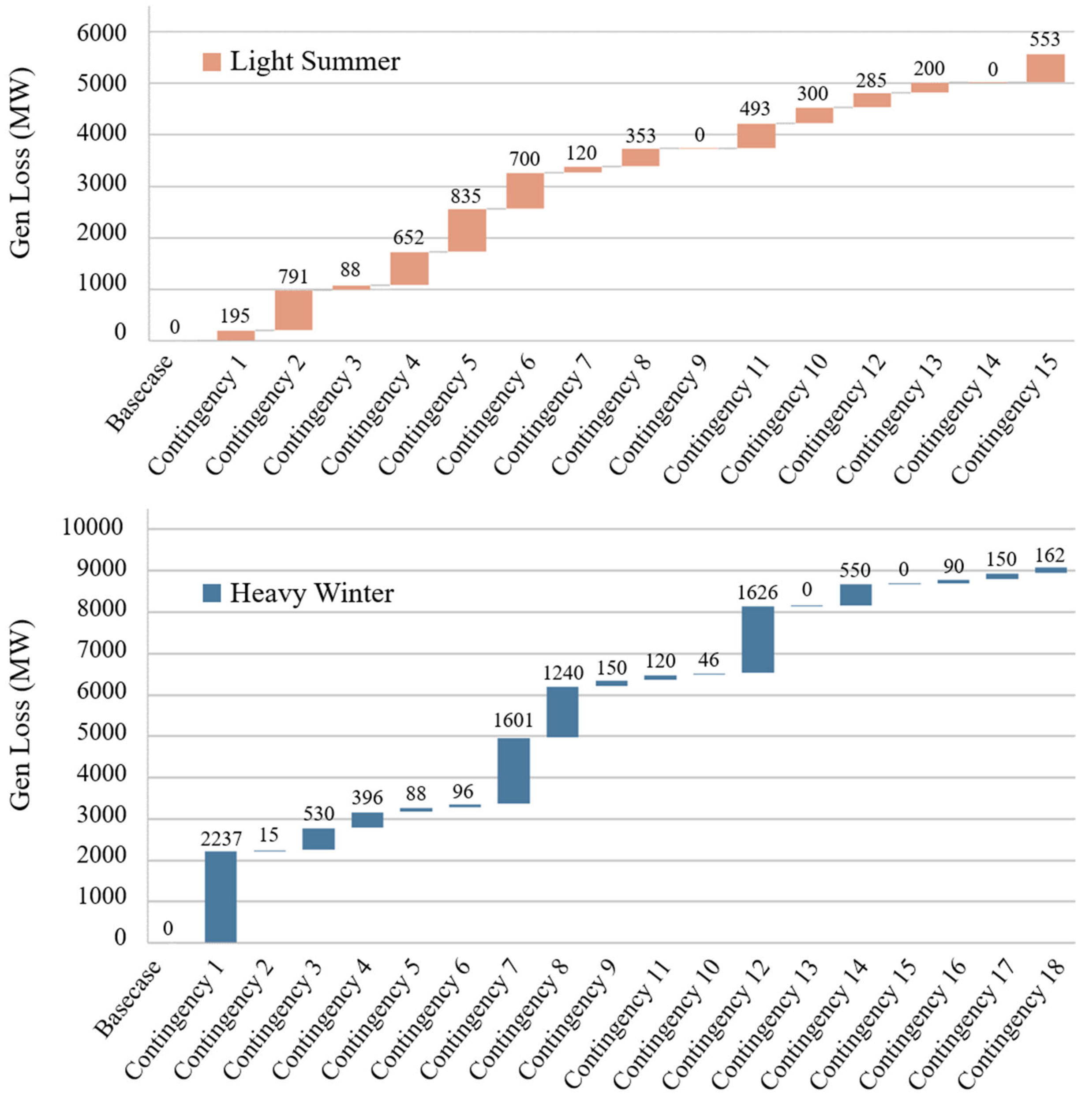

Figure 17. Sequence of loss of natural gas plant in HW case and LS case.

Simulation Methodology

Dynamic simulations were performed using a 1-minute windows after the occurrence of each contingency; the HW case, for instance, was assumed to have a sequence of 19 contingencies, with multiple plants tripping during each contingency. Each of these moving windows were stitched together to describe the overall sequence of events. The results of each minute's simulation were used to identify the power system status at the beginning of the next contingency, with frequency restored to 60 Hz, all performance violations (out-of-range voltages, transmission overloads, etc.) resolved, operating (online) reserves committed to generate power, and any additional natural gas generator outages accounted for by removing those plants from the generation mix.

Each new dynamic simulation starts with the assumption that system frequency is back to 60 Hz. This assumption is a limitation of all simulation software. Every dynamic simulation tool initializes dynamic simulation from a load-flow case. In actual operations, if there are multiple generators tripping in a short timeframe, AGC (also known as secondary control) might not have time to recover frequency to 60 Hz. Although AGC is not explicitly modeled, frequency is assumed to be returned at 60 Hz. The objectives of AGC are to regulate frequency to nominal value and to maintain the interchange power among balancing authorities according to predefined schedules by adjusting output of selected generators. The consequences of not modeling AGC are small differences in interchange and in generation dispatch; the differences are minor because very few units are on AGC compared with the number of units providing governor response.

Simulations were done on the 2018 WECC planning cases discussed above using power flow and dynamic simulation. Dynamic simulation is initialized from power-flow model and then numerical integration is performed on each case and each contingency using WECC dynamic models. The WECC dynamics database consists of generator, governor, stabilizer, and exciter models for generators of different types; dynamic models for loads; static compensator and static VAR compensator models, high-voltage DC models, etc. It also includes a limited set of relay models found in the case. Additional dynamic data are modeled in Positive Sequence Load Flow format; this includes the generator protection relays (low/high-voltage ride-through, low/high-frequency ride-through) that are added to the existing relay protection models in the WECC HW case that includes generator, governor, stabilizer, and exciter models for generator-side dynamics.

Dynamic simulation is performed to accurately depict the impact of cascading tripping actions and the effects they can have on other elements due to frequency and voltage swings. Corrective actions are considered and can be performed with several participating components of the system. These components can be generators, phase shifters, tap-changing transformers, switched shunts, loads, etc. The first set of corrective actions are performed with control phase shifters; tap-changing transformers and switched shunts are used to eliminate voltage violations. If the voltage and flow violations remain, manual operator actions such as generation redispatch and load shedding are used next. The detailed framework and simulation methodology are presented in Appendix A.

System State after the Outage of Natural Gas Plants

In the case of HW scenario, approximately 9,000 MW of generation was assumed to be lost, while in the LS case, approximately 6,000 MW of generation was assumed to be lost. Consequently, the requirements to help stabilize grid conditions after each contingency, such as (but not limited to) inertial and primary frequency response, reactive power, etc., differed between these scenarios. The effects of ensuing generator outages were analyzed using traditional dynamic and steady-state simulation.

Figure 18 shows the frequency movements resulting from a subset of contingencies under both LS and HW conditions and presents the inertial and primary frequency response provided, collectively, by resources north of the COI. This measurement represents the aggregate response of resources that help to arrest initial frequency drop and then restore frequency to a stable operating point.

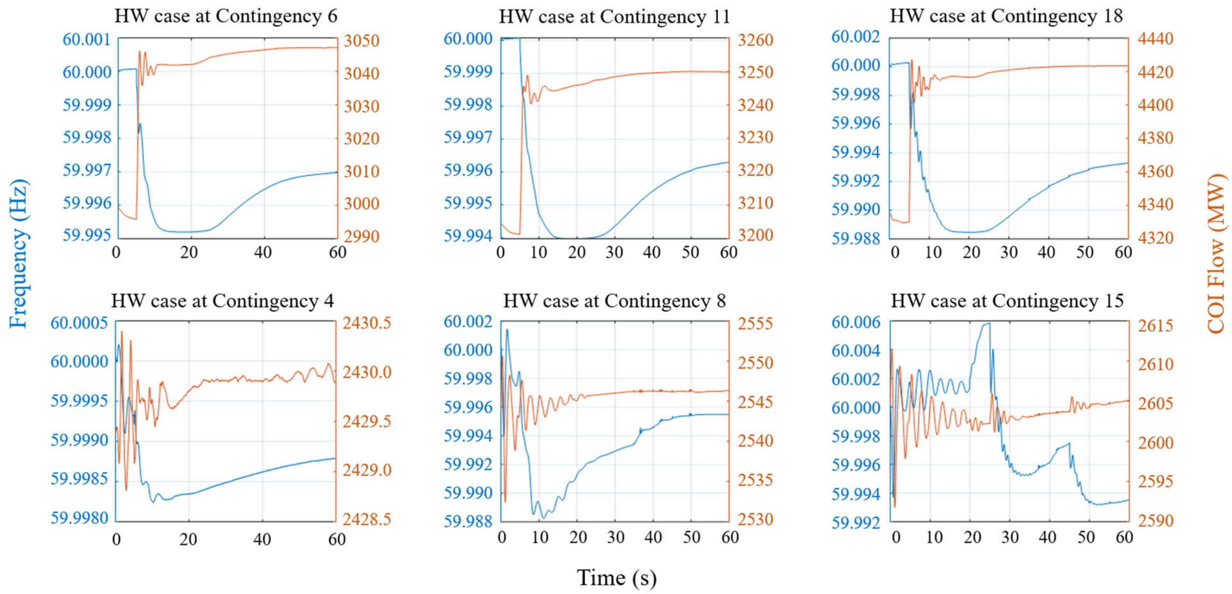

Figure 18. Frequency response and COI flow at various time intervals of the natural gas event scenario—simulation results for HW and LS cases.

Simulation Results: Hydropower's Response to Outage of Natural Gas Plants

To quantify the contribution of hydropower resources in the process of recovering from outages of natural gas plants, rea and reactive power variation metrics were analyzed.

Evaluation Criteria #1: Frequency Response—Inertial and Governor Response
As mentioned earlier, the contributions by hydropower resources to support frequency will depend on specific grid conditions, such as time of year, system load, water availability, etc. Hydropower's contribution to frequency response requirements due to outages of natural gas plants under different system conditions will be presented next.

<u>Frequency Response: Effects of Seasonal and Loading Conditions</u>
Overall in the WI, hydropower's contribution to primary frequency response was observed to be as high as 51% under light-load conditions in the summer and 56% under HW conditions, as seen in Table 10. The contribution of hydro generators toward primary frequency response is different for each contingency event and ranged from ~20–55% over the entire set of contingencies. On average, the contribution from hydropower resources towards primary frequency response was observed to be ~32% in LS and 38% in HW, while hydropower generators constituted only ~20% and ~25% of online generation capacity in the two cases, respectively. It should be noted that governor response does not bring back the system to 60 Hz, but to a stable operating frequency less than 60 Hz after the event.

Table 10. Hydropower contribution toward primary frequency response after widespread outages of natural gas power plants in the WI.

Light Summer				Heavy Winter			
After Contingency #	MW lost due to natural gas trip	Hydro Governor Response MW	% gen loss compensated by hydro governor response	After Contingency #	MW lost due to natural gas trip	Hydro Governor Response MW	% gen loss compensated by hydro governor response
15	5565	1788	$=\frac{1788}{5565}$ =32%	18	9096	3477	$=\frac{3477}{9096}$ =38%

Note: In Section 0, PMU data from various historical events were used to quantify the contribution of hydropower resources to frequency response. The simulation results presented in Table 10 closely align with responses shown by historical PMU data and thus provide increased confidence of the simulation-modeling procedures used in this report.

It should also be noted that that water usage is not explicitly modeled in the simulations presented in this section. If the events are spread across a longer duration, the capability of hydro resources to provide frequency support may lessen as water levels are depleted. In the natural gas plant outages scenario presented here, the outages are assumed to take place within 60 minutes, and it is reasonable to assume that hydropower capacity does not change during this interval. In other words, water availability is assumed to not become an issue for the duration and intensity of responses required from hydropower resources. Future work in this area should further explore this aspect.

It should be noted that unit commitment process is not modeled in this simulation approach. In actual operations, operators can commit additional hydropower and other resources during an emergency state,[1] which may help in providing additional frequency and voltage support. Hence, the contribution of hydropower from these simulation results is likely to be on the conservative side. As more and more natural gas units start tripping, operators may commit more hydropower units online (especially in light-load conditions) to support the grid.

Figure 19 shows the comparison of governor response for various resources, based on real-power variations from the start of the event until the final contingency for the HW and LS cases. After a large portion of natural gas fleet is lost as part of the contingencies, hydropower was observed to contribute significantly in making up the deficit for both loading conditions and seasons. It should be noted that all the natural gas plants were not assumed to be impacted, and hence the change in generation at the online plants is a response to the contingencies.

It was observed that hydropower and (remaining) combined-cycle plants provide the highest contribution to the contingencies in terms of governor action to replace the generation capacity lost in the contingencies. As AGC is not modeled in the simulation studies, it can be assumed that AGC actions are blocked by the operators during the emergency system state. Therefore, only generator governor action, from contingency reserve resources with high ramping capacity, is responsible for maintaining system frequency.

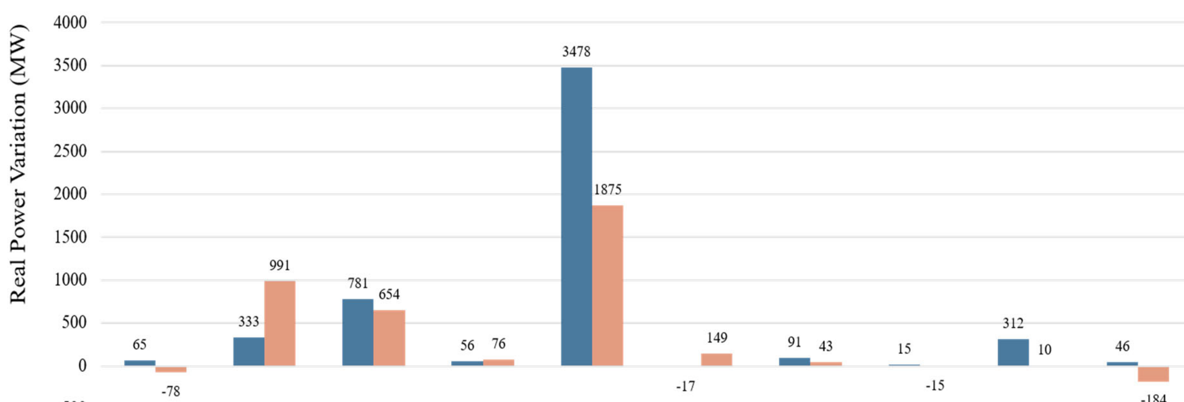

	Biomass	Combined Cycle	Combustion Turbine	Geothermal	Hydro	Others	Pumped Storage	Solar	Steam Turbine	Wind
Heavy Winter	65	333	781	56	3478	-17	91	15	312	46
Light Summer	-78	991	654	76	1875	149	43	-15	10	-184

[1] As discussed in Section 3.3, hydropower facilities can be brough online quickly.

Figure 19. Real-power variation for various resource types relative to base case and after Contingency 18 (HW case) and Contingency 15 (LS case).

Figure 20 shows the comparison of resource real-power variations across WECC areas; PG&E and Arizona are assumed to lose major amounts of their natural gas fleets, and the deficit in real power is observed to be made up by hydropower-rich areas in the Northwest and by BC Hydro in Canada. The results are consistent across the seasonal and loading conditions. These results do not include any natural gas resources that were lost during the contingency events.

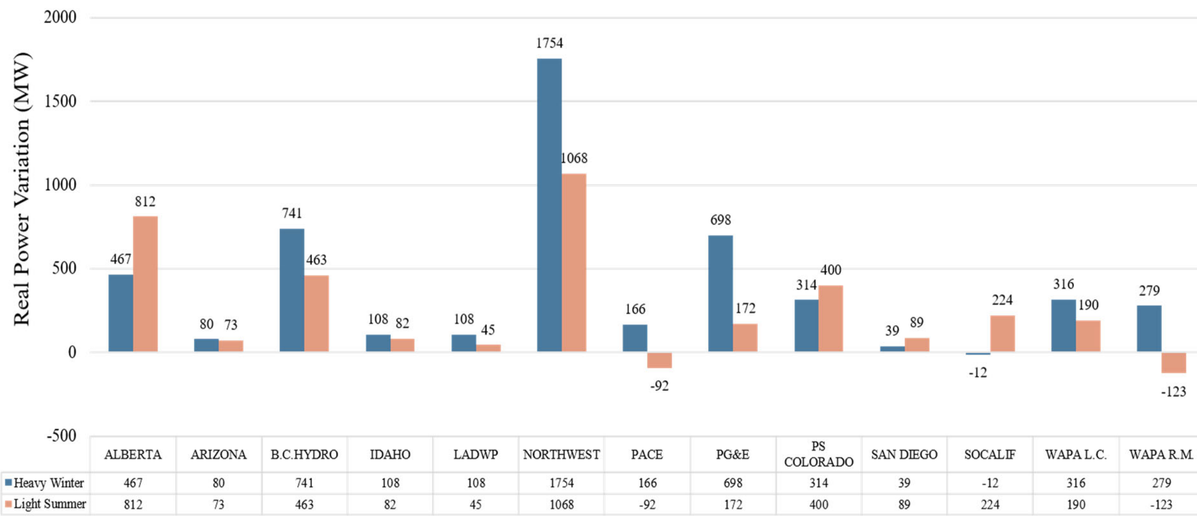

Figure 20. Real-power variation for different WECC regions relative to base case after Contingency 18 (HW case) and Contingency 15 (LS case).

These results show that hydropower was essential in ensuring that the WI system was able to withstand the impact of the outage of several natural gas plants. The contributions under LS load conditions are especially significant because the available online generation from other types of resources is much lower than in HW load conditions. The total contribution of hydropower to support system frequency was relatively equal under the two system states.

The operational differences between the HW and LS scenarios can be quantified by looking at some of the additional metrics that represent the system state and vulnerabilities for various contingencies, as presented in Appendix E. The flow-violation metrics in Appendix E (Figure E.4) show that the HW case is more prone to flow violations due to high loading conditions, and the amount of generation rescheduling and number of corrective actions to manage flow violations will be high even though there is enough hydropower capacity to provide replacement generation capacity. On the other hand, looking at the voltage-violation metrics in Appendix E (Figure E.4), the LS case is more vulnerable to voltage violations and voltage-stability issues, and actions to correct voltage levels are more pronounced. The contribution of hydropower resources in providing voltage support will be discussed later in the report.

Frequency Response: Effects of Water Availability

Water availability during LS conditions can impact the response of hydropower resources to grid events. To test the impact of water availability, the plant outages scenario was applied to the WI system with below-average water availability. In the case of a dry hydrological year, the hydropower resources in the Northwest were modified to reflect reduced maximum available capacity and a consequent reduction in overall reserve margin.

Figure 21 shows the contribution of real power from the various resource types; hydropower is the most significant contributor for all scenarios. However, for dry-hydro conditions, due to reduced reserve margin from hydropower resources, natural gas plants contribute an additional 500 MW compared to the regular LS case. Figure 22 shows the real-power variation across different WECC areas. As observed earlier, generation lost due to outages in PG&E and Arizona are compensated by contingency reserves from other available generators. The increased generation from hydropower comes mostly from the Northwest, BC Hydro, the Western Area Power Administration, Southern California, Idaho, and Alberta. However, the dry-hydro case shows that with reduced reserve margin, the system may not be able to survive all the contingencies.

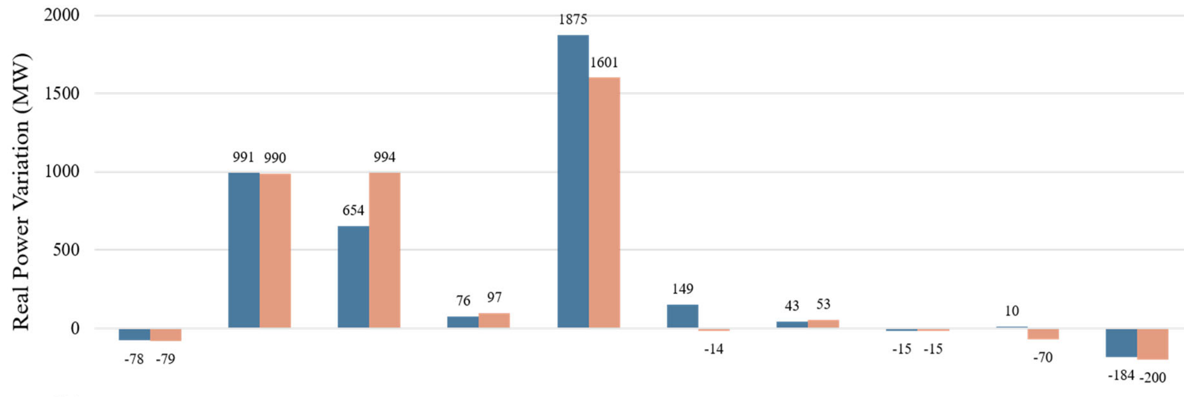

	Biomass	Combined Cycle	Combustion Turbine	Geothermal	Hydro	Others	Pumped Storage	Solar	Steam Turbine	Wind
Normal Hydro	-78	991	654	76	1875	149	43	-15	10	-184
Dry Hydro	-79	990	994	97	1601	-14	53	-15	-70	-200

Figure 21. Total generation variation by resource type relative to the base case and after Contingency 15 (LS—normal) vs. Contingency 15 (LS—dry-hydro conditions).

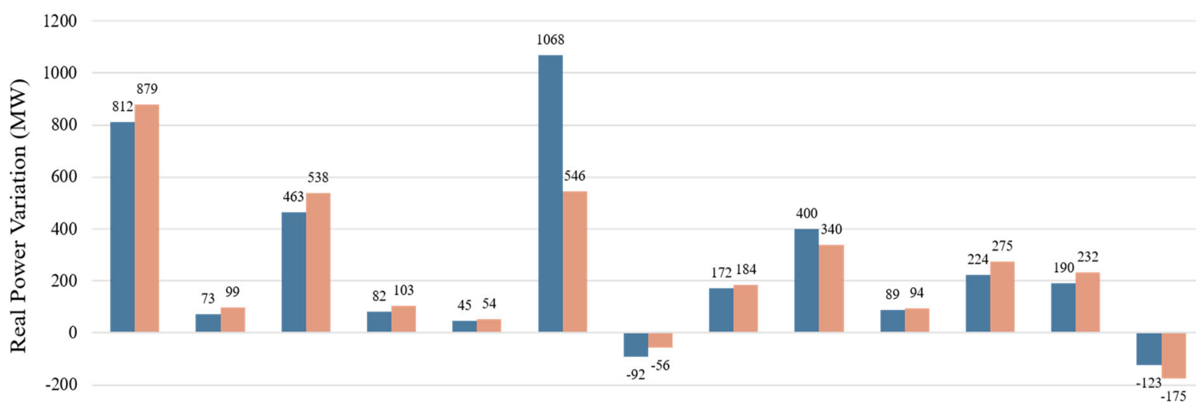

	ALBERTA	ARIZONA	B.C.HYDRO	IDAHO	LADWP	NORTHWEST	PACE	PG&E	PS COLORADO	SAN DIEGO	SOCALIF	WAPA L.C.	WAPA R.M.
Normal Hydro	812	73	463	82	45	1068	-92	172	400	89	224	190	-123
Dry Hydro	879	99	538	103	54	546	-56	184	340	94	275	232	-175

Figure 22. Total generation variation by area relative to the base case and after Contingency 15 (LS—normal) vs. Contingency 15 (LS—dry-hydro conditions).

Due to reduced availability of hydropower generation during dry conditions, more stress is placed on the system. These results additionally prove the reliance of the WI system on its hydropower resources. System performance degraded a little under dryer conditions: the system could only overcome 14 contingencies, as against all 15 contingencies in normal water year conditions. However, hydropower's contribution was still instrumental in ensuring that the system survived for as long as it did.

Evaluation Criteria #2: Reactive Power Contributions
As noted earlier, system voltages must be held within predefined limits. The voltage-violation metrics presented in Appendix E (Figure E.4 and Figure E.5) show that voltage violations are more prominent under light-load conditions due to a reduced number of online units that can provide reactive power support. Furthermore, in the dry-hydro case, the reduced reserve margin results in a further reduction of available reactive power capacity from existing resources, mostly hydropower. Hence, the contribution of hydropower resources to reactive power is presented for the case with dry conditions only.

Figure 23 shows the increase in reactive power generation from resources in the different WECC areas. It can be observed that the Northwest, Alberta, PG&E, and BC Hydro are the main contributors of reactive power in the system to maintain voltage stability. Figure 24 shows that hydropower resources contribute the most reactive power in the system, followed by gas turbines and the combined-cycle units. Figure 25 shows hydropower resources contributing to reactive power in the different areas. PG&E underwent a substantial generation loss due to outages, resulting in substantial loss of reactive power that was compensated locally by other online resources. Figure 26 shows that, in the PG&E area, almost 35% of the reactive power support was provided by hydropower resources.

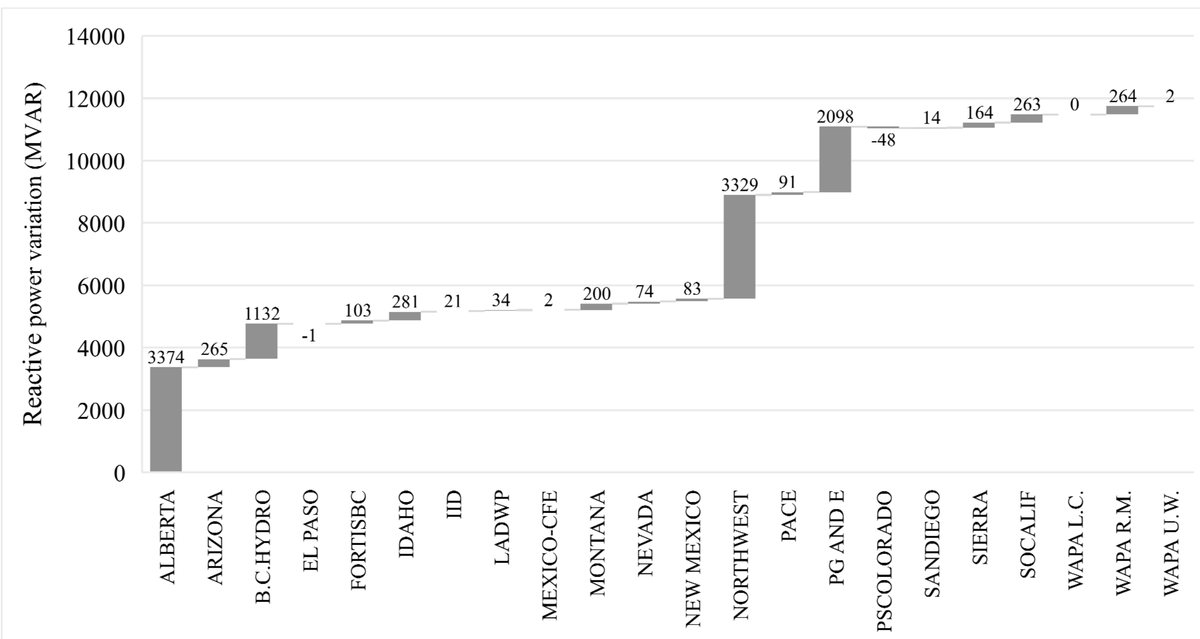

Figure 23. Reactive power variation by area for the base case and all contingencies for LS, dry-hydro case.

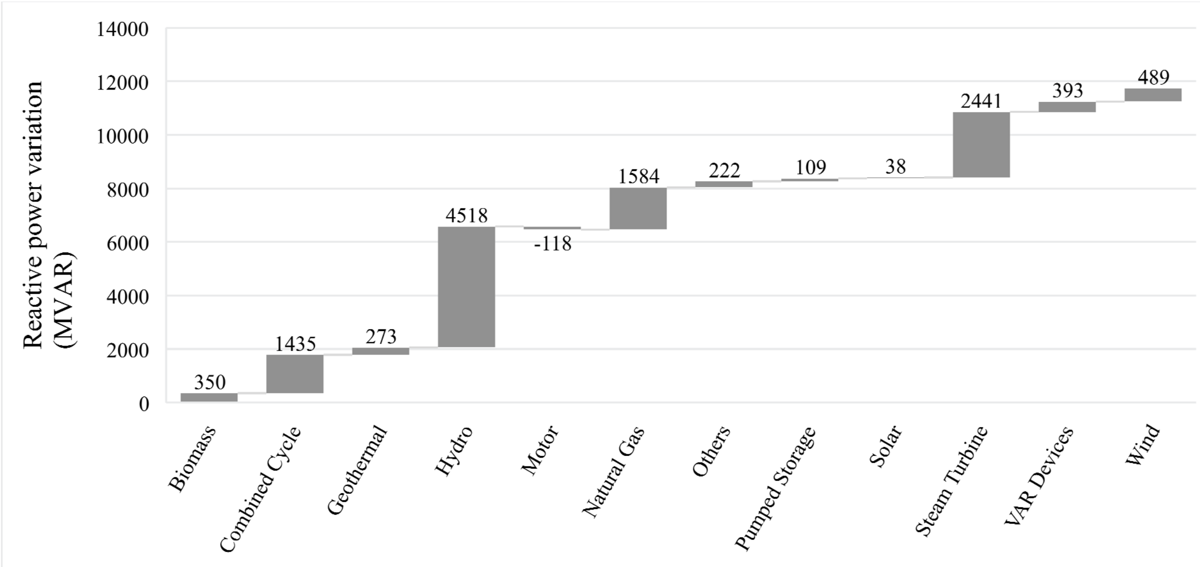

Figure 24. Additional reactive power supplied by various generation types for the base case and all contingencies for LS–dry-hydro case.

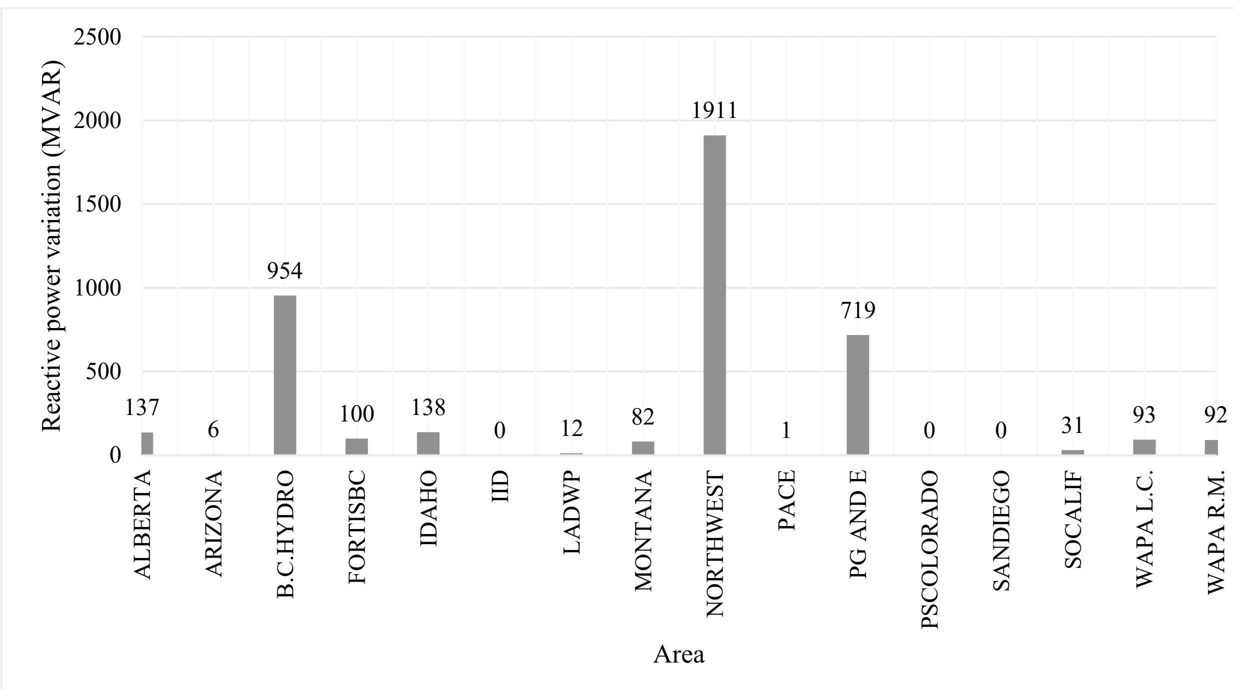

Figure 25. Hydro-only reactive power variation by area for the base case and all contingencies for LS–dry-hydro case.

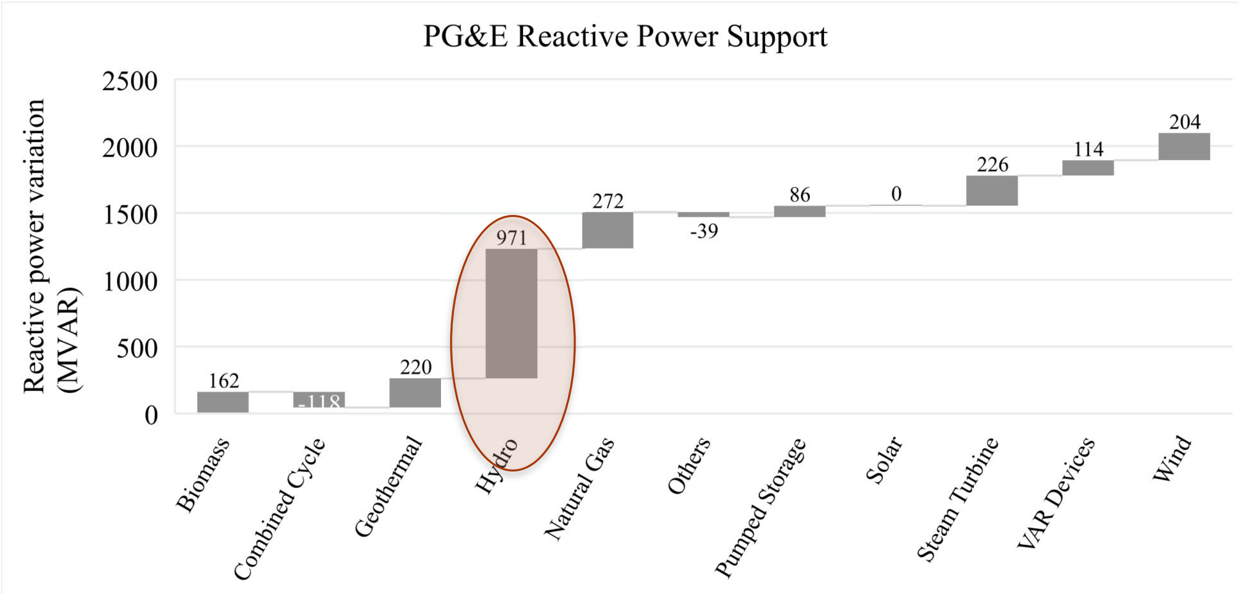

Figure 26. Reactive power variation in PG&E for the base case and all contingencies for LS–dry-hydro case.

It should be noted that while every synchronous machine (generator and motor) as well as inverter-based resources can provide reactive power, reactive power capability of resources is limited by capability curves. Capability curves are mostly limited by the amount of current that can flow through machine stator (thermal rating or megavolt amperes capacity) or, in case of inverter-based resources, by maximum current allowed through power electronics switching devices. Here we are addressing permanent and not short-term voltage support. Therefore, since hydro resources are generally operated with more headroom, they also have more available reactive power capability to increase permanent voltage support when needed. On the other hand, in WI thermal and nuclear plants operate at or near their rated capacity almost all the time (since that is the most economical way to operate), so they typically do not have room to provide long-term reactive power support unless they reduce MW output.

Additional evaluating criteria from the simulation results are presented in Appendix E.

3.2.4 Other Advantages of Hydropower Generators

3.2.4.1 Frequency Ride-Through Capabilities of Hydropower Resources

One of the major concerns in power systems is that, during large frequency disturbances, generators can trip due to underfrequency protection of turbines. Underfrequency load shedding (UFLS) is supposed to prevent this, but if UFLS is not fast enough—that is, not enough load can be shed in time—or if the disturbance is too large, generators can trip due to under or overfrequency protections. This can cause wide-scale blackouts because it would lead to additional frequency decay.

Hydro generators have an advantage over other resources because they can operate over significantly wider frequency range,[1] hence they are much less sensitive to changes in system frequency. The reason is

[1] ANSI/IEEE. 1987. *IEEE Guide for Abnormal Frequency Protection for Power Generating Plants*. C.37.106-1987. ANSI, New York City. "The abnormal frequency limitations for hydraulic turbine generators are much less stringent than that for STGs and CTGs. Generally, hydraulic turbine generators are designed to withstand more severe over-speeds than steam and combustion turbines, in some cases up to 100% overspeed (200% speed). Bucket designs on

that hydro turbines are rotating at a much slower speed compared to steam and gas turbines. Steam and gas turbines are very sensitive to variation in speed changes and are prone to permanent damage if they operate above or below rated speed for some cumulative time over lifecycle. For example, for steam turbines, operation between 58.5–57.9 Hz may be permitted for 10 minutes before turbine blade damage is probable. This time is cumulative, meaning if a unit operates within this frequency band for 1 minute, then 9 more minutes of operation within this band are permitted over the life of the blades. On the other hand, hydro turbines do not have such a limitation. This advantage can be inferred from the NERC Protection and Control PRC-024 standard; Figure 27 illustrates generation frequency ride-through requirements for different interconnections. The no-trip zone in the figure illustrates the area where generators are required not to trip. Because the Quebec interconnection is decoupled from the Eastern Interconnection through DC links, and the fact that Hydro-Québec relies exclusively on large hydro resources, the no-tripping zone for Quebec (green line) was established to be much wider than the other interconnections (Western, Eastern, and the Electric Reliability Council of Texas) for both lower and higher frequency operation. It should be noted though that a generator may not necessarily trip even if it is operating outside of the no-tripping zone.

Because operating at low frequencies does not cause problems for hydro turbines, they do not have underfrequency protection. They might have only the quality protection that would, at some point, reflect that performance of auxiliary loads would be affected but only below the frequency levels at which UFLS (steam turbine tripping) occur. Loads like fans or pumps might have reduced flows due to lower frequency, because of which these resources might eventually trip. However, these problems would not happen immediately, allowing additional time to ride through the event and for the frequency to return to normal. Another reason for underfrequency tripping of hydro generators is that they may be part of a utility's underfrequency protection program. When steam and gas turbines (which are damaged by operating at low frequency) trip due to underfrequency, the hydro units may be dramatically overloaded. Because of this situation, these hydro units might be included in the utilities' generator underfrequency protection program. Utilities must coordinate their generator underfrequency tripping with NERC regional load-shedding programs.[1]

hydro units are therefore more rugged than the tapered blade designs found on other turbines. While manufacturers should be consulted for their specific recommendations, the abnormal frequency capability for continuous operation of a hydro unit is generally outside of the range from 57–63 Hz."

[1] WECC. 2011. *WECC Off-Nominal Frequency Load Shedding Plan*. Salt Lake City, Utah. https://www.wecc.org/Reliability/Off-Nominal%20Frequency%20Load%20Shedding%20Plan.pdf

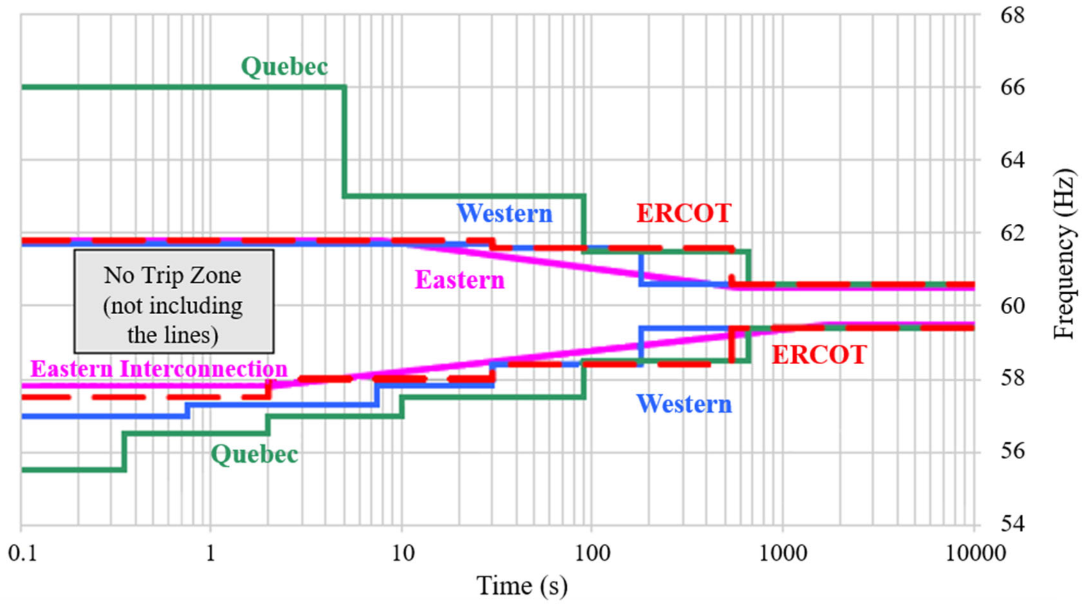

Figure 27. No-tripping zone requirement per NERC PRC-024 for different interconnections.[1]

The province of British Columbia is similar in its generation portfolio as the province of Quebec, Canada. Almost all generation resources are hydropower, but unlike Hydro-Québec it is not separated from neighbors (WI) by DC links; it is connected through Path 1 with Alberta Electric System Operator and through Path 3 to the United States (Bonneville Power Administration), so all are synchronized. This implies that the region is not shielded from frequency excursions due to events in its neighbors' footprints. However, owing to the large penetration of hydropower resources, BC Hydro can tolerate much larger frequency excursions, as will be shown in a modeling-based example below.

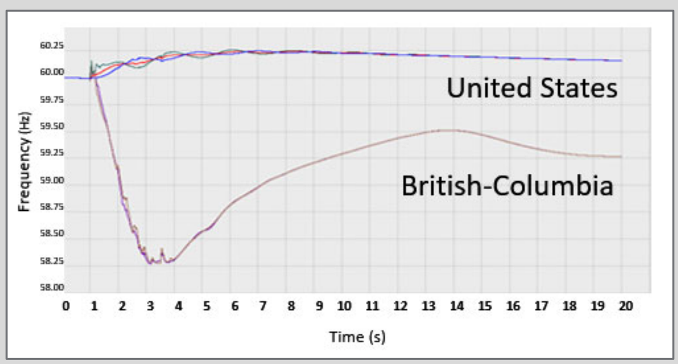

BC Example: During conditions of heavy imports from the United States, tripping of two Ingledow-Custer 500 kV lines (same right of way) causes the tripping of a 230 kV line that forms Path 3 because of a remedial action scheme to prevent them from overloading. Under this circumstance BC Hydro is islanded. As imports can account for a significant percentage of total energy needed, the frequency decreases significantly and load is shed to prevent frequency from going below 58 Hz. This figure illustrates such a case using the planning model.

Frequency in BC Hydro does indeed go very low while frequency in the United States does not change too much. This example highlights how low frequency can dip in some nonfrequent events, without any consequences, thanks to hydro resources in British Columbia, remaining online to maintain the grid support. While this frequency dip is still within the no-tripping zone requirement for WI, typically frequency within WI does not dip below 59.5 Hz for N-1 and credible N-2 contingencies. In this case,

[1] NERC. 2015. *Generator Frequency and Voltage Protective Relay Settings*. Standard PRC-024-2. Atlanta, Georgia. https://www.nerc.com/pa/Stand/Reliability%20Standards/PRC-024-2.pdf

since BC Hydro separated from interconnection, frequency reached 58.25 Hz and recovered due to load shedding and governor response. If the frequency had remained at 58.25 Hz for a longer time, hydro resources in BC Hydro would have remained in operation still providing support to the system, because hydro units usually do not need underfrequency generation tripping. Here is the sequence of events:

1. Light-load spring case with 2,424 MW loading on Path 3 (import into British Columbia)
2. UFLS tripped 25% of load in British Columbia
3. Frequency recovered at 59.25 Hz after initial nadir point dipped to 58.25 Hz
4. No generation tripped by underfrequency generation protection.

3.2.5 Hydropower's Role During Events Leading to Sudden Loss of Generation

In this section, the role of hydropower during sudden loss-of-generation events was explored. Hydropower usually has large rotational masses and, as a result, the stored kinetic energy in the rotational masses can provide significant inertial response to arrest the drop in the frequency during large disturbances. Fast governor action also allows hydro resources to act and recover from the drop in the frequency effectively compared to other resource types. The benefit of the hydropower resources in frequency response was explored both for historical events and through simulation studies. The observations from the historical events closely align with the simulation results showing the impact of hydro resources during grid disturbance events.

Simulation results show that hydroplants in the WI are a major resource for inertial and governor response during an extreme event that results in outage of a significant generation capacity in a short period. It can be concluded that the more hydro units online during such an extreme event, the better the interconnection's frequency response is. Table 11 shows the summary of contribution of hydropower toward primary frequency for the historical events as well as for simulation results. For all the cases examined, at least 30% of the primary frequency response came from hydro resources and can go as high as 60%.

Table 11. Summary of hydropower contribution towards primary frequency response.

Event Type	Hydropower Contribution
Historical Events in WI	30–61%
(Simulated) Largest contingency in WI	47–56%
(Simulated) Widespread NG plant outages in WI	32–38%

Loading and water availability conditions can lead to different levels of stress on the system. However, frequency response from hydropower units is consistent at different loading (high/low) and seasonal (winter/summer) conditions. During dry conditions, when there are fewer hydropower units online, interconnection frequency response could be negatively impacted.

Simulation results show that hydropower units have significant reactive power capability that helps in maintaining grid voltage stability during extreme events. Hydropower units provide additional reactive power support to maintain the local voltage schedule and, by extension, support interconnection-wide voltage stability. Local voltage support offered by hydroplants also ensures that hydropower plants can provide additional real power, which helps in recovering system frequency to the precontingency state.

While the simulation results are based on two events—the single largest contingency event in the WI and widespread outages of natural gas plants—they can be generalized to other extreme events where significant generation may be lost. Additionally, hydropower resources also provide frequency ride-through capabilities during large grid events, which is a unique characteristic of hydro resources compared other conventional generators.

3.3 Responses to Events Caused by Extreme Weather

This section examines the expected response of the future (2028) BES to two weather events: a late February 2008 cold wave and a summer heat wave in July 2011. As the penetration of wind and solar increases, the operation of the BES will be more closely coupled. Understanding which historical weather events will further stress the future system, and which are no longer concerning, is vital to valuing system resilience provided by different components of the system. This section investigates the resilience value provided by hydropower to ensure the future BES can withstand the 2008 cold wave and 2011 heat wave.

3.3.1 Scheduling Hydropower Flexibility During Weather Events

Production cost modeling (PCM) was used to simulate scheduling and dispatch of the system during long-term weather events and understand the value of hydropower flexibility to the system. Figure 28 shows the steps that can be involved in PCM. For this project the top two steps—namely, Hydro and Storage Scheduling and Day-Ahead Simulation—were used. Many hydro units are modeled as energy-limited resources to capture the water storage behind dams that exists at many hydropower plants. The first step decomposes those energy limits, which are typically modeled as monthly constraints, to daily constraints that can be used in the next step—i.e., Day-Ahead Simulation. In the first step, longer term storage, such as large pumped-storage generators, are also given daily targets that allow their longer-term operations to be represented in shorter, daily optimization horizons.

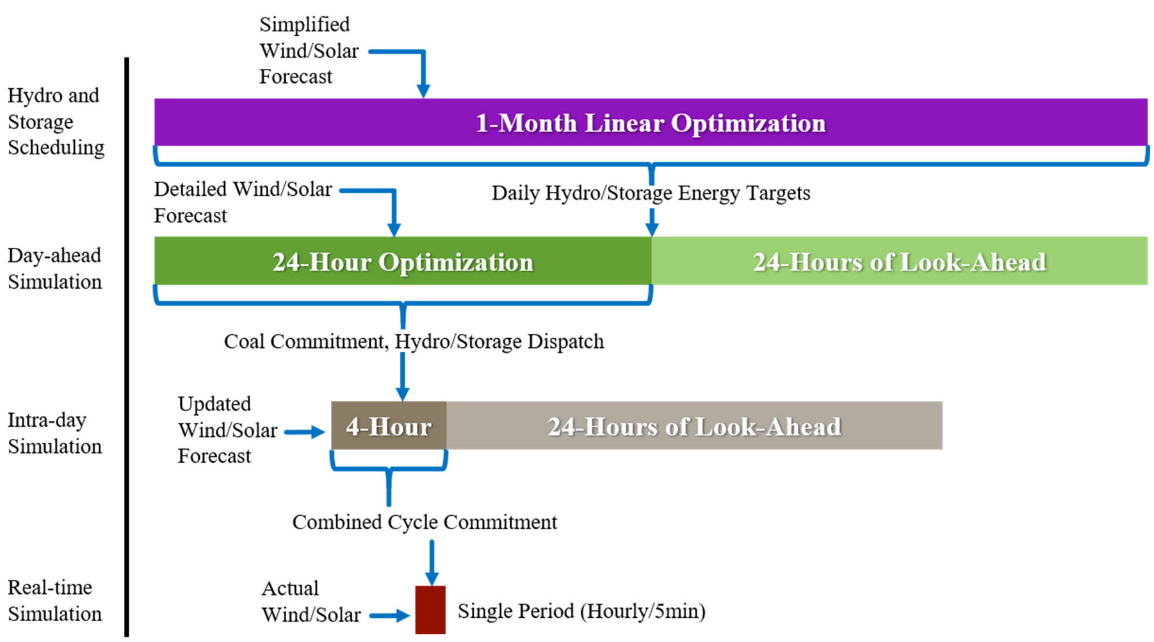

Figure 28. Flow diagram of the steps used in PCM to simulate system operations.

The next step simulates hourly operations of the system. To properly capture system ramping and minimum on and off times that exist at many large thermal generators, system dispatch is optimized for each full day. This is similar to the way an ISO or regional transmission organization would operate a day-ahead market. Chronological time series for load, wind, solar, and fixed or ROR hydro are included in full detail in this step. The PCM then runs an optimization for each day, minimizing the full system cost to meet load under a variety of technoeconomic constraints. More detail on what is and is not considered in PCM can be found in the *Eastern Renewable Generation Integration Study.*[1]

Often PCM is used to model a full year of system operations; however, this project used PCM to focus on system operations during particular, pre-identified weather events,[2] namely a February cold wave and a July heat wave. For that reason, the first step in Figure 28 was only modeled for the month around the weather event; the second step was only run for the days most impacted by the weather of the system.

A key requirement to model a specific weather event in a future infrastructure is to provide synchronous wind, solar, and load time-series profiles along with historical hydro energy limits, such that they all reflect the meteorology the system would experience if the event happened again. Applying the synchronous time-series data and hydro energy limits to a future system infrastructure allows investigation of that system's possible reaction to the historical weather event. In other words, the PCM has both a meteorological and an infrastructure year. The meteorological year is determined by providing wind, solar, load, and hydro profiles and limits that reflect historical meteorology. The tools used to create the profiles and limits are described in Appendix C. The infrastructure year is modeled using WECC's planned generation and transmission capacity in 2028 as given in the WECC 2028 Anchor Dataset (ADS). That infrastructure is used to model two weather events: a cold wave in February 2008 and a heat wave in July 2011.

The intent of the PCM is to simulate how the system might operate when confronted with particular conditions. However, there are a number of key limitations to PCM's ability to simulate system operations. In this project, all of WECC is modeled as one system, with a single objective function. In other words, there is a single system operator making dispatch decisions for the entire WI. In reality, a number of systems operators make unit commitment and dispatch decisions for their respective territories. In this project, a cost to exchange power between regions is included to capture the inefficiencies that exist when different system operators in the WI trade power with each other. This helps capture the effect of multiple decision makers within a single objective function model.

The system modeled for this project represents the WI in 2028, including generation and transmission capacity planned for the future. The case was built from the WECC 2028 ADS.[3] Figure 29 shows the generation capacity modeled for each aggregated region. In the future, results from the PCM, such as dispatch states of generators and flows on transmission lines, could be provided as inputs into power flow and contingency modeling covered in Section 4.1. Such additional load flow and dynamic modeling would provide a fuller picture of weather event impacts on the power system, system resilience vulnerabilities, and resilience benefits of hydropower. Appendix C describes the creation of the WECC 2028 ADS in PLEXOS. Having this database in PLEXOS allows for sharing of results back and forth between the PCM and power-flow modeling.

---

[1] Bloom A, A Townsend, D Palchak, J Novacheck, J King, C Barrows, E Ibanez, M O'Connell, G Jordan, B Roberts, C Draxl, and K Gruchalla. 2016. Eastern Renewable Generation Integration Study. NREL/TP-6A20-64472. National Renewable Energy Laboratory. Golden Colorado. https://www.nrel.gov/docs/fy16osti/64472.pdf.
[2] Novacheck J et al. "Extreme Weather Events in High Variable Generation Systems." Forthcoming.
[3] WECC. 2015. *Anchor Data Set* web page. https://www.wecc.org/SystemStabilityPlanning/Pages/AnchorDataSet.aspx

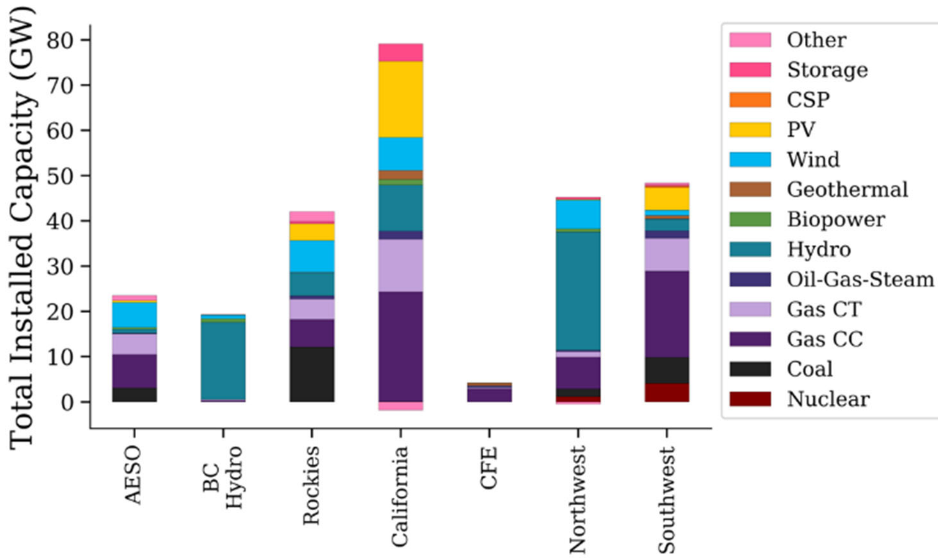

Figure 29. Installed generation capacity by region in the WECC ADS 2028 case.

3.3.1.1 Scenario 3: Hydropower Response during Cold Wave

A weak cold wave drifted down from Canada along the front range of the Rocky Mountains and into the Midwest between February 20–23, 2008. This led to cooler, but not dramatically cold temperatures across most of the West. Figure 30 shows high and low temperatures, along with pressure-gradient maps for the four key days of the event.

The front trapped weak storms and cloud cover in the WI. Not only did this limit solar generation in California and the Southwest, but it also led to stagnant air with little wind across much of the West. Low wind speeds combined with prevailing high pressure yielded light winds, clouds, and widespread light fog. Daily high temperatures were not especially cold, but overnight lows dipped into the 20s and 30s across most states in the West, except California. This led to cold mornings and elevated electric load during the morning peak across much of the WI, as will be shown later. Further details of the meteorology that drives this cold wave and its impact on the wind and solar resource can be found in the *Extreme Weather Events in High Variable Generation Systems* report.[1]

Impact on Wind and Solar Outputs, System Load, and Net Load

Figure 31 shows a heat map of the wind-resource deviation from average across the continent for this 4-day period in February 2008. The data used to create the map are modeled wind resources from the WIND Toolkit;[2] the average for each location on the map was calculated using the modeled wind resource for all days of the month around this event (15 days before and 15 days after) for the meteorological years 2007–2013. The deviation from the average shown in the figure is the difference between the 2008 wind generation output and the average output in 2007–2013 for this time of year. A darker red means less generation than average while blue indicates more generation than average. As seen in Figure 31, the wind resource is between below normal and well below normal across most of the country for the entire period; details are provided later in this section. This includes much of the WI, especially on February 20 and 21.

---

[1] Novacheck J et al. "Extreme Weather Events in High Variable Generation Systems." Forthcoming.

[2] National Renewable Energy Laboratory. 2021. *Wind Integration National Dataset Toolkit* web page. Golden, Colorado. https://www.nrel.gov/grid/wind-toolkit.html.

Figure 32 shows the deviation of the modeled solar daily capacity factor. The solar data used were created from the National Solar Radiation Database.[1] The average for each location on the map was calculated using the modeled solar generation for all days of the month around this event (15 days before and 15 days after) for the meteorological years 2007–2013. The deviation from average is the difference of the 2008 solar resources' output from that average. As seen in Figure 32, much of California and the Southwest has below-average daily capacity factors for this time of year.

Figure 33 summarizes total wind generation, solar generation, load, and net load for the entire WI during the 4-day cold wave. Time-series plots for wind and solar show the available generation (before curtailment) at all wind and utility-scale solar photovoltaic (PV) generators modeled in the WECC 2028 ADS. The solid-colored lines (blue for wind and gold for PV) show the available wind and PV generation for the cold wave event in 2008, while the dotted line shows the average output for this time of year based on 2007–2013 data. The statistical distributions shown on the right side of Figure 33 compare the daily average generation for wind and PV relative to two distributions. The colored distribution is all days in the same month as this event for 2007–2013. The dotted grey distribution is average daily generation for the entire wind and PV generation dataset; in other words, it contains all days between 2007–2013.

Similarly, the load and net load (load minus available generation from wind and PV) compares to the average for this time of year in WECC. This is done both on an hourly basis on the left side of the figure and based on daily load on the right. The grey dotted distribution on the right side of the figure also compares the load and net load to the full dataset, rather than just a seasonal comparison.

---

[1] National Renewable Energy Laboratory. N*ational Solar Radiation Database* web site. Golden, Colorado. https://nsrdb.nrel.gov

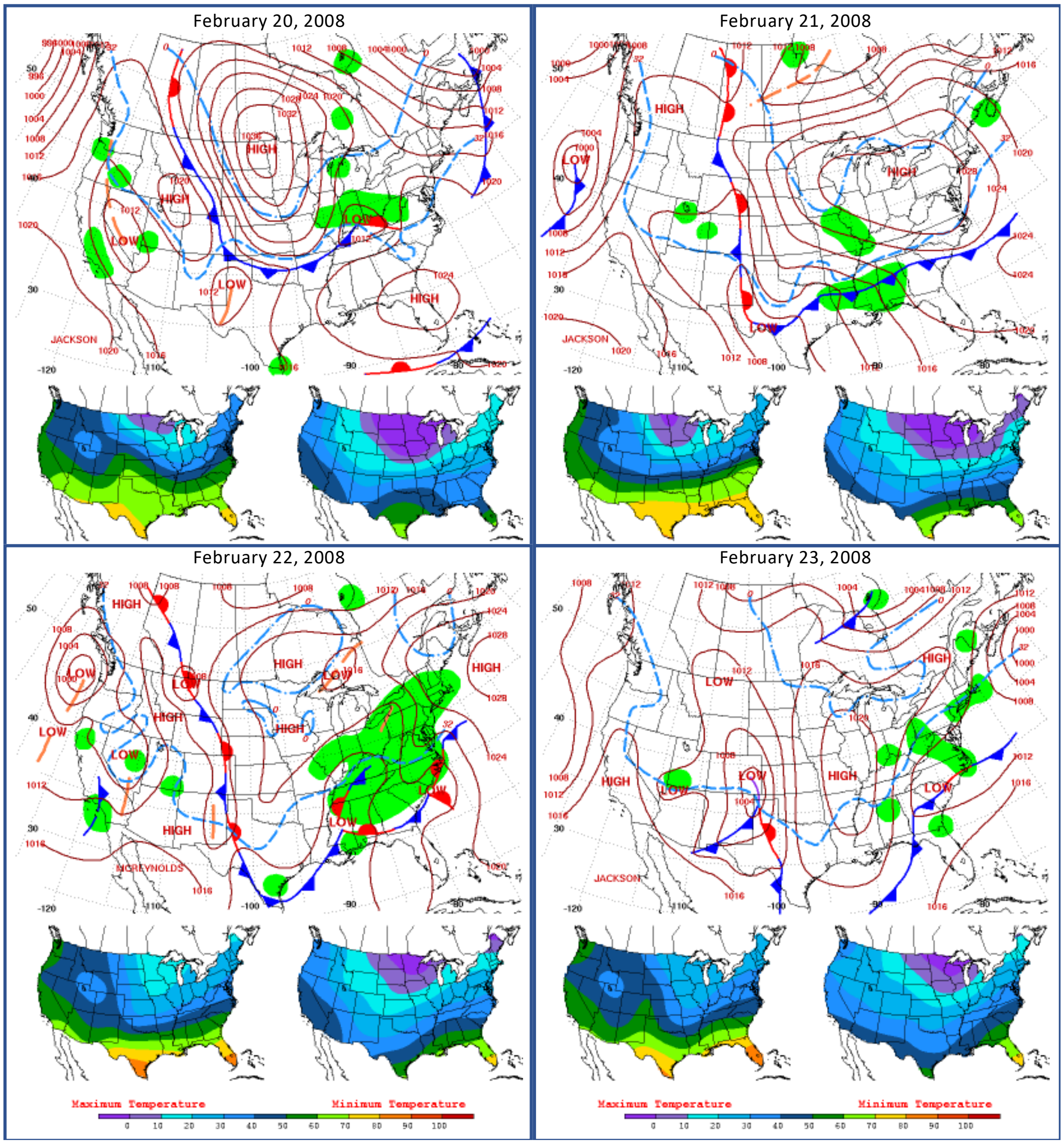

Figure 30. Surface weather and temperature maps valid at 7 am EST[1] for the cold wave case.

[1] Novacheck J et al. "Extreme Weather Events in High Variable Generation Systems." Forthcoming.

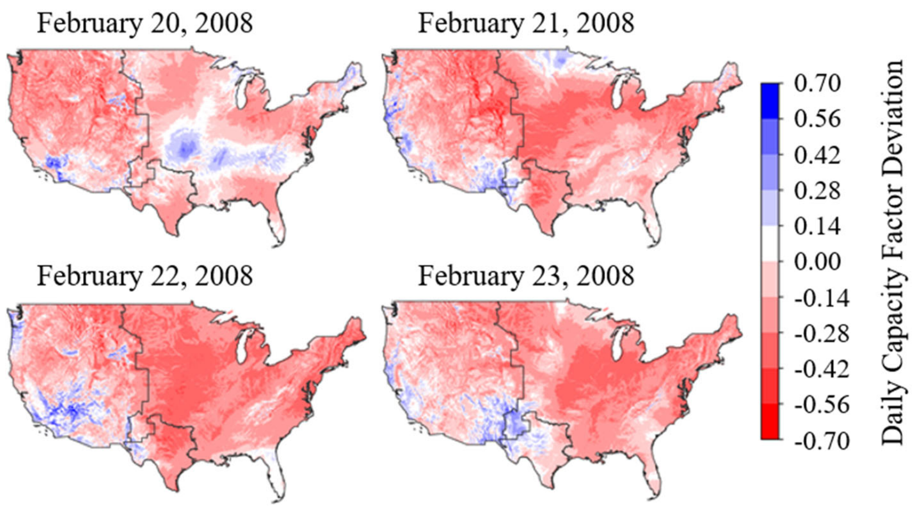

Figure 31. National daily average wind capacity factor deviation during the February 2008 high net-load event.

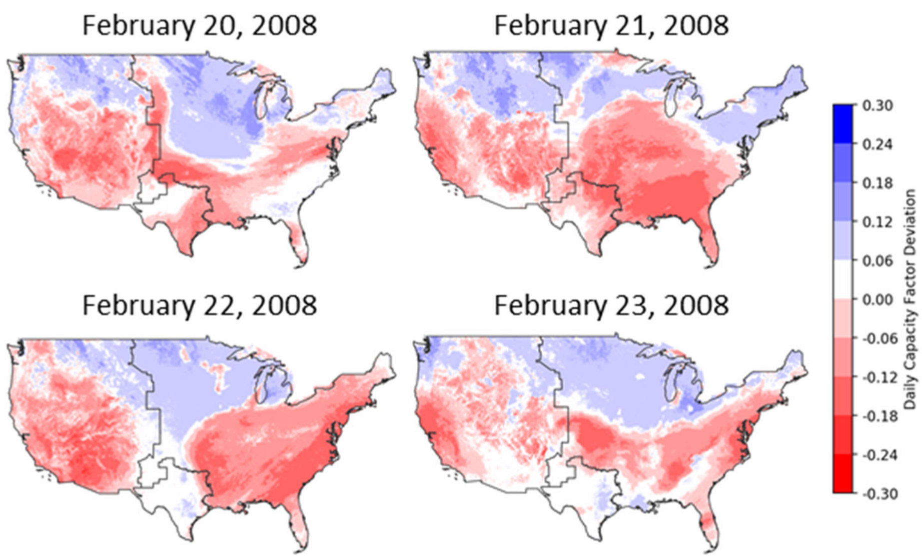

Figure 32. National daily average solar resource deviation during the February 2008 high net-load event.

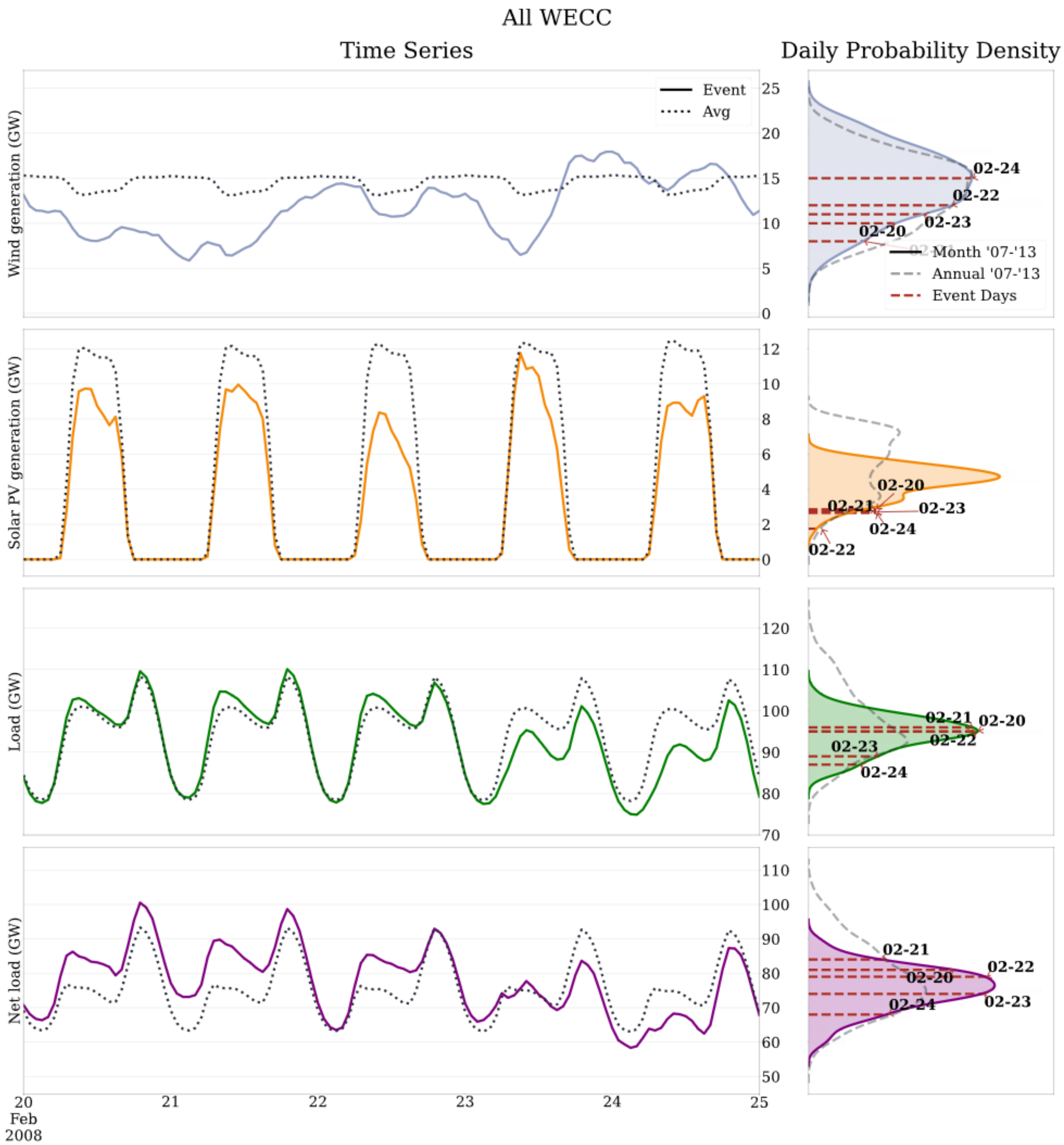

Figure 33. (Left) Hourly total wind generation, solar generation, load, and net load for all of WECC during cold wave event in February 2008 (solid color) relative to the average hourly generation for that time of year (dotted line). (Right) Distribution of average daily output/load for the time of year (colored distribution) and for the entire year (dotted grey distribution). Dotted red lines show the average output/load for one of the days of the event.

Figure 33 highlights how the wind and utility-scale solar PV generation is observed to be well below normal for all hours for the first 3.5 days of the simulated 2028 event. For wind, the 21st is in the low end of the tail of the seasonal and full dataset distributions. For much of the day on the 21st wind hovers between 30–60% of normal (~4–9 GW of aggregate generation). This is driven by low wind generation output in Canada, the Pacific Northwest, and the Rockies, where much of the installed capacity of wind in the WECC 2028 ADS exists. The other days of the event are not as extreme but are still below normal and in the lower half of the distribution.

Similar to wind, PV sees reduced output for all days of the event relative to normal conditions, as shown in Figure 33. Most of the utility-scale solar PV is in California and the cold wave kept much of California and the Southwest in a hazy fog. The 22nd, or third day of the event, has significantly depressed generation, especially in the afternoon when generation is 40-50% below normal. At 11 a.m., there is an 8.3 GW shortfall in PV output relative to average. This day is in the low end of the tail of both the seasonal and annual distributions, averaging only 2.6 GW of output (or a 10% capacity factor) throughout the day. It is one of the lowest output days for utility-scale PV generation in the dataset.

The weak cold wave does not create extreme loads; however, morning loads are elevated above normal, for the first 3 days of the event. This can be seen in the green hourly time-series plots in Figure 31. However, other than the higher morning peak, the daily average load is in the middle of the seasonal load distribution. The net load, however, is a different story. The combination of below-average wind and solar drive the net load above average for all hours for this time of year for the first 2.5 days of the event, as is shown by the purple hourly time series in Figure 33. February 21st, which is the lowest day for wind generation, approaches the high tail of the net-load seasonal distribution, suggesting this day, in particular, is one of the more challenging days for the system to have adequate resources to meet load. Hydro and other resources will have to help make up the deficit caused by this event.

Impact on System-wide Resource Dispatch and Hydropower Response

Figure 34 shows available dispatchable hydro energy in the WI between 2007–2013 for the month of February. This plot does not include data from hydro facilities that follow a fixed profile in the WECC 2028 ADS. February tends to be the lowest winter hydro generation month because water availability hits a low point before being recharged by spring runoff in March. February 2008 had average water availability relative to the rest of the dataset. The peak February water availability occurred in 2011 and was only 2.3% higher than 2008.

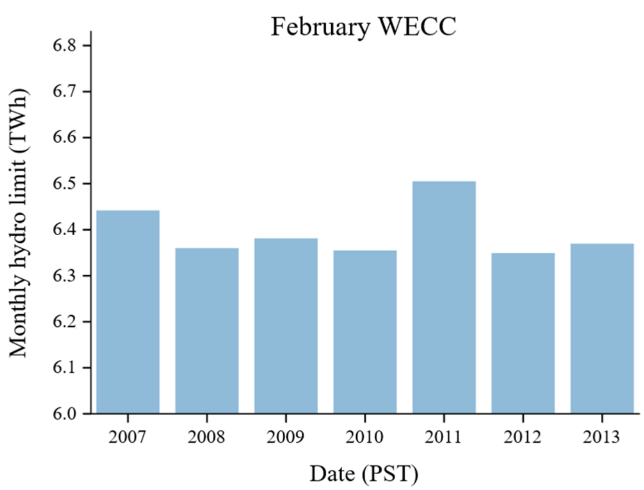

Figure 34. WECC hydro historic energy available for dispatchable hydro in February for 2007–2013.

Figure 35 shows results from the PCM of this cold wave event. The top dispatch stack shows the aggregate generation across the interconnection by type. Throughout the event, the interconnection aggregate thermal fleet barely changes its output. Nuclear (red) and coal (black) are essentially flat throughout the event. Natural gas (light and dark purple) ramp slightly throughout the week, but are also mostly flat. This leaves hydro (dark teal) to both load follow and make up for wind and solar resource deficits described earlier.

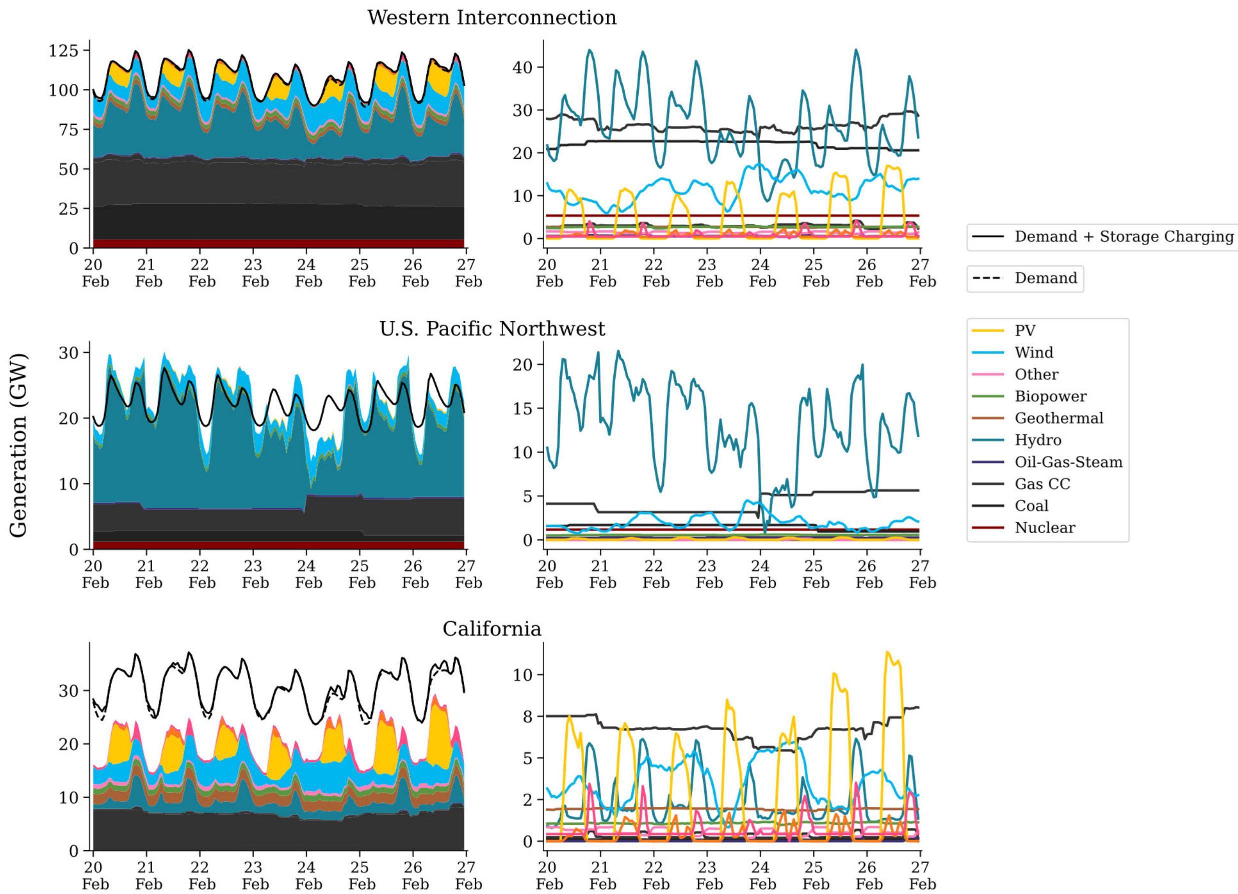

Figure 35. Generation dispatch stacks for the entire WI (top), the Northwest (middle), and California (bottom), February 20–26, 2008.

The dispatch results of this event show the value of dispatchable hydro, especially in the Pacific Northwest, to fill in the gap both by shifting generation hourly and changing total daily output. Figure 36 shows the daily dispatchable and nondispatchable hydro from the region during the event. Hydro generation has the highest houly peak (Figure 35) and provides the most daily energy (Figure 36) on February 20, 21, and 22, the highest net-load days of the event. On those days, daily energy from aggregate dispatchable hydro is between 15–33% higher than the monthly average, as shown by the horizontal dotted line in Figure 36. By operating above this level on these three days, hydro resources must reduce output at other times in the month to make up the difference. This is valuable flexibility provided by hydro at this time. Notice that even on these days, hydro still follows the load in the Northwest and California (Figure 35), reducing its output in the middle of the day and at night. Throughout the event the correlation coefficient between hydro generation and WI net load is greater than 0.9. This is especially obvious and dramatic overnight between February 21and February 22 when the wind resource recovers throughout the interconnection, and Northwest hydro takes an opportunity to ramp down to save water for generation later in the day. Three of the four days that follow February 22 have less hydro generation relative to the evenly split monthly energy limit. As the wind and solar resources recover and the cold wave disappates, hydro takes the opportunity to reduce output.

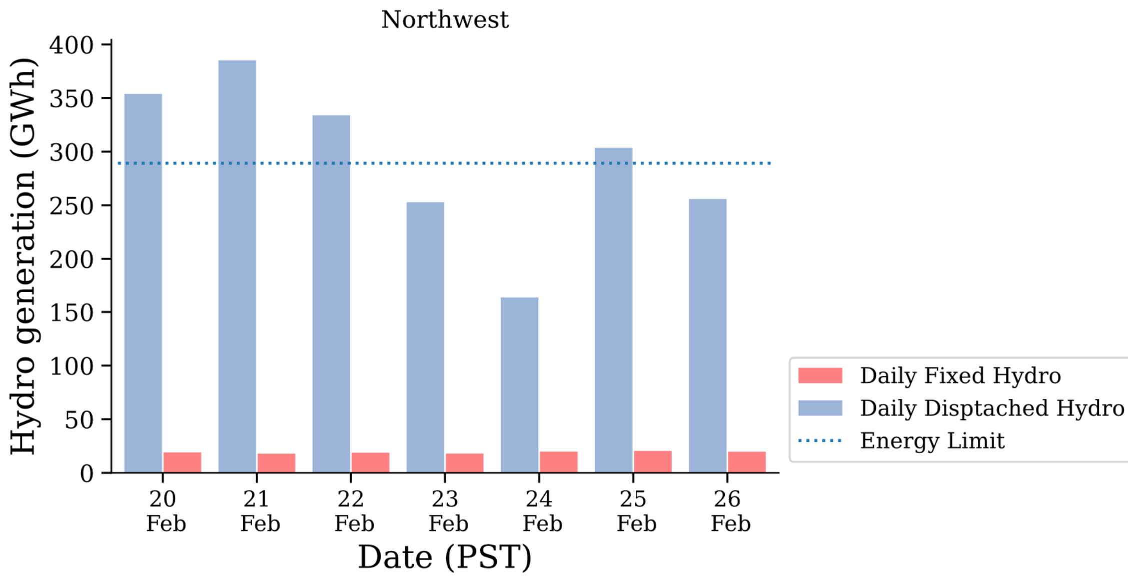

Figure 36. Daily dispatchable and fixed hydro generation in the Pacific Northwest with a dotted line showing the average generation from dispatchable hydro if the monthly energy limit was equally allocated over every day.

Figure 37 shows the net interchange of power from the Pacific Northwest to its neighbors, including California. On February 20 and 21, the Pacific Northwest exports to California throughout the day, maxing out export capability in the evening when California hits its net-load peak. Transmission is key in this case to enable the system to take advantage of the Northwest's hydro flexibility. Combined, the two infrastructures (transmission and hydro) make up for the reduced output from California solar and wind throughout the WI.

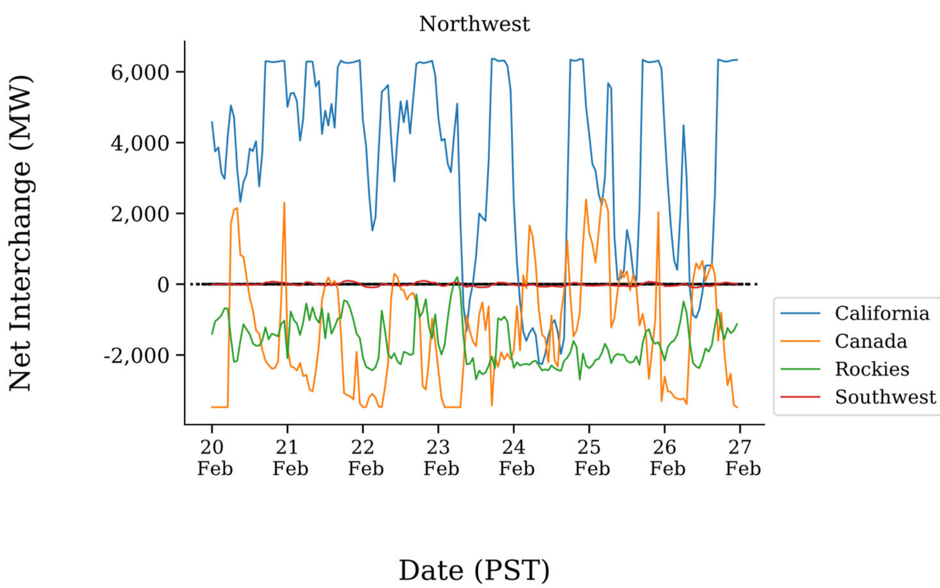

Figure 37. Net exports from the Pacific Northwest to its neighbors. Positive values are exports from the Pacific Northwest and negative values are imports into the Pacific Northwest.

After February 22, California solar recovers enough, as does interconnection-wide wind, for Pacific Northwest hydro to turn down and import excess solar from California during the middle of the day. However, Northwest hydro ramps up in the evening again to make up for the ramp down in solar generation at sunset in California. At this time of year, sunset also concides with regional and interconnection-wide peak load.

Dispatchable California hydro exhibits similar behavior to hydro in the Northwest; however, California's hydro is much more inflexible. Figure 38 shows the hourly generation of dispatchable and fixed hyrdo resources and demonstrates that generation of dispatchable and fixed hydro in California is not well correlated. Fixed hydro is mostly load following, while the dipatchable hydro is used almost exclusively at the daily net-load peak. More flexible operations of the fixed hydro would yield higher value and be more benefical to the system during events such as when California solar generation is depressed.

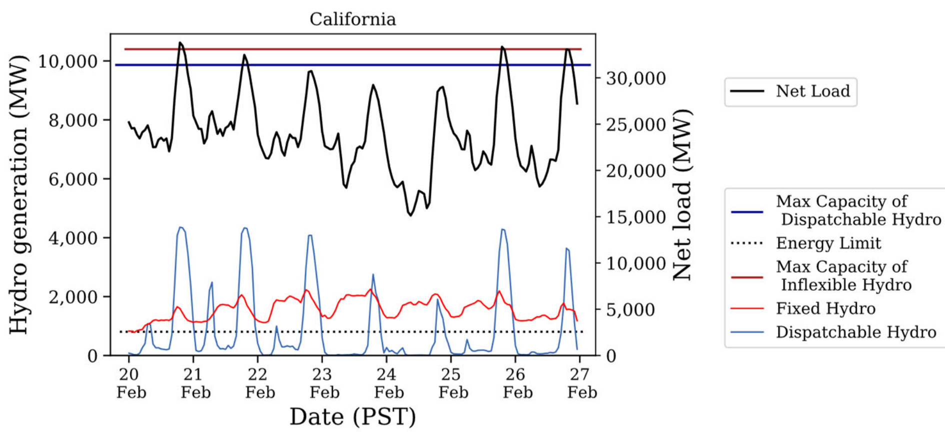

Figure 38. Hourly dispatchable and fixed hydro generation in California with dotted line showing the average generation from dispatchable hydro if the monthly energy limit was equally allocated to every hour.

1.1.1.1 Scenario 4: Hydropower Response during Heat Wave

Summer 2011 broke heat records across U.S weather stations with either the daytime high temperatures or overnight low temperatures hotter than ever recorded for the contiguous United States for that period. The average U.S. temperature was 74.5°F, which was 2.4° above the long-term (1901–2000) average. This record-breaking heat wave hit the western U.S., with Arizona breaking the record for the day at 111°F and California recording 110°F on July 18, 2011. Temperatures in Nevada and Colorado reached 105°F and 100°F, respectively. New Mexico had its warmest summer ever recorded, peaking at 102°F during the day and 80°F overnight on July 20, 2011. Apart from these actual extreme high temperatures during the day, the endurance of the heat made it even more remarkable, with exceptionally warm nights. These pervasive high temperatures can be seen in Figure 39. Further details of the meteorology that drove this significant heat wave and its impact on wind and solar resources can be found in the *Extreme Weather Events in High Variable Generation Systems* report .[1]

[1] Novacheck J et al. "Extreme Weather Events in High Variable Generation Systems." Forthcoming.

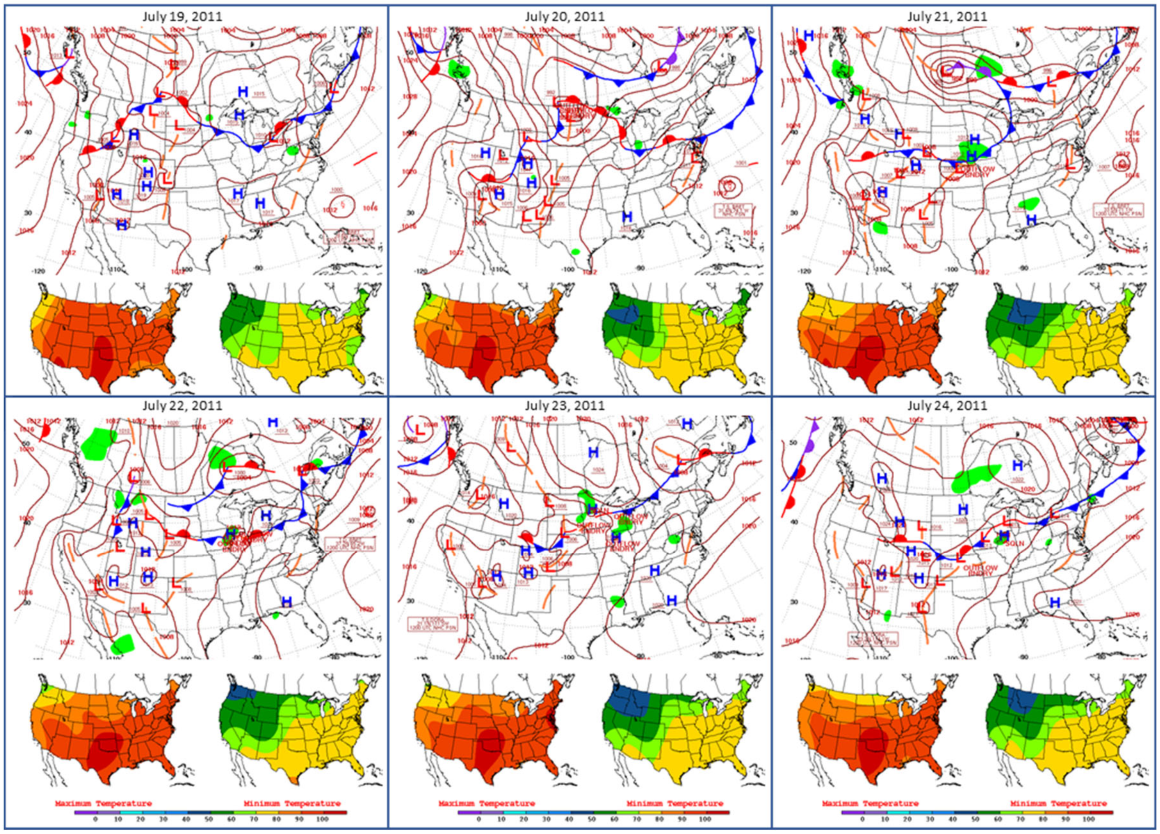

Figure 39. Surface weather and temperature maps valid at 7 a.m. EST.[1]

Impact on Wind and Solar Outputs, and System Load and Net Load

Figure 40 summarizes the total wind generation, solar generation, load, and net load for the entire WI during the week of July 16, 2011. See the discussion of Figure 33 to understand details of the various plots.

Figure 40 shows that both wind and solar resources were near normal for the time of year in the WI. Wind was depressed slightly relative to the higher resource seasons, as seen in the difference between the grey dotted and blue distributions on the right-hand side of the figure, besides July 20, which was above average for the season. Also, wind followed a strong diurnal pattern that is typical of this time of year. Wind generation hit minimum output as the sun began to rise and then increased again in the evening as the sun began to set, staying high for the evening and overnight hours. Utility-scale PV had nearly uniform generation every day of the event, as the heat wave had little impact on the PV resource. Load was slightly elevated on July 18, 19, and 20 relative to normal conditions for the time of year, showing some impact of the heat wave, but was hardly extreme given the daily average load was not in the extreme tail of the seasonal distribution in Figure 40. The combination of elevated, but not extreme load and above-average wind and solar resource, the net load was also near normal if not slightly depressed from average.

[1] Novacheck J et al. "Extreme Weather Events in High Variable Generation Systems." Forthcoming

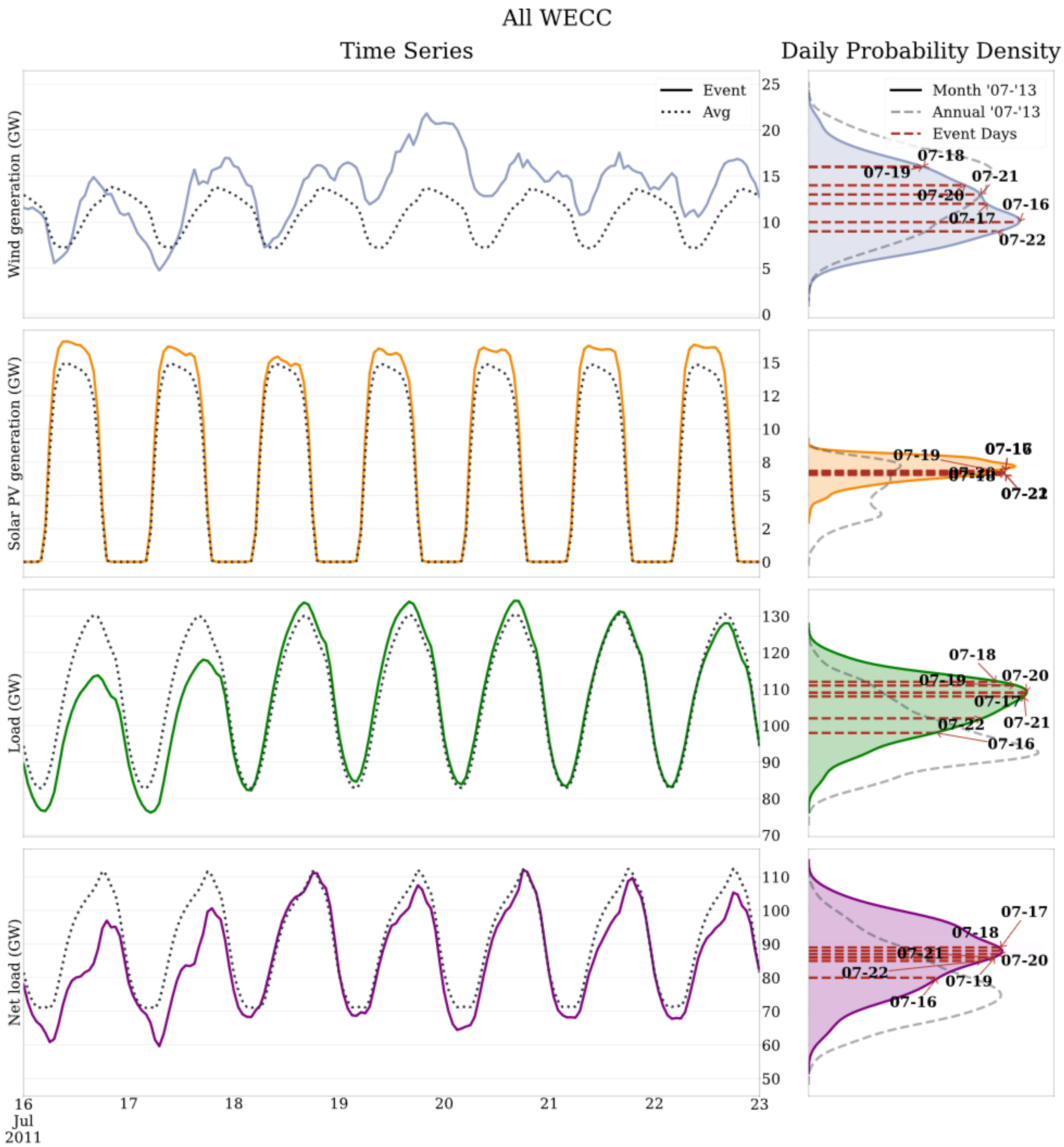

Figure 40. (Left) Hourly total wind generation, solar generation, load, and net load for all of WECC during a heat wave in July 2011 (solid color) relative to the average hourly generation for that time of year (dotted line). (Right) Distribution of average daily output/load for the time of year (colored distribution) and for the entire year (dotted grey distribution). Dotted red lines show the average output/load for one of the days of the event.

Impact on system-wide resource dispatch, and hydropower's response

Figure 41 shows how 2011 dispatchable hydro energy availability in WECC compared to the years between 2007–2013 for the month of July. This plot does not include hydro facilities that follow a fixed profile in the WECC 2028 ADS. July can be quite variable in hydro availability depending on the timing of the spring runoff and its magnitude. July 2011 was the wettest July in the 2007–2013 datasets, as seen in Figure 41.

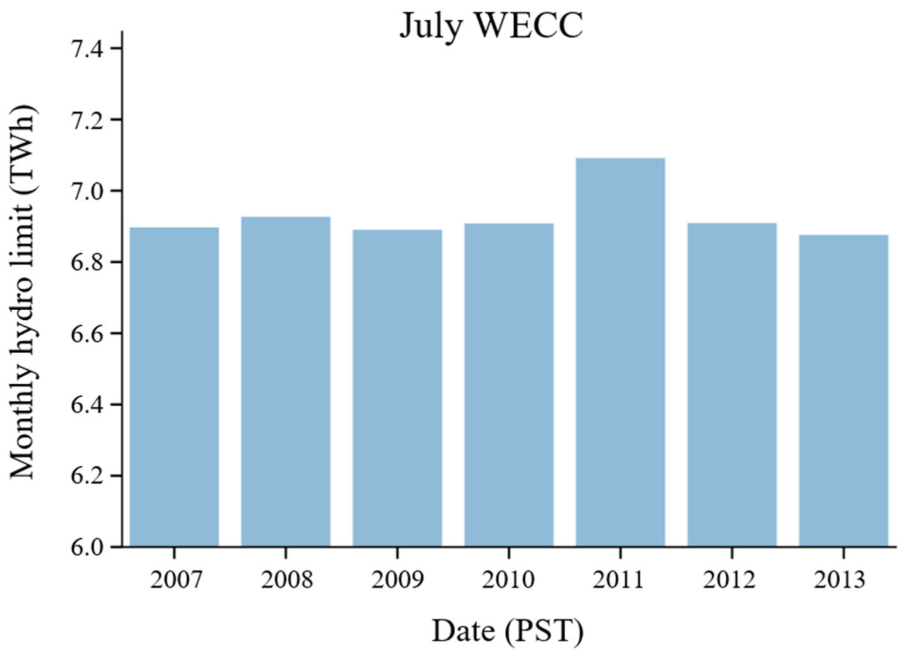

Figure 41. WECC historical energy availability for dispatchable hydro in July for 2007–2013.

Figure 42 shows the generation dispatch results from the PCM. Even though the heat wave did not lead to a significant wind and solar resource deficit, hydro still played a vital role in ensuring resource adequacy and balancing of the system. Hydro contributed the most energy of any generating resource while ramping and following net load, when allowed to provide its flexibility. The first row of Figure 42 shows the dispatch for the full interconnection. Except for a few overnight hours on the 16th and 22nd, hydro generation was always greater than 25 GW, interconnection wide. Most days hydro ramped up in the daytime hours, increasing its output by approximately 70%. The timing of the hydro peak typically occurred after sunset and even after the actual peak load, to provide capacity when it was needed most, at peak net load.

The difference in operations between California and Northwest hydro shows some of the limits to the value of hydro flexibility. The heat wave particularly increased loads in California. The solar resource was strong in California, as shown in the last row of Figure 42. However, load is still elevated when solar generation begins to decrease. Dispatchable hydro in California delayed its ramp up until at solar peak or after in order to provide needed capacity at the peak net load.

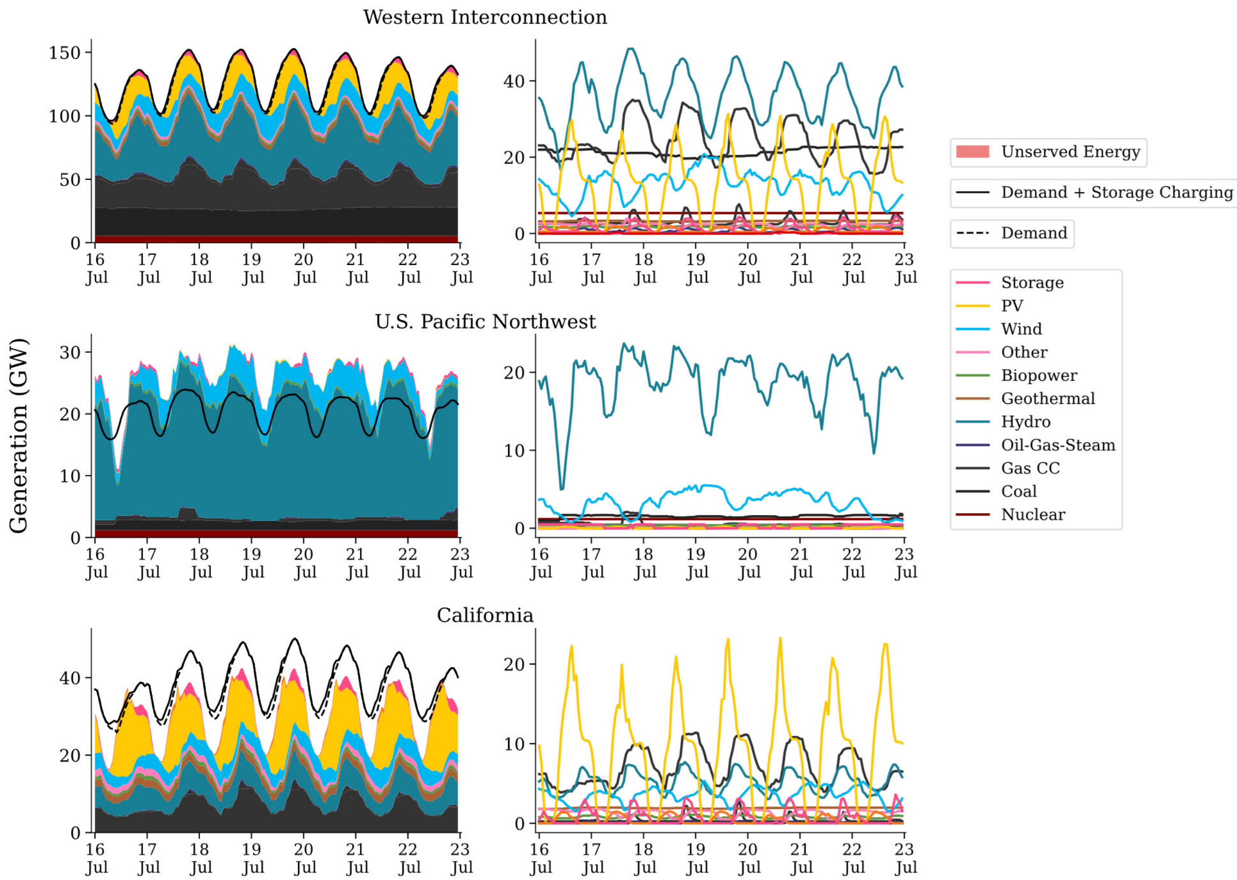

Figure 42. Generation dispatch stacks for the entire WI (top), the Pacific Northwest (middle), and California (bottom) between July 16–22, 2011. The left-column shows the total generation stacked, while the right-hand corner shows each generating technology as its own time series.

On the other hand, hydro in the Northwest followed local load, which was not particularly impacted by the heat wave, very closely. Ideally, the hydro would have been most valuable to follow the net load in California instead. However, as shown in Figure 43, there was little to no transmission availability for hydro to provide this value. The figure also shows the net interchange from California to its neighbors during this event. The lines and interfaces connecting the Northwest and California were predominately used to export power from the Northwest to California and operated near their maximum transfer capability for nearly all hours of the heat wave. Without more transfer capability, the Northwest's hydro value is limited to assist California through the event.

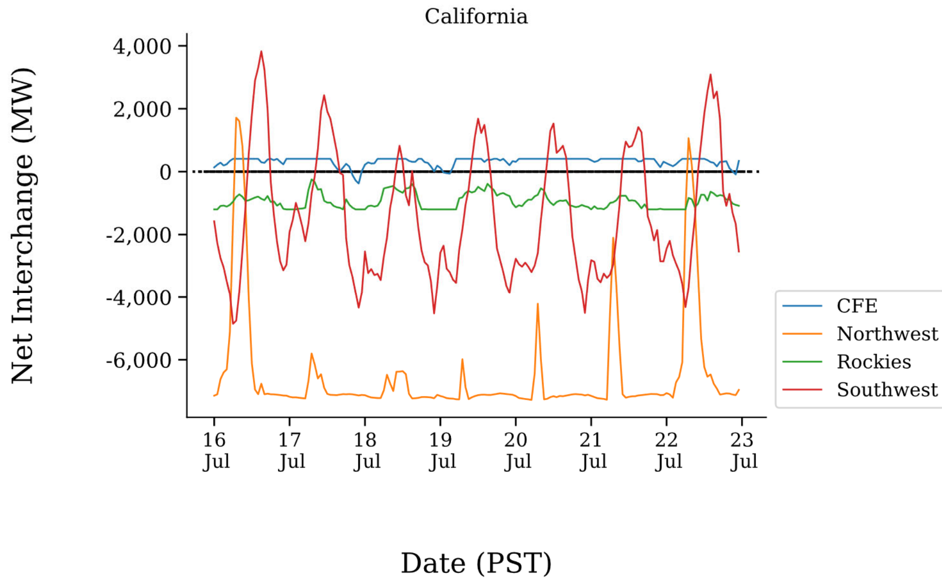

Figure 43. Net exports from California to its neighbors. Positive values are exports from California and negative values are imports into California.

3.3.2 Summary of Hydropower's Role During Extreme Weather Events

In summary, as the penetration of wind and solar increases, cold and heat waves like these will continue to present operational and planning issues to the BES. Future systems will see more weather events that have a larger impact on wind and solar generation availability than they do on load. For example, while the February 2008 cold wave was not so severe as to cause a dramatic increase in load, it did depress wind and solar generation, as shown in Figure 33. In this case, hydro used its flexibility to fill the gap by using its long-term storage and hourly ramping flexibility to provide energy and capacity when needed. In the July 2011 heat wave, wind and solar total energy were not negatively impacted by the resulting weather. However, hour-to-hour variability of the resource shifted the peak net load until after solar PV had peaked, but before wind had increased its output in the evening. In this case, the flexibility of California hydro resources enabled them to supply energy during hours around sunset, as shown in Figure 43. The flexibility compensated for the more severe hour-to-hour variability introduced to the system by the increased wind and solar capacity. The Northwest's hydro was unable to provide that same flexibility because export capacity to California was already at its maximum. This demonstrates how other infrastructure, transmission in this case, is key to enable hydro's full flexibility and resilience value to a high variable generation system, such as the modeled WECC 2028 ADS.

To further the understanding of hydropower's resilience value to the BES during extreme weather events, future work should focus on a variety of hydro flexibility and availability sensitivity analyses. For example, sensitivities that increase or decrease hydro's ability to shift its monthly water availability around from day to day or to limit the amount dispatchable hydro can ramp down at any one hour. Many hydro facilities will be up for relicensing in the coming decade and in many cases this flexibility is at risk. This sensitivity analysis would help inform resilience impacts of losing flexibility. Also, understanding how changing water availability (i.e., wet and dry years) impacts hydro's resilience value is important. For both categories of sensitivities, comparing how the production costs change and how the system changes its operations will allow more direct quantification of hydro's value. Finally, linking the system dispatch with power flow and contingency modeling would create better understanding of risk and hydro's value in both modeling domains.

4.0 Summary

In this study, the role of hydropower resources in supporting grid reliability and resilience was analyzed for a range of extreme events. These assessments were conducted using a combination of historical data and simulation-based analysis. The report highlights different methodologies, tools, models, and datasets that are needed to carry out analyses on the role of hydropower in maintaining grid reliability and resilience. The main findings from the study are:

1. Hydropower is critical in stabilizing the WI after events causing sudden large loss of generation. The contributions of hydropower resources were observed to be consistent across different combinations of seasons, system loading, and water availability conditions. Hydropower's contributions also were consistent across different types of scenarios resulting from sudden loss of online generation capacity.

   - Analysis of historical data and simulation results shows that hydropower plants are a major resource for inertial and governor response during extreme events in the WI. Specifically, it was observed that hydropower facilities, collectively, contribute between 30–60% of governor response[1] to help stabilize system frequency after outage events. It should be noted that hydropower generation constitutes between 20–25% of generation capacity in the WI grid.

   - Hydropower units have significant reactive power capability that helps maintain voltage stability during extreme events. Hydropower's ability to provide reactive power is similar to other conventional generation resources. However, conventional resources, especially baseload steam turbines (coal) and nuclear plants, operate close to their rated power capacities, which leaves little room to provide reactive power. Hydropower resources (and natural gas plants) generally operate at less than full capacity, which allows them to provide more reactive power support when needed. Simulation results for the WI show that hydropower units are a major source of reactive power support under all seasonal, loading, and water availability conditions.

   - Other characteristics of hydropower units that can enhance a system's response and recovery attributes include a wide band of frequency ride-through ability and black start support. Analysis of past events and existing regulatory standards, such as North American Electric Reliability Corporation Protection and Control Standard 24, demonstrate that hydropower units can withstand a much wider range of frequency deviations compared to other conventional resources. This capability of hydropower resources can allow them to stay online longer than conventional resources after extreme events, which can help with quicker system recovery after those events.

2. Hydropower's storage capability and dispatch flexibility are critical to ensure system reliability during extreme weather events. Simulation results from extreme weather scenarios for the western United States showed significantly depressed wind and solar generation even though the impact on system load was not extreme. It was observed that hourly flexibility of hydropower resources was used to fill the resulting energy and capacity gaps. The cold wave scenario lasted over multiple days, and hence, hydropower resources' long-term storage capability was key in ameliorating the situation.

[1] In a study conducted by American Governor Company, *The Impact of Hydroelectric Power and Other Forms of Generation on Grid Frequency Stability for the WECC Region*, the authors estimate that for the WI grid as a whole in 2008, hydropower generation contributed between 25–90% of the primary frequency control response in the first 10 seconds after an underfrequency event, before intervention from automatic generation control.

In the past and in simulated future event scenarios, this study demonstrated that hydropower resources contribute significantly to grid reliability and resilience during extreme events. The analyses in this study suggest that as the magnitude and frequency of extreme and stressful grid conditions increase, hydropower will continue to play a vital role in power system reliability and resilience. However, more work needs to be done to fully assess the role of hydropower under all potential combinations of future grid states and extreme events. The modeling framework developed in this project can be leveraged to assess some of these combinations, such as contingency events during extreme weather conditions with different water availability conditions. The toolchain established for this analysis also can be combined with capacity expansion models to determine hydropower's role in maintaining grid resilience under different realization of future grid states, such as those achieving 80-100% decarbonization by 2035.

Appendix A

Dynamic Contingency Analysis Tool Framework

Appendix A

Dynamic Contingency Analysis Tool Framework

A.1 Story Line: Hydropower During an Extreme Event

Dynamic and steady-state hybrid simulations were performed to determine the impact of the extreme events and to better understand how well hydro generation can help the system to recover from such events. Simulations were performed on the WECC 2018 LS case by using Pacific Northwest National Laboratory's Dynamic Contingency Analysis Tool (DCAT).[1] The simulation results are helpful to assess the impact of an extreme event and potential subsequent cascading events across systems and interconnections. DCAT simulations
provide insight into where reinforcements or other mitigation measures on the BES may
be most effective.

The main framework of the DCAT procedure was built with General Electric Positive Sequence Load Flow (PSLF) codes. Figure A.1 shows the main flow chart of the DCAT procedure. It includes the following steps:

- *Step 1*: The dynamic simulation of the given system is run with a flat start.
- *Step 2*: A severe disturbance, such as loss of a substation or power plant, is applied (the simulation time after the disturbance is defined by the user). The dynamic remedial action scheme (RAS) criteria are tested during the simulation.
- *Step 3*: Incremental dynamic simulation is run for every 3 s of simulated time, checking whether the system reaches steady state when the speed variances of all the synchronous machines are within a user-defined tolerance.
- *Step 4*: If the steady-state condition is reached, the steady-state RAS is tested and the power-flow case is extracted from the dynamic simulation.
- *Step 5*: The extracted post-dynamic simulation power-flow case is solved.
- *Step 6*: Corrective actions are applied to the solved post-dynamic simulation power-flow case to mitigate the voltage and line and transformer overloading violations.
- *Step 7*: Overloaded lines and transformers are checked and ranked based on overload after corrective actions. If there are no overloaded facilities, the DCAT procedure stops; otherwise, the DCAT procedure starts a new dynamic simulation by tripping the overloaded facilities with highest rank and the procedure goes back to Step 3.

[1] Samaan NA, JE Dagle, YV Makarov, R Diao, MR Vallem, TB Nguyen, LE Miller, BG Vyakaranam, S Wang, FK Tuffner, and MA Pai. 2015. *Dynamic Contingency Analysis Tool – Phase 1*. PNNL-24843. Pacific Northwest National Laboratory. Richland, Washington.
http://www.pnnl.gov/main/publications/external/technical_reports/PNNL-24843.pdf.

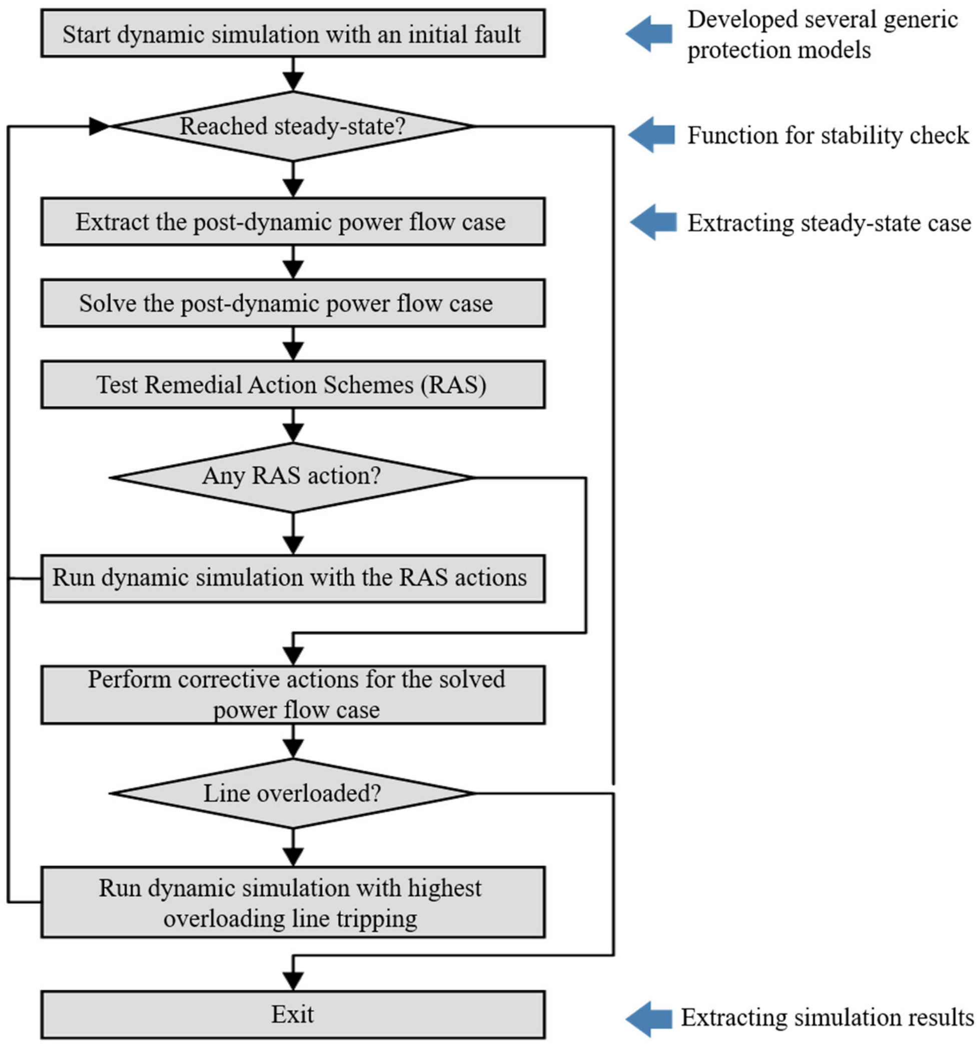

Figure A.1. Modeling approach using DCAT for a single natural gas contingency.

A.2 Dynamic Models

The modeling of protection was demonstrated as were features added to PSLF to achieve the sequence of events that follow a major disturbance, which are dynamic and steady-state cascading outages caused by various relay and protection devices.[1] Generic protection schemes that are currently implemented in DCAT using PSLF include the generic generator protection system (*gp2*), low/high-voltage ride-through (*lhvrt*) generator protection, low/high-frequency ride-through (*lhfrt*) generator protection relay models, transmission distance protection relays (Zone 1, Zone 2 and Zone 3 protection using the *zlin1* model) and transformer-protection relays (time-inverse overcurrent relay: *tiocrs*). The settings for generator

[1] Vyakaranam B, N Samaan, B Thomas, WW Price, M Vallem, R Huang, R Diao, and Y Makarov. 2018. "Modeling of Protection Relays using Generic Models in System-Wide Power System Dynamic Simulation Studies." *IEEE PES General Meeting*, Portland, Oregon.

protection relays are taken from National Energy Reliability Council (NERC) Standard PRC-024-1[1] These models are added to the existing dynamic models in the real-world case, which includes generator, governor, stabilizer, and exciter models for generator-side dynamics. A more detailed version of protection modeling, depending on the area of investigation, will be added in future phases of the project.

A.3 Dynamic Simulation

Dynamic simulation is a computationally intensive task. An appropriate tradeoff is necessary to run the dynamic simulation long enough to capture the dynamic response of the system. The appropriate time can be determined by having stability checks at intermediate times that could stop the dynamic simulation.

To extract a useful power-flow case at the end of dynamic simulation for a corrective action task, the system must reach a steady state at the end of dynamic simulation. An EPCL script was developed to run a stability check at the end of each dynamic simulation period. The script has the following steps:

Step 1: Run dynamic simulation for the required period, T0 (T0 = 60 s in this study). The dynamic RAS is tested during dynamic simulation.

Step 2: Run the stability check.

Step 3: If the system reaches a steady state, steady-state RAS criteria are also tested. Otherwise, continue to run dynamic simulation for $\Delta T = 3$ more seconds and then go back to Step 2. This process will continue until the maximum simulation time Tmax is reached. The simulation will print out the status and save the power-flow case.

Step 4: Extract the power-flow case and go to the corrective action stage.

The algorithm for stability is shown as a flow chart in Figure A,2.

[1] NERC Standard PRC-024-1. *Generator Frequency and Voltage Protective Relay Settings.* https://www.nerc.com/pa/Stand/Reliability%20Standards/PRC-024-1.pdf.

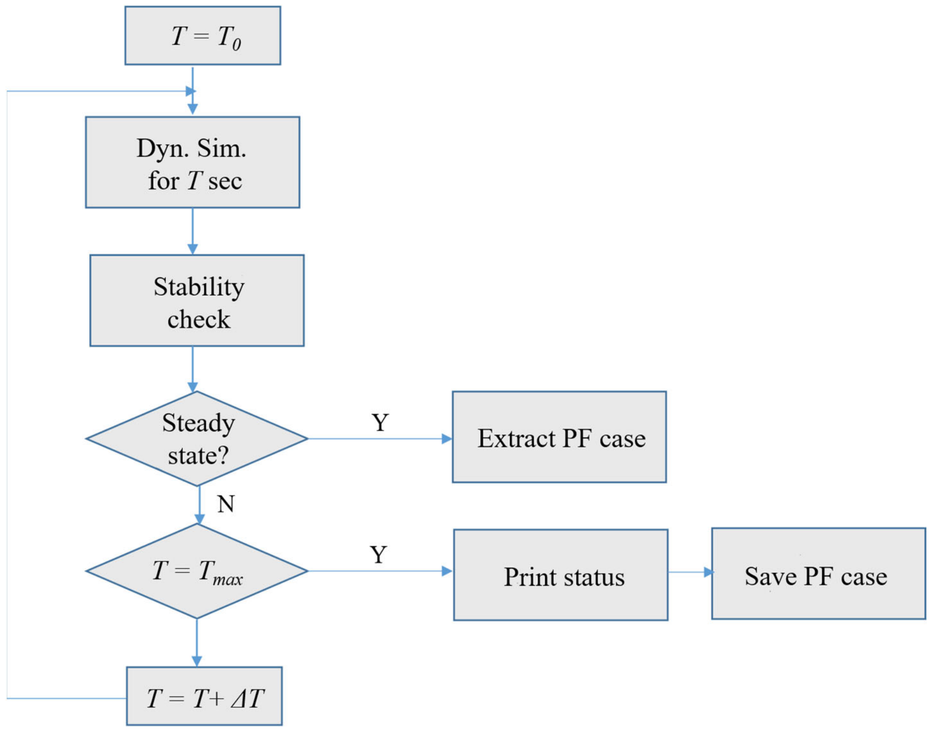

Figure A.2. Algorithm for stability check.

A.4 Modeling of Corrective Actions

Utility operators perform corrective actions,[1,2] such as generation redispatch, capacitor switching, transformer-tap changes, phase-shifter tap changes, line switching, load shedding, generator tripping, etc., aimed at alleviating system problems caused by contingencies. These corrective actions can have different implementation times and different effects on the system. For example, redispatch is constrained by the ramp rates of the generators and generally can alleviate system overloads. However, capacitor switching and transformer-tap changing can be faster and have the potential to rectify system bus voltage violations. There could be other faster acting controls, such as line switching, load shedding, and generation tripping.

[1] Vaiman M, P Hines, and J Jiang. 2013. "Mitigation and prevention of cascading outages: Methodologies and practical applications." 2013 IEEE Power & Energy Society General Meeting, pp. 1–5. Vancouver, Canada. DOI: 10.1109/PESMG.2013.6672795.

[2] NERC Standard PRC-023. 2014. *Transmission Relay Loadability*. NERC, Atlanta, Georgia. http://www.nerc.com/_layouts/PrintStandard.aspx?standardnumber=PRC-023-3&title=Transmission Relay Loadability&jurisdiction=United States.

For the current implementation of DCAT, generation redispatch,[1] shunt switching, transformer-tap changing, phase-shifter tap changing, and load shedding are the corrective actions considered. The process of identifying corrective actions is formulated as an optimal power-flow[2,3] problem with the objective function of minimizing control shifts subject to constraints of control limits and operating conditions. The goal is to restore the system to a reliable and secure state in a given short period with as little control movement as possible. Switching actions will be implemented by protection relays in the dynamic simulation block of DCAT.

An optimal solution thus represents a minimal corrective action scheme that resolves system security violations. This section gives a condensed formulation of this minimal corrective action, optimal power-flow problem. The optimization solver is based on linear programming. Discrete controls, such as shunt susceptance and transformer-tap ratio, are treated as continuous variables at first, and when the solution reaches some tolerance, they are fixed at the nearest steps. The details on objective functions and various corrective actions and their constraints can be found in Dong et al.[4]

A.5 Simulation Automation Simulation

An automation capability is developed for DCAT to simulate natural gas contingencies. Figure A.3 shows the simulation approach used in this study. In this approach, the first dynamic simulation is initiated using DCAT by considering the first set of generator outages from a natural gas contingency list. The final power-flow case at the end of the first DCAT simulation is used as an input to run the second natural gas contingency, and the process continues until the DCAT runs are completed for all the list contingencies or system divergences. DCAT saves power-flow cases, along with the sequence of events, at various stages of simulation. Figure A.4 shows the flowchart of the automated process of running a multicontingency study.

---

[1] Wang C and M Shahidehpour. 1994. "Ramp-rate limits in unit commitment and economic dispatch incorporating rotor fatigue effect." *IEEE Transactions on Power Systems*, vol. 9, no. 3, pp. 1539–1545. 9(3):1539–1545. DOI: 10.1109/59.336106. Available at https://ieeexplore.ieee.org/document/336106.
[2] Capitanescu F and L Wehenkel. 2008. "A New Iterative Approach to the Corrective Security-Constrained Optimal Power Flow Problem." *IEEE Transactions on Power Systems* 23(4). DOI: 10.1109/TPWRS.2008.2002175. https://ieeexplore.ieee.org/document/4620169.
[3] Dong F, L Huang, B Lam, and X Xu. 2012. "Practical applications of preventive security constrained optimal power flow." *2012 IEEE Power & Energy Society General Meeting*, San Diego, California. DOI: 10.1109/PESGM.2012.6344734. https://ieeexplore.ieee.org/document/6344734.
[4] Dong F, B Vyakaranam, N Samaan, R Huang, B Thomas, WW Price, and M Vallem. 2018. "Restoration of System Security with Optimized Corrective Actions." *IEEE PES General Meeting*, Portland, Oregon.

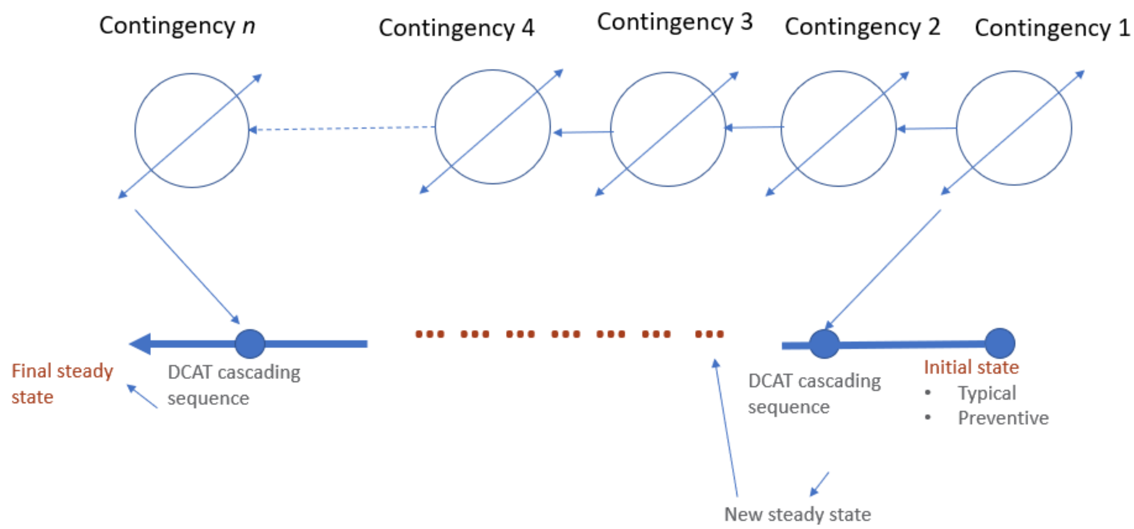

Figure A.3. Natural gas BES simulation approach for a multicontingency study.

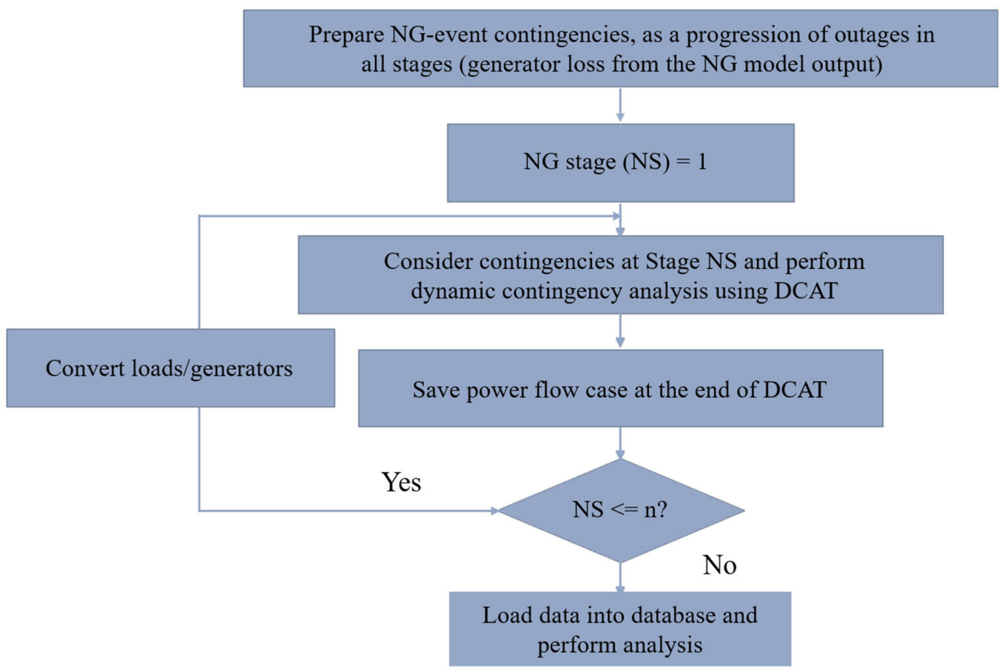

Figure A.4. Automated process flowchart of running a multicontingency study.

A.6 Database Management Module Framework

DCAT simulations for a large, interconnected power system produce valuable engineering information that can be used to develop actionable recommendations; however, the information is difficult to extract. The difficulty comes not only from the number of events analyzed, but also from the different types of result data produced in DCAT: system intermediate power-flow cases, time series from dynamic simulations, corrective actions, and a summary of relay operations. We developed a module to extract DCAT output information from multiple scenarios and multiple stages of cascading outages and to save that data to MongoDB. Figure A.5 illustrates various datasets that can be extracted using this module.

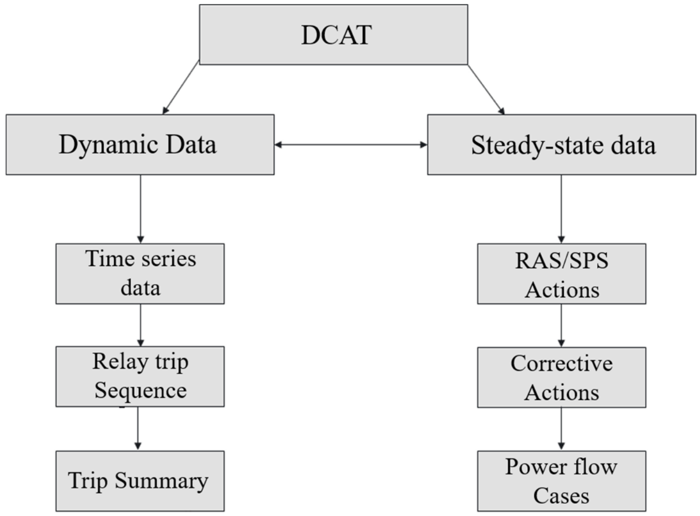

Figure A.5. DCAT data sets.

The datasets are described below:

1. *Time-Series Data*
   This dataset has all the time-series data for all simulation variables (machine shaft speeds, bus voltages and angles, real and reactive flows) during each contingency that are monitored during dynamic simulation runs.
2. *Relay Trip Sequence and Trip Summary*
   This summary lists all the tripping information for actions immediately after each contingency event that are captured in the dynamic simulation. A summary of the sequence of relay trips observed during the dynamic simulation is saved for analysis.
3. *RAS Actions*
   A new dynamic simulation is allowed to run for a few seconds from a flat start and a special protection system (SPS)/RAS action is then implemented. The dynamic response of the interconnected system to such SPS/RAS action is captured and loaded into the database.
4. *Corrective Actions*
   All modifications that the corrective actions[1] have made on the case for each contingency are recorded. In the current implementation, generation redispatch, shunt switching, transformer-tap changing, phase-shifter tap changing, and load-shedding transformer taps are considered.
5. *Power-Flow Cases*
   Static data from each steady-state case are extracted and saved in the database. This includes bus, branch, load, generator, and interface data.

A.7 Database: MongoDB

An advanced data management module is being developed for DCAT using MongoDB with existing simulation results. We need this capability and an enhanced interactive visualization for DCAT to analyze and better understand the DCAT simulation results. Several Python scripts are prepared to save DCAT simulation results directly into MongoDB.

[1] Dong F, B Vyakaranam, N Samaan, R Huang, B Thomas, WW Price, and M Vallem. 2018. "Restoration of System Security with Optimized Corrective Actions," *IEEE PES General Meeting*, Portland, Oregon.

A.8 Commonly Used Parameters in Database Collections

DCAT uses a hybrid dynamic and steady-state approach to simulate cascading outage sequences that include fast dynamic and slower steady-state events. Table A.1 shows parameters commonly used in database tables during dynamic and steady-state processes; they are depicted in Figure A.6.

Table A.1. DCAT commonly used parameters.

Parameter	Description
INIT_EVENT_ID	Events used in DCAT simulation (different hurricanes)
SCENARIO	Options applied to DCAT simulation, such as with or without corrective actions
COUNT_ID	Contingency number in hurricane contingency list
STAGE_ID	Dynamic simulation stage, automatically assigned according to result file names
SNAP_ID	Steady-state stage, automatically assigned according to result (1 after DCAT reaches steady state; 2 after RAS/SPS actions; 3 after corrective actions)

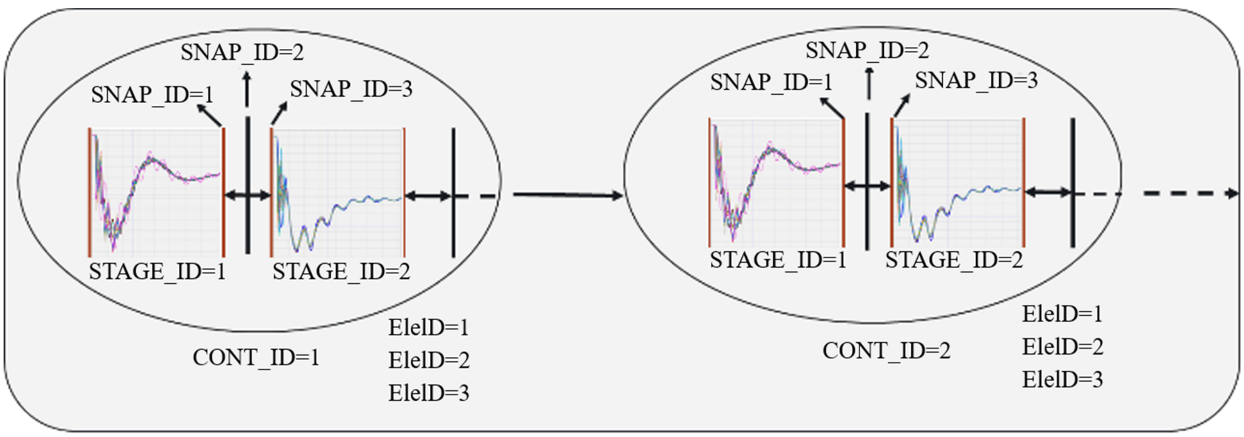

Figure A.6. DCAT parameters used in database collections.

A.9 Graphical User Interface for Analytics and Visualization

The graphical user interface for DCAT analytics and visualization was developed as a standalone Windows application based on a Windows Presentation Foundation framework. This application accesses MongoDB to display a list of contingencies and generates graphs illustrating system responses for various initiating events. It also allows query development to extract information from the database. Engineering knowledge and experience analyzing extreme events are factored into the design of the interface. The complete automation capability for analyzing hurricane contingencies using DCAT is shown in Figure A.7.

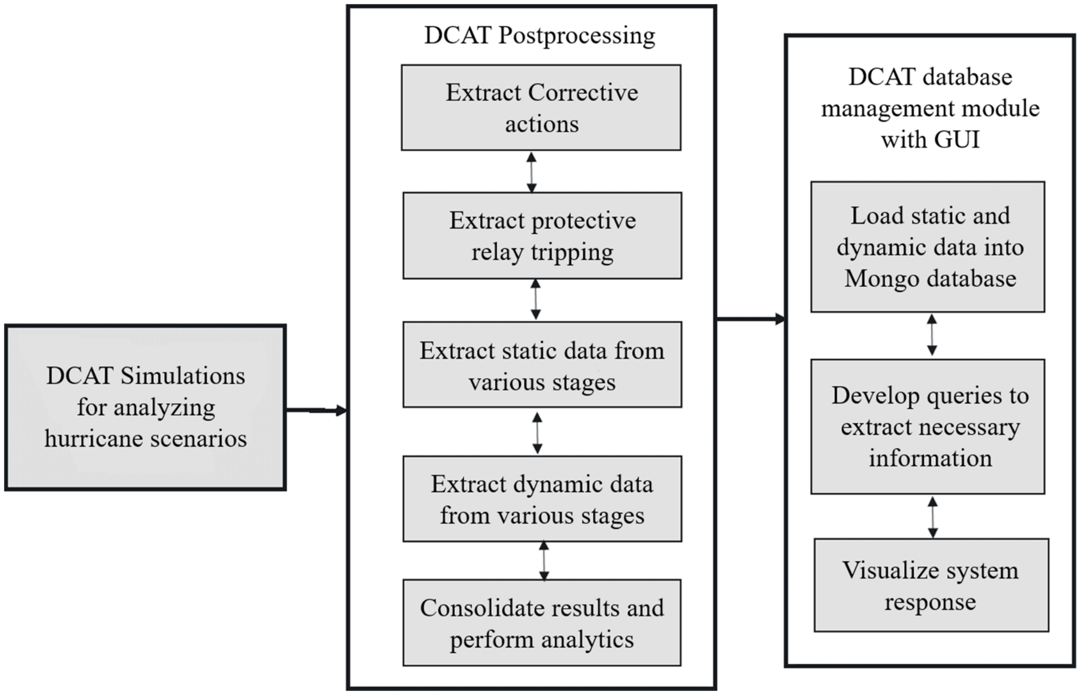

Figure A.7. Complete automation capability for analyzing hurricane scenarios.

Appendix B

Development of Dry Hydrological Cases

Appendix B

Development of Dry Hydrological Cases

To simulate dry-year conditions, U.S. Army Corps of Engineers (USACE) data for Northwest hydro resources 2015 (dry-hydro year) were used. The power flow and dynamic cases were adapted using the base 2018 WECC Planning case. Figure B.1 shows a comparison of Grand Coulee hydropower availability across seasons and different hydrological conditions.

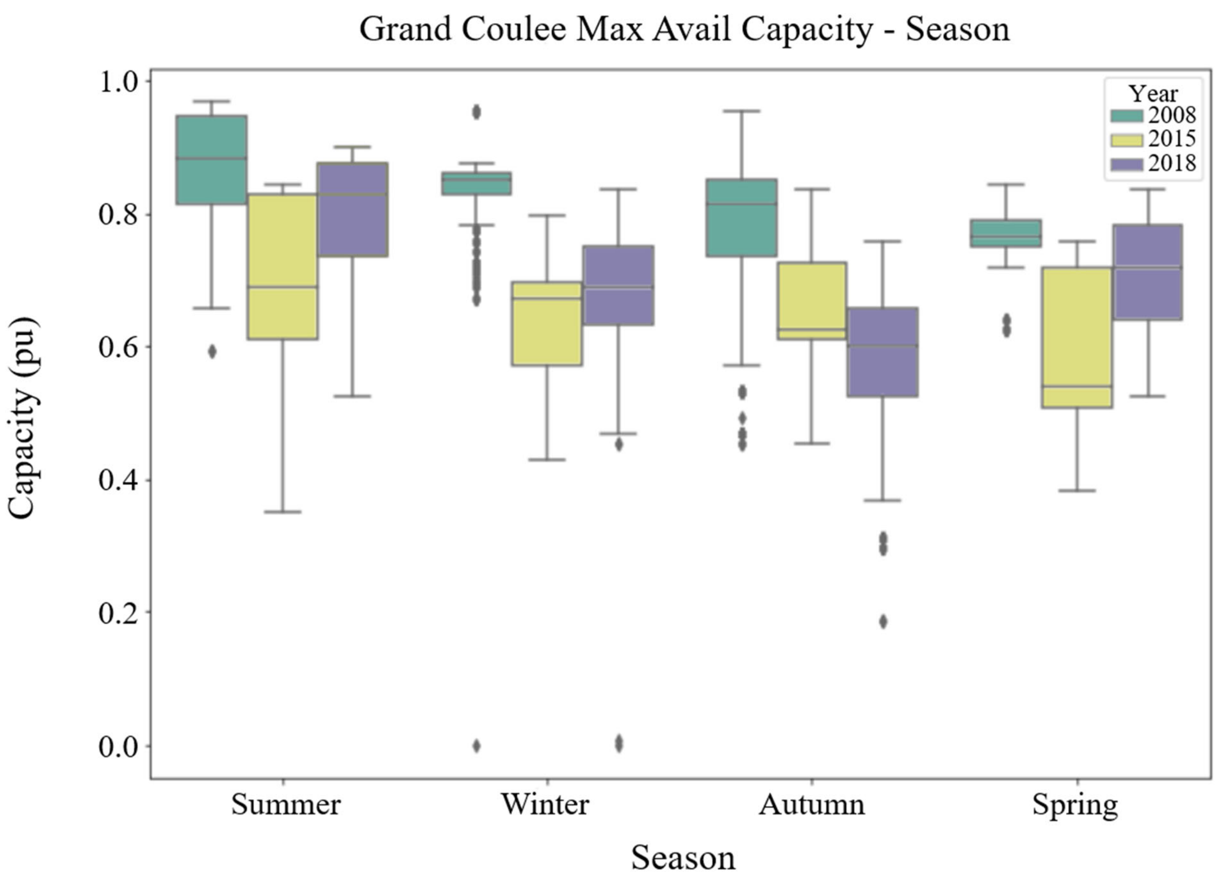

Figure B.1. Comparison of Grand Coulee hydropower max available (per unit) capacity across seasons and different hydrological conditions.[1]

Methodology used for approximate representation of dry-hydro conditions with minimal changes to generation and load dispatches:

- USACE available capacity (MW) for Northwest hydro resources
- Adjust area 40 hydro resources with Pmax >30 MW
- Summer Pmax_dry = 85% average year Pmax

[1] USACE. 2021. *Query Timeseries from USACE Northwestern Division* web page. https://www.nwd-wc.usace.army.mil/dd/common/dataquery/www/

- Winter Pmax _dry = 72% average year Pmax
- Units where Pgen >Pmax _dry,
- Pmax _dry = Pgen+2% reserve margin
- Parameters changed in PSLF cases:
- Power-flow data: Pmax= Pmax_dry and Mbase = Pmax_dry/0.95 (using 0.95 power factor) for selected generators
- Dynamic data: mwcap = P_{max_dry} and mva = P_{max_dry}/0.95 for selected generators.

Appendix C

Long-Term Weather-Based Extreme Events Scenarios

Appendix C

Long-Term Weather-Based Extreme Events Scenarios

C.1 WECC 2028 Anchor Dataset Translation

This section describes the process of translating the WECC ADS from ABB's GridView to PLEXOS by Energy Exemplar. Although WECC uses GridView for its modeling and analysis, this effort is intended to leverage the already existing capability in modeling extreme events at the National Renewable Energy Laboratory (NREL) using PLEXOS.

The ADS 2028 PCM represents the expected projection of load, resource mixes, and transmission topology 10 years into the future for a given reference year. The initial stage of this translation focused on relevant data collection from GridView's Microsoft Access database files for various objects. A high-level breakdown of these data is shown in Table C.1.

Table C.1. Summary of key assumptions in the WECC 2028 ADS.

Unit Category	Description	Modeling Methodology
1. Hourly Renewable	Wind and solar (solar tracking/fixed axis/behind the meter)	Hourly shape based on NREL hourly profiles
2. Hourly Hydro	Inflexible hydro insensitive to load or price with load shapes. This includes hydro and hydro renewable portfolio standard units (plants with capacities from 10–30 MW in California) with hourly profiles	Hourly shape
3. Proportional Load Following Hydro	Hydro sensitive to load and locational marginal pricing	Proportional load following
4. Pump Storage	Pump storage	Pumped storage
5. Dispatchable Thermal	Conventional resources, such as gas and coal-fired	Units dispatched if cost effective and needed
6. Must Run Thermal	Biomass, biogas, geothermal, cogeneration, and combined heat and power	Thermal that must run if available, with output typically set to a high minimum value
7. Plant Parts	Operationally tied units, typically units within a combined-cycle plant	Same as dispatchable thermal
8. DC Interties	DC tie flows (e.g., Blackwater DCI)	
9. Motor Load	Negative generation representing synchronous pump motor loads	Hourly shape based on historical data
10. Volt-amperes reactive (VAR) Device	Power-flow resources representing VAR support devices	
11. Off-Line	Resources that should be considered offline (e.g., retired, out of service, indefinitely on standby)	Turned off in the model

Unit Category	Description	Modeling Methodology
12. Energy Efficiency/ Demand Response	Loads being reduced to reflect energy efficiency and demand response	Energy efficiency: Hourly shape based on area load shapes Demand response: Hourly shape based on response forecasts
13. Generic Storage	Storage facilities with unknown details, battery storage	Pumped storage
14. Other Hourly Resources	Resources that exist or are planned but whose modeling is uncertain or incomplete	

Figure C.1 shows steps involved in creating the PLEXOS database, using NREL's PLEXOS Input Data Generator tool[1] to aggregate the data into a PLEXOS database. Other NREL additions to the model included time-synchronous wind, solar, load, and monthly hydro limits for the historical metrological years of 2007–2013.

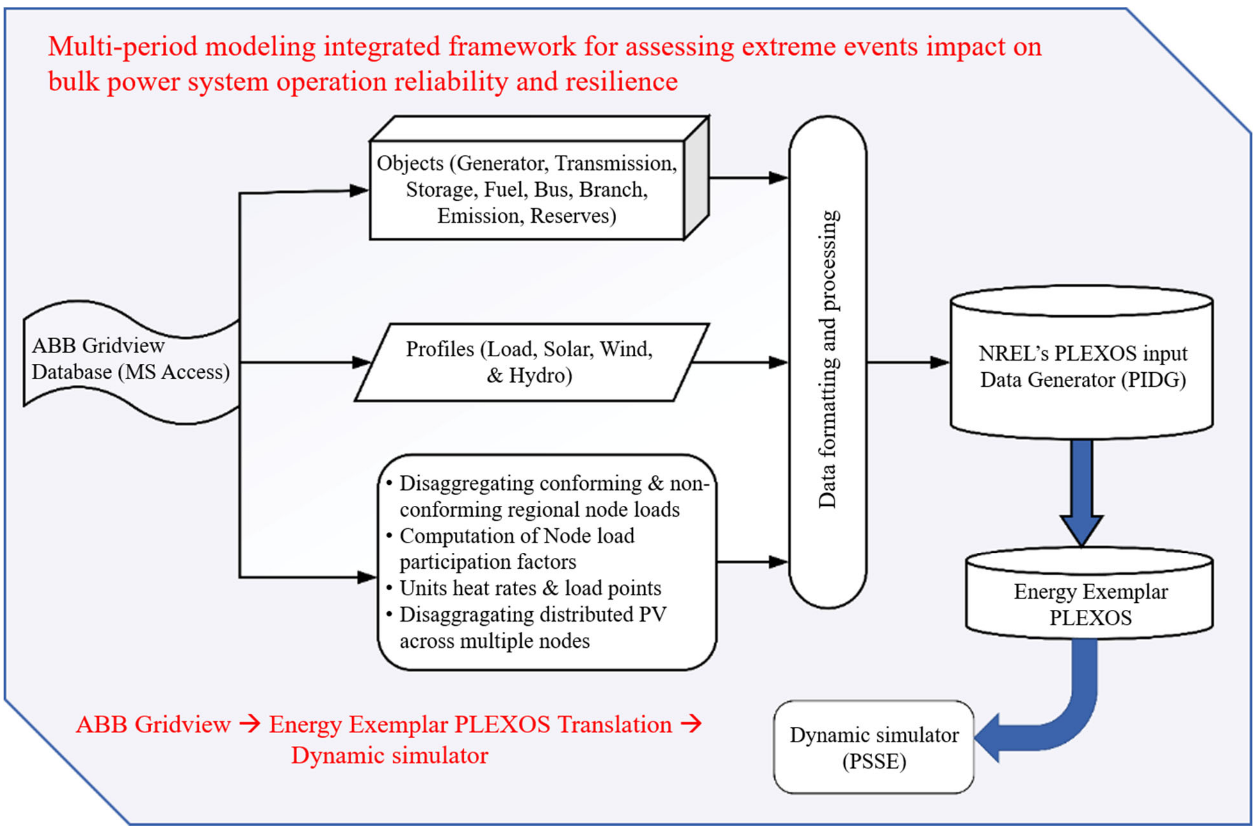

Figure C.1. Workflow of steps involved to create WECC 2028 ADS case in PLEXOS.

The translated model in PLEXOS was validated by GridView's total generation across the WI regions, as shown in Figure C.2. Except for the Northwest and Rockies, the percentage difference between PLEXOS and GridView databases was below 10% for the year.

[1] National Renewable Energy Laboratory. 2021. *NREL/PIDG GitHub* web page. https://github.com/NREL/PIDG

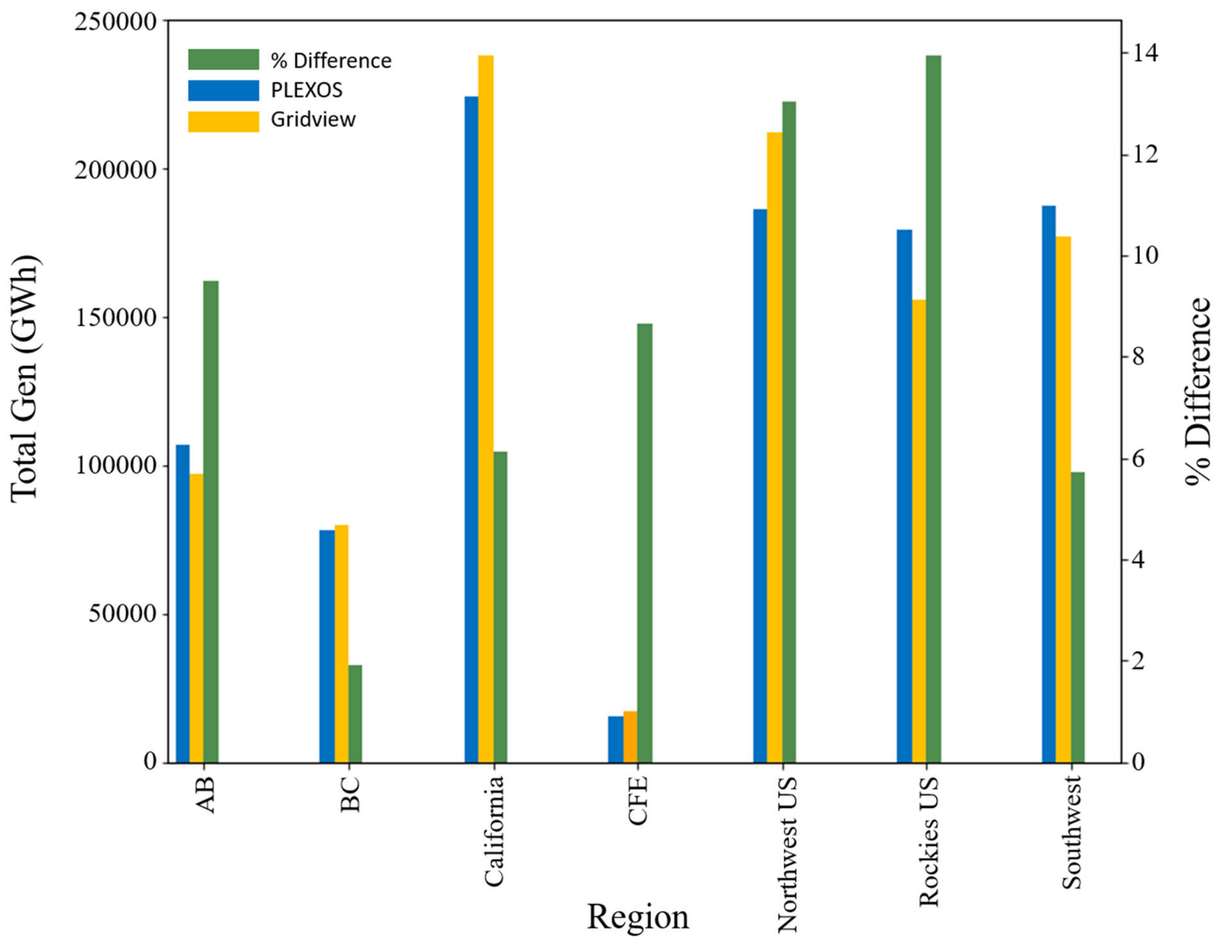

Figure C.2. Comparison of GridView and PLEXOS generation results by region for WECC 2028 ADS.

Listed below are additional translation assumptions made to create the database in PLEXOS and characterize the network as represented in GridView:

- 2028 retired generation units were removed.
- Transmission elements with STATUS = FALSE were turned off.
- Loads with STATUS = FALSE were turned off.
- Negative conforming and nonconforming load were modeled “Fixed Generation” provided they have STATUS = TRUE.
- The behind-the-meter distributed PV system were disaggregated to top 20 high-load nodes with the assumption that distributed PV will offset peak load in the system. This is important for dynamic modeling since GridView assumes the distributed PV is connected to only one bus with participation factor equal to 1.
- Simplified reserves for five reserve sharing groups. We assumed 4% of load to account for spinning regulation and contingency reserves. This will be improved in the near future to better reflect actual reserve assumptions.

C.2 Renewable Energy Data

Figure C.3 shows maps of the modeled wind and solar resources used to generate profiles for the PCM. Wind data come from the WIND Toolkit,[2] which creates high temporal and spatial resolution wind data using weather research and forecasting modeling. Wind data are readily available for the weather years 2007–2013; therefore, this model focused on those historical weather years. Solar data are produced using the National Solar Radiation Database.[3] Generation profiles are produced using the Renewable Energy Potential model.[4]

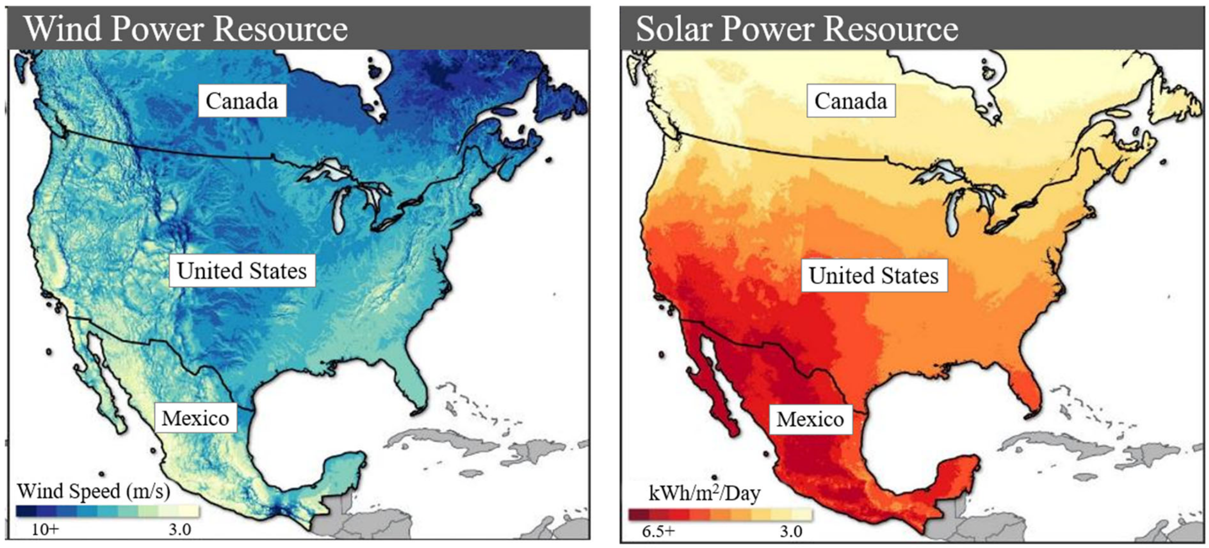

Credit to Billy Roberts for map

Figure C.3. Resource quality maps of the modeled wind and solar data for North America.

Figure C.4 shows the approximate locations of hydroplants in North America and the aggregate monthly energy availability for the contiguous United States. Energy Information Administration-923[5] data are used to create monthly generator-level energy limits. This process was also informed by the Renewable Energy Potential model.

---

[2] National Renewable Energy Laboratory. 2021. *Wind Integration National Dataset Toolkit* web page. Golden, Colorado. https://www.nrel.gov/grid/wind-toolkit.html.
[3] National Renewable Energy Laboratory. N*ational Solar Radiation Database* web site. Golden, Colorado. https://nsrdb.nrel.gov
[4] National Renewable Energy Laboratory. 2021. *reV: The Renewable Energy Potential Model.* https://www.nrel.gov/gis/renewable-energy-potential.html
[5] U.S. Energy Information Administration. 2021. *Electricity* web page. Washington, D.C. https://www.eia.gov/electricity/data/eia923/

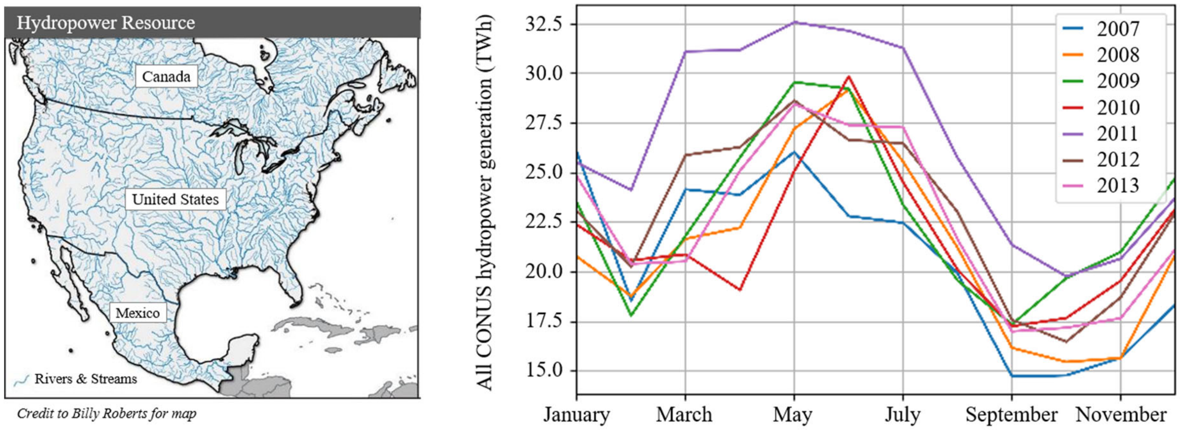

Figure C.4. Waterways where many of the major hydropower resources exist (left) and the hydropower monthly energy availability for the contiguous United States (right).

Appendix D

Interaction Graphs

Appendix D

Interaction Graphs

In principle, both natural and human-related grid contingencies are usually a chain of events during which any of several external events may trigger the same internal event. Therefore, hardening certain critical components that impact internal events would significantly reduce the risk of blackouts. Understanding the disturbance propagation process—where the external event penetrates the electric grid as a major cause for internal events—would be crucial to designing an optimal hardening strategy in both the short and long term.

Interaction models are normally employed to express the interactions between component failures and to capture the general propagation patterns of the cascades.[1] To this end, we use the approach shown in Figure D.1 to illustrate the aforementioned events in Sections 2 and 3. We categorize all events as *external events*, *external-to-internal events*, and *internal events*. The external and internal events are denoted as rectangles with different colors. The external-to-internal events are denoted as double-arrow lines with necessary descriptions. Other evaluations of events are denoted as single-arrow lines.

A systematic principle to categorize different events is the key to this approach. We regard an event as an object, denoted as Event *A*. If another event, Event *B,* is a unique consequence of Event *A*, then we regard Event *B* as an attribute of Event *A*. In this case, we do not categorize Event *A* causing Event *B* as an event propagation. Conversely, if multiple events could lead to Event *B*, then Event *B* is regarded as an independent event with its own attribute and the evolution from Event *A* to Event *B* is defined as an event propagation. In general, a spontaneous occurrence is usually an attribute (e.g., ash fall and lava are clearly and immediately caused by volcanic activity, and thus the attributes of the volcanic activity). On the other hand, a tree falling can be caused by many events, like wind and flooding, and can therefore be considered an independent event. The internal events of a power system could be complicated and multifaceted. Based on statistical information from historical blackouts, we conclude several common categories of internal events. It is also worth noting that events that are not externally caused, which are mainly in the technical and human-unintentional category, are illustrated because this paradigm is used to study disturbance propagation from external to internal.

With such a graphical model, key external-to-internal events can be identified and mitigated to enhance grid resiliency. As shown in Figure D.1, several weather-related external events may cause trees to fall, which may in turn damage power lines and poles. This is the key step that the external disturbance propagates into the electric grid that further leads to customer interruption, cascading outages, and even blackouts. The 2003 blackout was initially triggered by a vegetation-induced fault. If such external-to-internal events can be identified and prevented, the event chain can be stopped. In this case, one mitigation strategy can be proposed immediately: retain safe distances between trees and electric components. Although the presented case is simple and straightforward, it indicates great potential for information discovery from complex events. It is also easy to observe that most frequent internal failures induced externally are equipment damage. Thus, the system degradation caused by external disturbances could be relieved if equipment could be hardened in the preparedness stage. Building a comprehensive database with graphical data structure could be valuable.

[1] Qi J, K Sun, and S Mei. 2014. "An interaction model for simulation and mitigation of cascading failures." *IEEE Transactions on Power Systems* 30(2):804–819.

In addition, the interaction graph also supports studies of interdependent infrastructure. In these scenarios, the damage to other infrastructure will be described as external-to-internal events. As shown in Figure D.1, extreme cold temperature can overload gas pipelines and thus cause gas fuel shortage for gas-fired generators. Drought-induced water shortage can pose challenges for cooling thermal-generation units. Physical attacks on telecommunication, gas networks, etc., can also impact power systems.

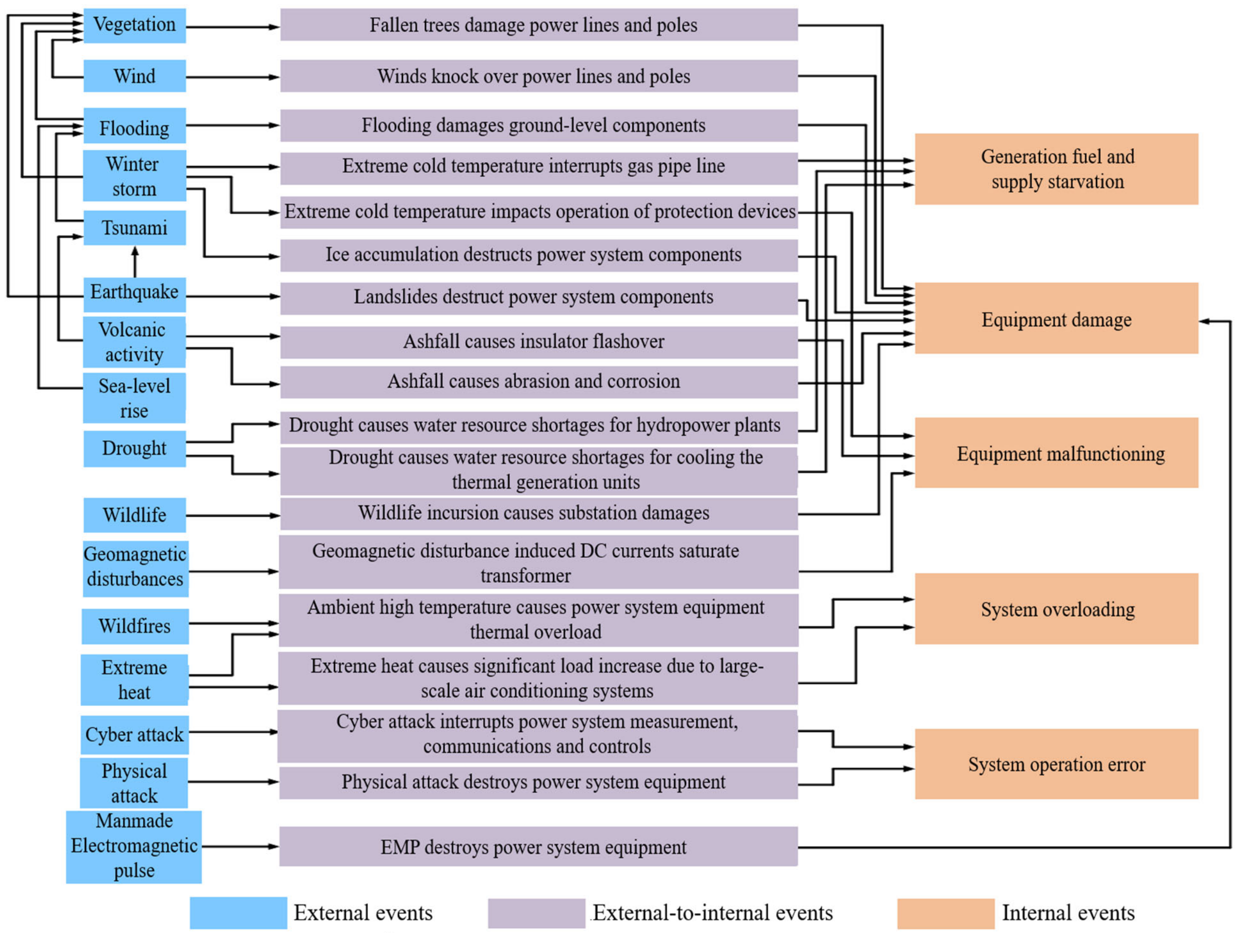

Figure D.1. Interaction graph to elaborate disturbance propagation from external to internal.

Appendix E

Supporting Simulation Results and Metrics

Appendix E

Supporting Simulation Results and Metrics

E.1 Additional Metrics for Quantifying System States

Several metrics are proposed in this section to compare the effect of seasonal, loading, and hydro condition variations. These metrics are used to compare the contribution of hydropower in extreme events.

In order to make sure simulations represent actual system operations and maintain different voltage limits and line-flow limit thresholds, several other evaluating criteria were estimated as part of the simulation procedure. These evaluation criteria are used by system planners and operators to make sure system operational states are feasible. The voltage-violation evaluating criteria demonstrate whether system voltages are within acceptable limits throughout the simulation process. If voltage violations are observed, it may result in voltage instability from tripping of certain loads due to operation over/under-voltage protection. Line-flow-ratings evaluating criteria demonstrate lines and transformers that are overloaded beyond their normal ratings. If transmission lines get overloaded, it may result in thermal damage, hence overcurrent protection will act and trip the transmission lines which may result in loss of load and islanding of the grid. The total-load-not-served evaluating criteria provide MW load, tripped following every contingency, to maintain system stability (i.e., load/generation balance). The total-load-not-served indicates loss of load to the customer and has high impact on the grid.

E.2 Voltage Violations Metrics

Voltage violations can result in instability/collapse, insulation, or induction motor tripping. Voltage-violation metrics that will be computed to compare various scenarios are:

1. Number of violations
2. Violations distribution at each voltage level
3. Voltage-violation heat maps
4. Under-voltage load-shedding relays.

Figure E.1 shows the voltage heat maps after Contingency 1 for the LS and HW cases. Corrective actions are performed after dynamic simulation to restore voltage within the thresholds. The number of corrective actions required to bring the voltage to nominal values is dependent on loading of the system and the number of resources online. Figure E.2 shows the voltage violations after every contingency for the HW and LS cases. The LS case had more voltage violations following each contingency than the HW case. This is mostly because the light-load case has fewer resources online to provide the required reactive power for maintaining voltage profile compared to the heavy loading case. Figure E.3 shows the voltage heat map after Contingency 1, before and after applying corrective actions.

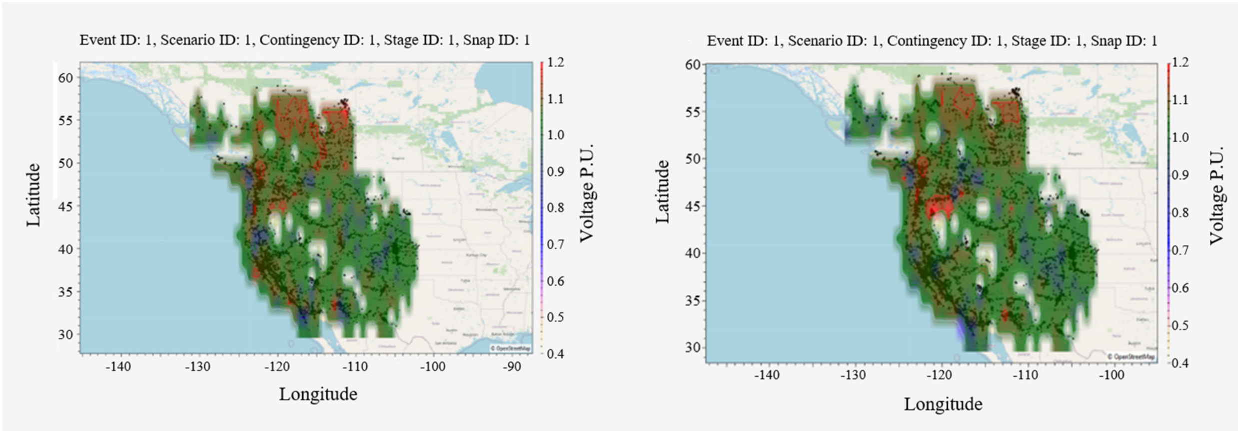

Figure E.1. Voltage heat map after Contingency 1: LS (left) and HW (right).

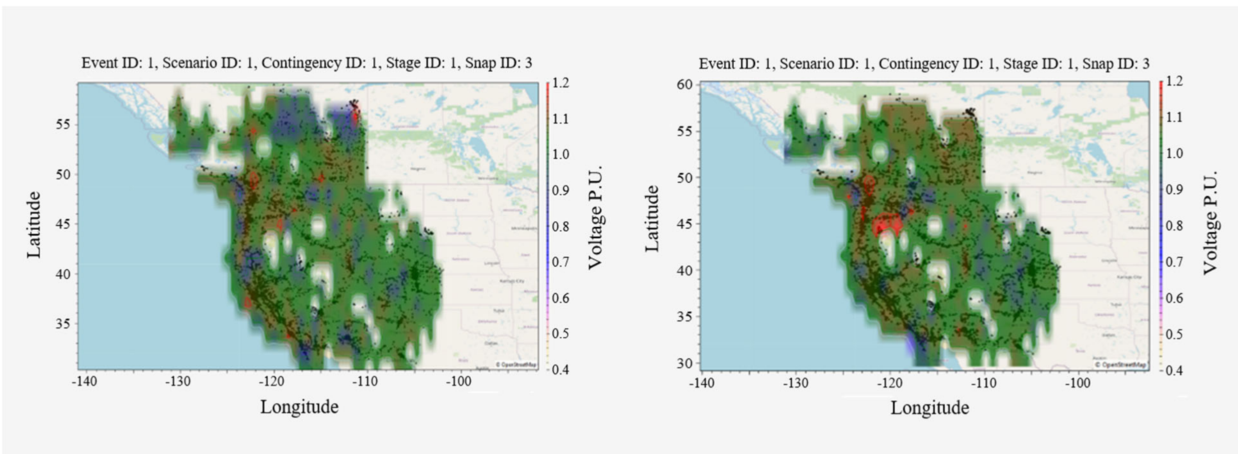

Figure E.2. Voltage heat map after Contingency 1, after applying corrective actions: HW (left) and LS (right).

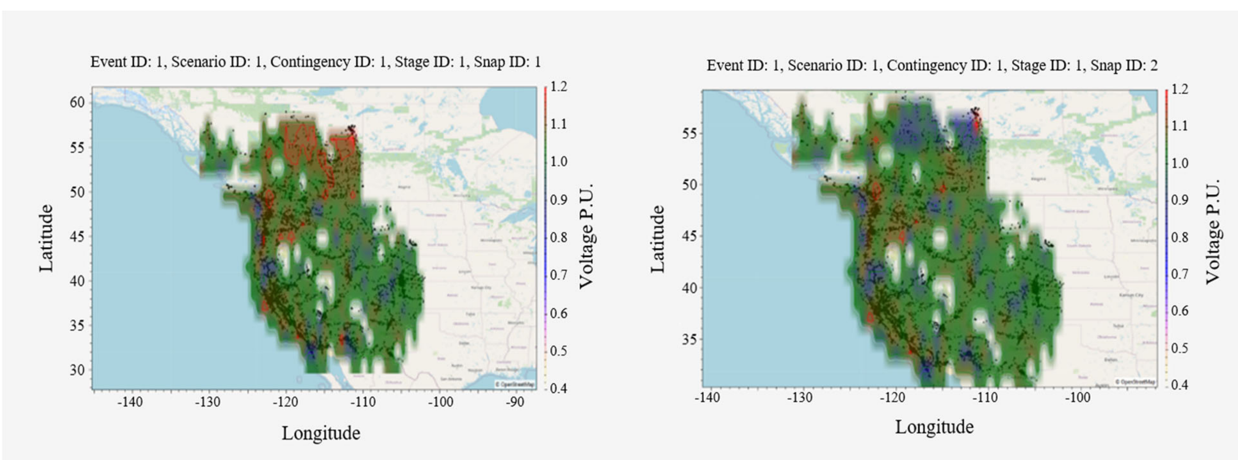

Figure E.3. Voltage heat map after Contingency 1, before (left) and after (right) applying corrective actions.

Figure E.4 shows the voltage violations after each contingency for LS and HW cases.

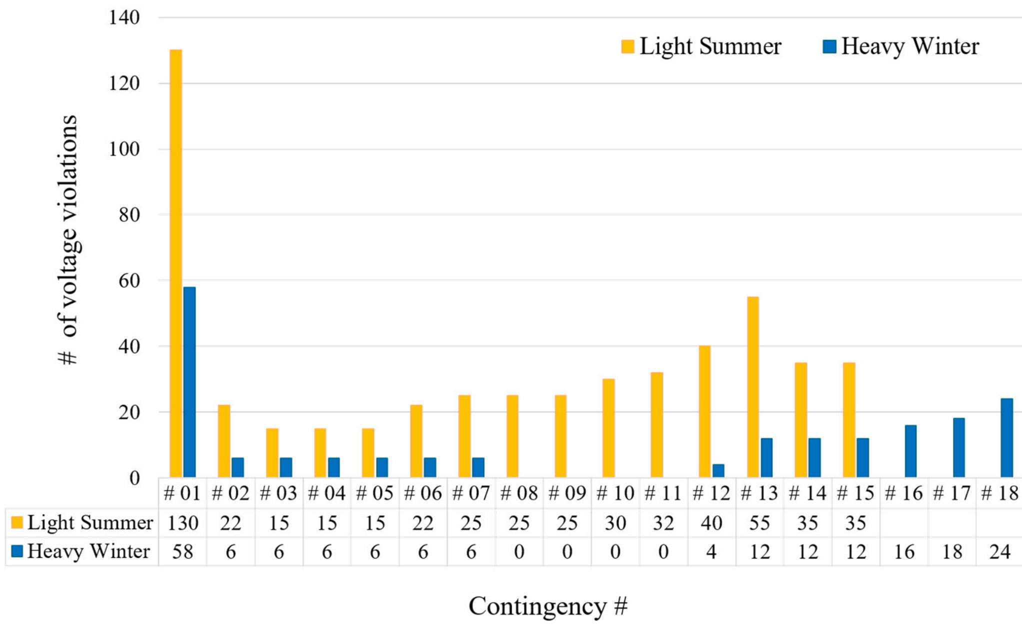

Figure E.4. Voltage violations after each contingency for LS and HW cases.

Figure E.5 shows the voltage violations after every contingency for the LS and the LS–dry-hydro cases. The dry-hydro-year case had more voltage violations following Contingency 1 than the average hydro year case. Figure E.6 shows the distribution of the nominal voltage levels and per-unit voltage violations for the LS and the LS–dry-hydro case. The dry-hydro case has more voltage violations at buses with nominal voltage level less than 69 kV. Also, voltage violations occurred more frequently below 0.8 pu for the dry-hydro case.

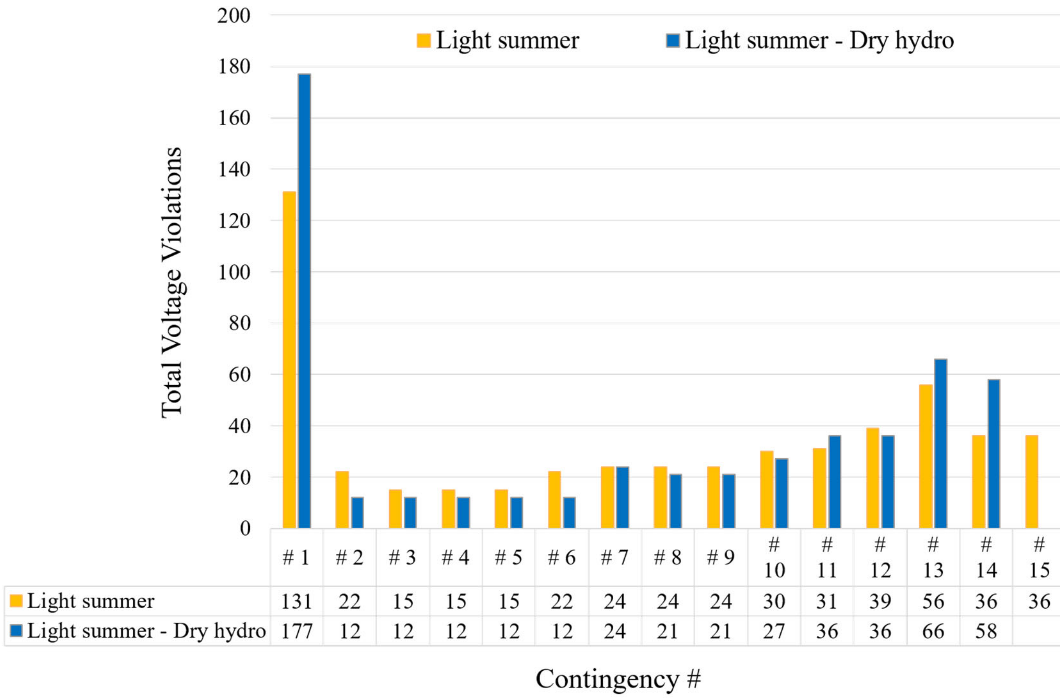

Figure E.5. Voltage violations after each contingency for LS–normal and LS–dry-hydro conditions.

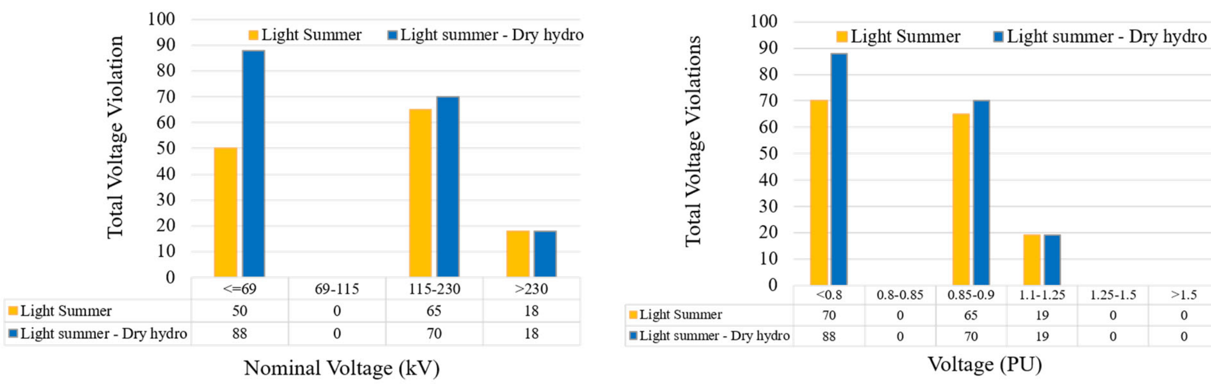

Figure E.6. Voltage-violation distribution for Contingency 1 for LS–normal and LS–dry-hydro conditions.

E.3 Load-Not-Served Metrics

Load-shedding metrics are beneficial in quantifying the severity of an extreme event. The metrics considered in the report include:

1. Underfrequency load shedding in MW
2. Under-voltage load shedding in MW
3. Operator load shedding as part of corrective actions in MW.

The total-load-not-served metrics provide MW load tripped following every contingency to maintain system stability. From this it can be observed that the LS case simulations resulted in increased load not served following each contingency compared to the HW case for certain contingencies as shown in Figure E.7. Given fewer resources are online in a light-load scenario, the result is reduced available reserve capacity to dispatch following contingencies. From the previous results comparing generation variation because the majority of the contingency reserve is provided by hydropower and combined-cycle power plants, the light-load case can be more severe with respect to unserved load than the heavy-load scenario.

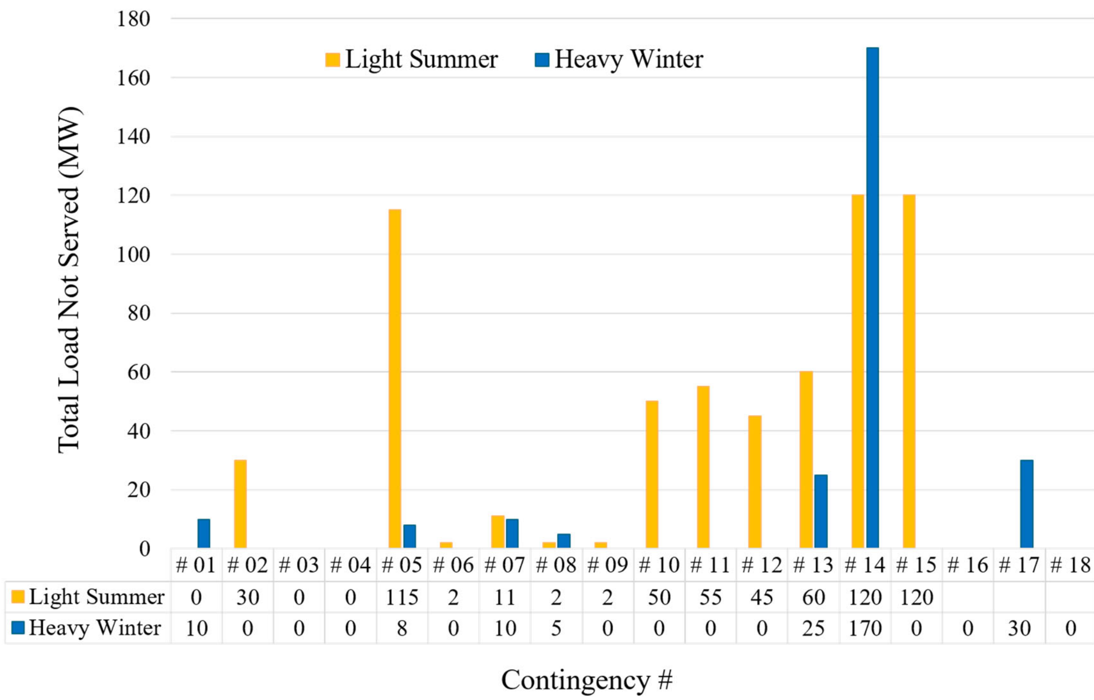

Figure E.7. Total load not served after each contingency—HW and LS cases.

The LS case simulations resulted in increased load not served following each contingency compared to the LS–dry-hydro case for certain contingencies as shown in Figure E.8. However, for the LS–dry-hydro scenario, the system fails to converge after Contingency 14.

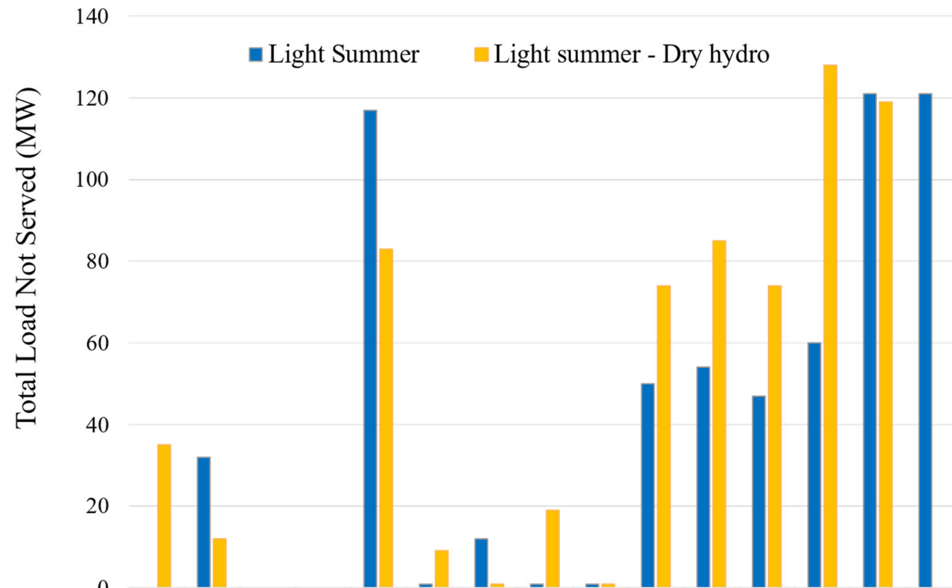

	# 1	# 2	# 3	# 4	# 5	# 6	# 7	# 8	# 9	# 10	# 11	# 12	# 13	# 14	# 15
Light Summer	0	32	0	0	117	1	12	1	1	50	54	47	60	121	121
Light summer - Dry hydro	35	12	0	0	83	9	1	19	1	74	85	74	128	119	

Contingency #

Figure E.8. Total load not served for each contingency for LSnormal vs. LS–dry-hydro conditions.

E.4 Transmission/Flow-Violation Metrics

Extreme events lead to overloading transmission lines and may require tripping if the stability and thermal limits of lines are exceeded. Transmission flow violations considered here include:

1. Number of lines tripped following an event
2. Number of lines above 100% loading but less than 150% during steady state conditions.

The flow-violation metric for the LS and HW cases is provided in E.9. It can be observed that the LS case has fewer flow violations compared to the HW case. Dynamic simulations are done in sequence, i.e., the steady-state power-flow case extracted at the end of the previous contingency is used as the input for the next contingency. The system is stable for this contingency, but there are a few load drops at the beginning of the simulation; thus, a slight increment in the frequency is observed initially, but then it settles down at a new value (~59.98) at the end of the simulation period. The flows through the Pacific DC Intertie (PDCI) and COI for all contingencies are shown in Figure E.10 and Figure E.11. Note that the flow in PDCI does not change significantly from the 1,945 MW value while the flow in COI increases from 2,800 MW and settles at 4,500 MW for LS case.

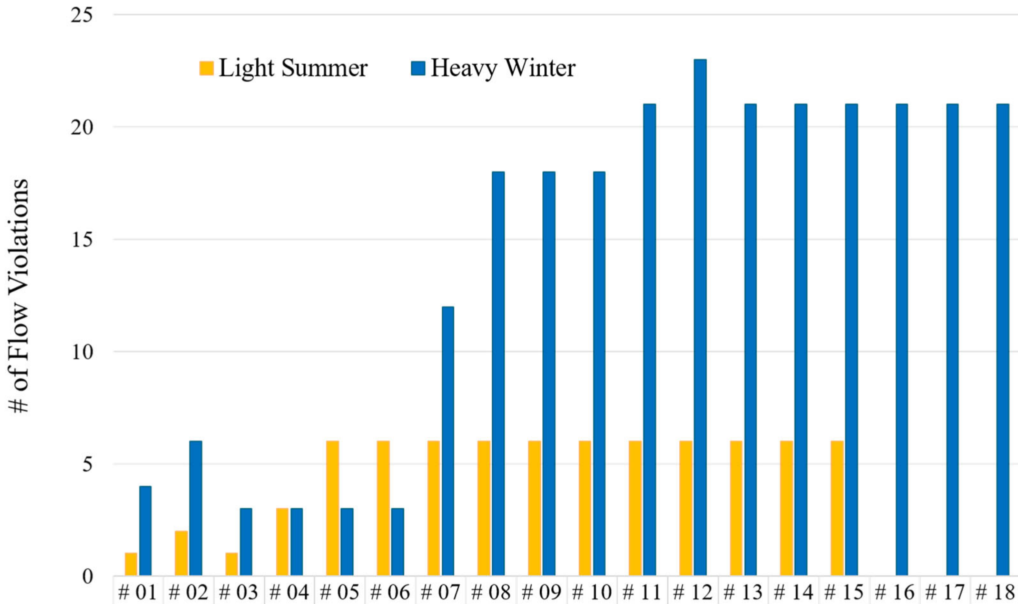

	# 01	# 02	# 03	# 04	# 05	# 06	# 07	# 08	# 09	# 10	# 11	# 12	# 13	# 14	# 15	# 16	# 17	# 18
Light Summer	1	2	1	3	6	6	6	6	6	6	6	6	6	6	6			
Heavy Winter	4	6	3	3	3	3	12	18	18	18	21	23	21	21	21	21	21	21

Contingency #

Figure E.9. Total flow violations after each contingency—HW and LS cases.

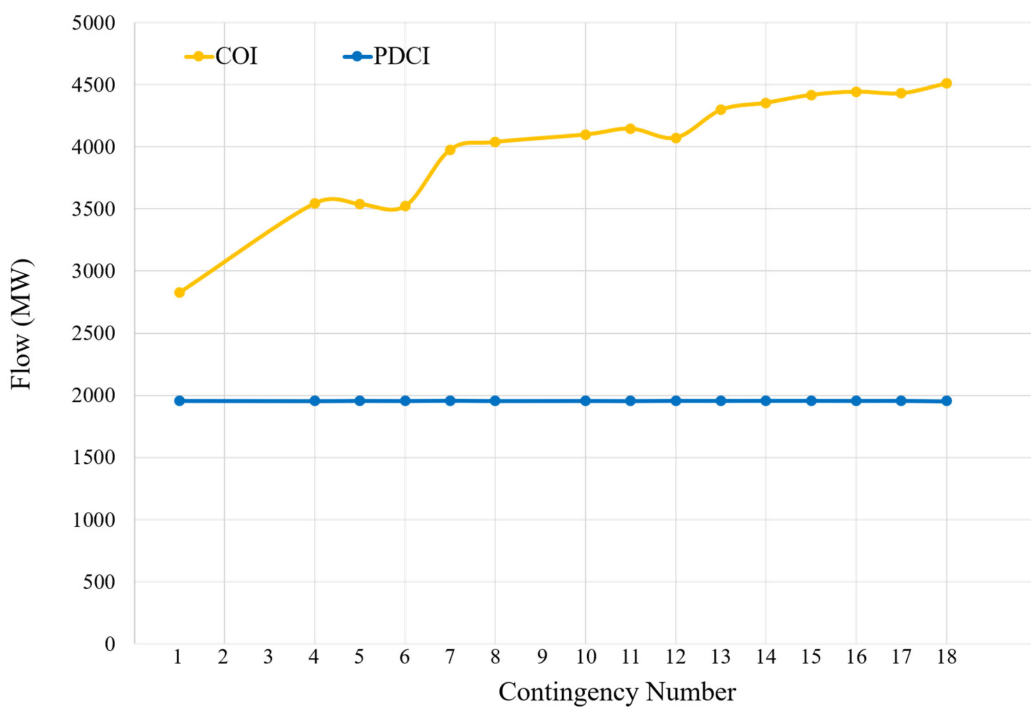

Figure E.10. PDCI and COI flows after each contingency—LS case.

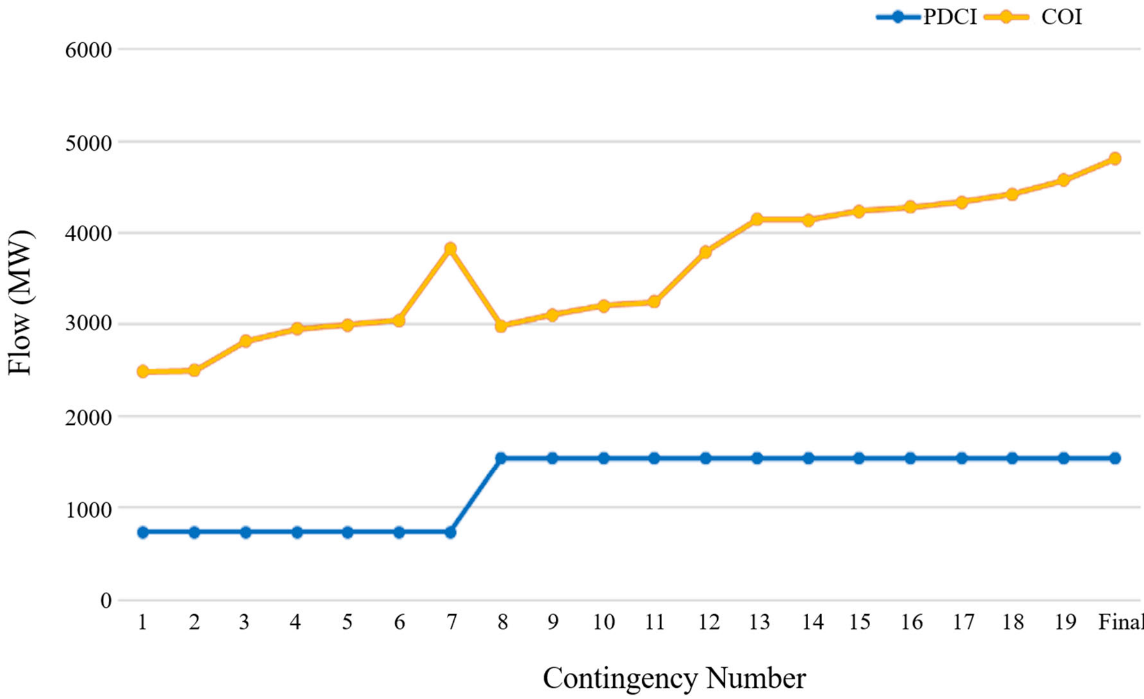

Figure E.11. PDCI and COI flows after each contingency—HW case.

The flow-violation metric for the LS and LS–dry-hydro case is provided in Figure E.12. For the LS–dry-hydro case, there are increased flow violations after the first contingency, but reduced violations after the first contingency. Figure E.12 shows the distribution of the per-unit flow-violation range after Contingency 1. The average hydro case only has one instance of flow violation in the 1–1.15 pu range; however, the dry-hydro case 10 instances of flow violation in >1.3 pu range and two instances of flow violations in the 1–1.15 pu range.

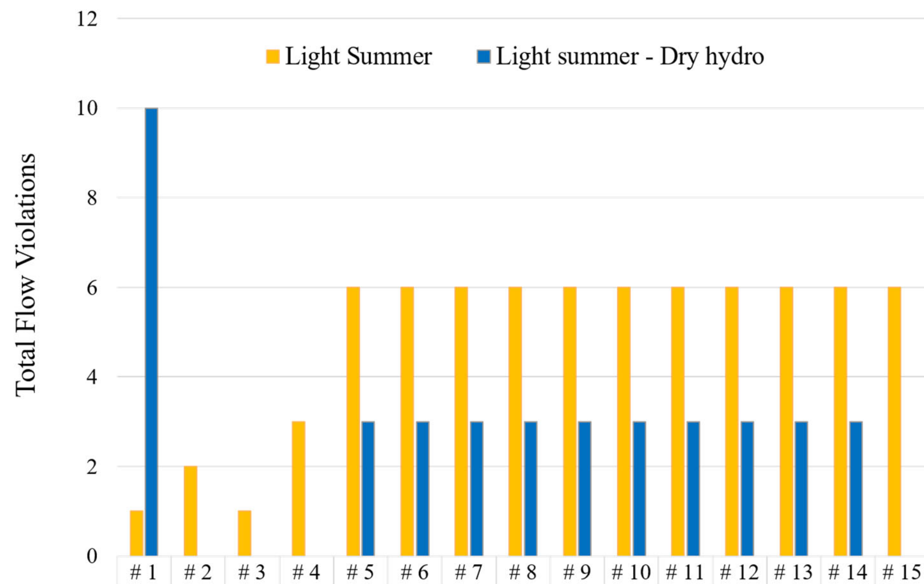

	# 1	# 2	# 3	# 4	# 5	# 6	# 7	# 8	# 9	# 10	# 11	# 12	# 13	# 14	# 15
Light Summer	1	2	1	3	6	6	6	6	6	6	6	6	6	6	6
Light summer - Dry hydro	10	0	0	0	3	3	3	3	3	3	3	3	3	3	

Contingency

Figure E.12. Total flow violations for each contingency for LS–normal vs. LS–dry-hydro conditions.

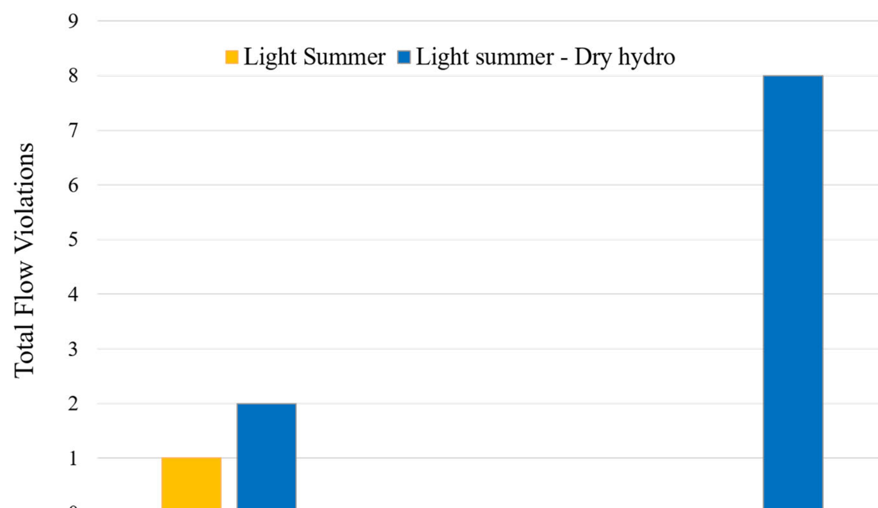

	1-1.15	1.15-1.3	>1.3
Light Summer	1	0	0
Light summer - Dry hydro	2	0	8

Percentatge of overloading

Figure E.13. Number of flow-violation distribution for Contingency 1 for LS–normal vs. LS–dry-hydro conditions.

E.5 Generator Unit Tripping

Figure E.14 and Figure E.15 provide the total number of generator unit tripped and the total MW of generator unit tripped after each contingency to maintain system stability. These results do include the generators tripped as a result of the natural gas contingencies.

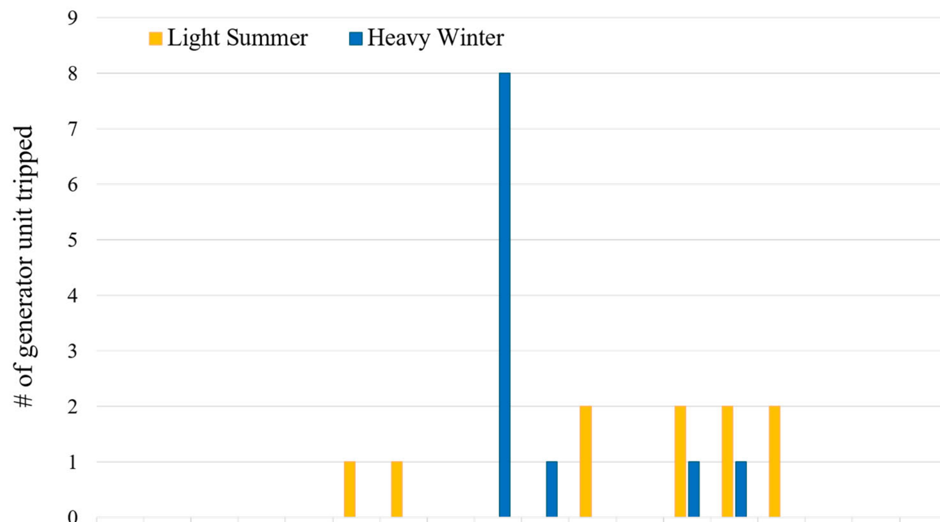

	# 01	# 02	# 03	# 04	# 05	# 06	# 07	# 08	# 09	# 10	# 11	# 12	# 13	# 14	# 15	# 16	# 17	# 18
Light Summer	0	0	0	0	0	1	1	0	0	0	2	0	2	2	2			
Heavy Winter	0	0	0	0	0	0	0	0	8	1	0	0	1	1	0	0	0	0

Contingency #

Figure E.14. Total number of units tripping after each contingency for HW vs. LS case.

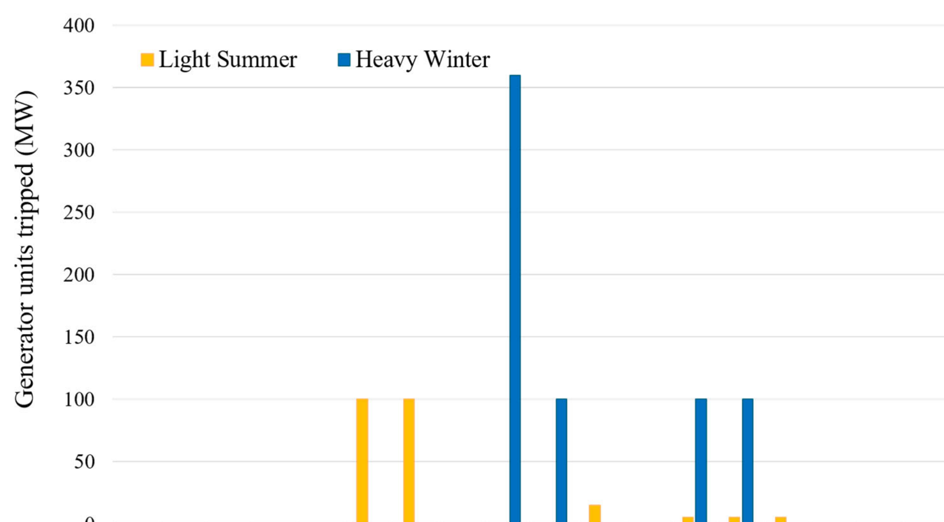

	# 01	# 02	# 03	# 04	# 05	# 06	# 07	# 08	# 09	# 10	# 11	# 12	# 13	# 14	# 15	# 16	# 17	# 18
Light Summer	0	0	0	0	0	100	100		0	0	15	0	5	5	5			
Heavy Winter	0	0	0	0	0	0	0	0	360	100	0	0	100	100	0	0	0	0

Contingency #

Figure E.15. Total MW generation tripped after each contingency for HW vs. LS case.

Appendix F

Model and Data Validation

Appendix F

Model and Data Validation

F.1 Steady-State Model Parameters

The hydrological and electrical measurement data have been verified to make sure that hydrological data such as head and water flow align with the electrical output of the plants.
The data is obtained for various hydropower resources in the Pacific Northwest from U.S. Army Corps of Engineers (USACE) data repository.[1] To validate the efficacy of using WECC planning models for simulations and quantify the contribution of hydropower it is necessary to ensure the WECC planning models reflect the actual plant output. Figure D.1 shows the comparison of the actual generator output and the data in the WECC planning models for P_{gen} (actual real power generated) and P_{max} (maximum power generation) for a hydropower resource in the Pacific Northwest for various seasons. The WECC planning models for light-load and heavy-load conditions may underestimate or overestimate the actual plant-state space. This is primarily because WECC planning cases are created ahead of actual operations, based on forecasted water availability. Additionally, based on discussions with industry experts, it may be because WECC planning cases are not usually updated to reflect forecasted water availability and may be based on nominal, average hydro-year data. It is important to be aware of these steady-state model inaccuracies when interpreting simulation results using such planning cases.

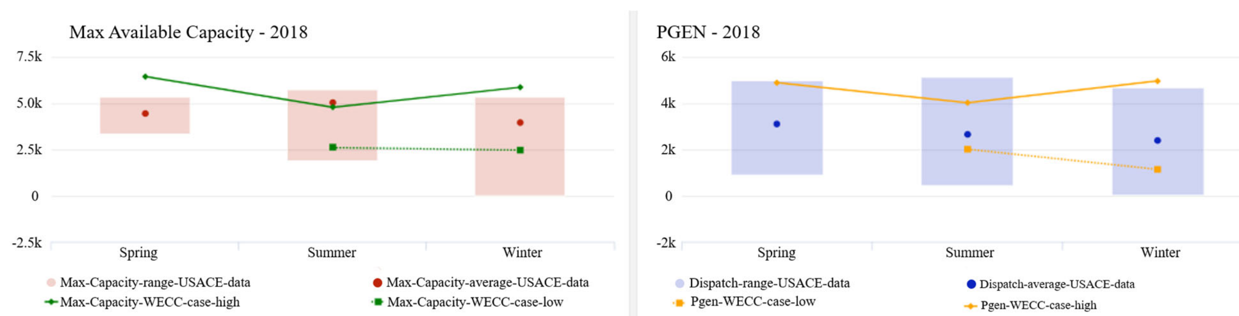

Figure F.1. Comparison of resource dispatch and max available capacity between WECC planning cases and historical data.

F.2 Turbine-Governor Parameters

Another interesting observation from the data validation task is the performance of the hydropower generator governor models in the 2018 WECC planning cases. There are several hydro turbine-governor models in the model as shown in Figure D.2. From the simulation results, it was identified that certain hydropower resources' output MW exceeded the MW capacity limit (mwcap) parameter in the governor models (Figure D.3). This may be because extreme events are being simulated that result in time domain simulations for an extended time period resulting in the exceedance. The issue will be investigated further in future projects in collaboration with industry experts and the WECC modeling subcommittee.

[1] USACE Hydro Data Repository: https://www.nwd-wc.usace.army.mil/dd/common/dataquery/www/ Accessed: July 26, 20221

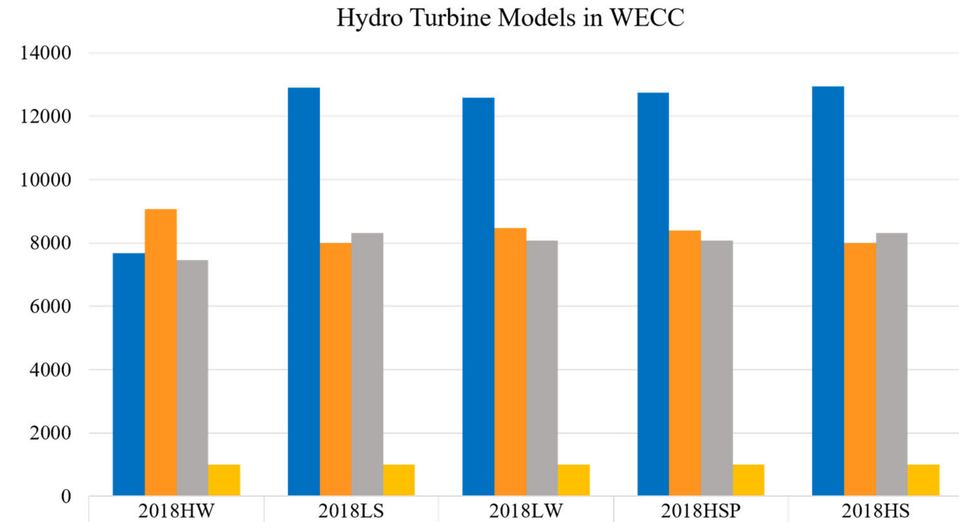

	2018HW	2018LS	2018LW	2018HSP	2018HS
hyg3	7673	12896	12589	12737	12934
hygov	9076	7998	8468	8388	7998
hygov4	7464	8310	8070	8070	8310
hygovr	1008	1008	1008	1008	1008

Figure F.2. Hydro turbine models in 2018 WECC planning models.

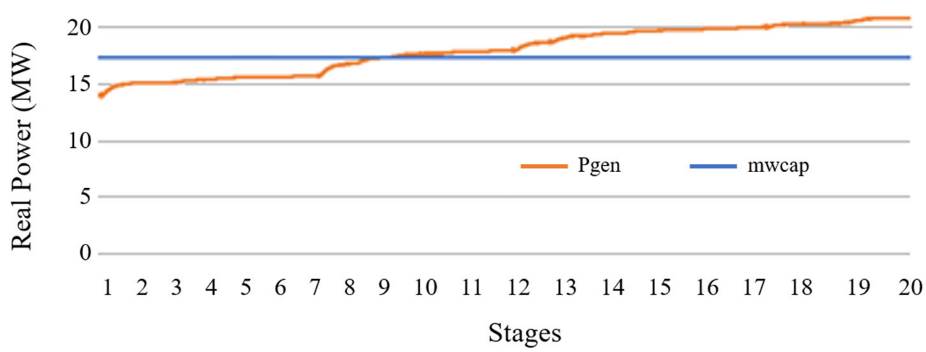

Figure F.3. GE Positive Sequence Load Flow time domain simulation results—hydro MW output (Pgen) exceeds MW capacity of that resource (mwcap).

Appendix G

Examples of Emergency Grid Events

Appendix G

Examples of Emergency Grid Events

G.1 2011 Southwest Blackout[1]

A mistake by a technician led to the accidental shutdown of a 500 kV line between Arizona Public Service's Hassayampa substation near the Palos Verdes Nuclear Generating Station in Tonopah, Arizona, and the North Gila substation in Yuma, Arizona. This transmission line is part of the Southwest Power Link. With the line shut down, the 500 kV Southwest Power Link went from San Diego, California, to Yuma, Arizona, but was not supplied by anything else.

Arizona Public Service (APS) estimated that reconnection would not take long. However, the line opening caused a large phase difference in the grid and the line could not be reconnected until the next day. Most of the power to the San Diego area was then rerouted through Southern California Edison's system through the San Onofre Nuclear Generating Station (SONGS) switchyard. At this point, the San Diego Gas and Electric (SDG&E) system was taking more power from Southern California Edison than it could supply through the SONGS switchyard, and this became worse as events progressed.

The Imperial Irrigation District (IID) sub-transmission system also ended up transferring a portion of the power between Southern California Edison's Palo Verde-Devers 500 kV line and SDG&E's 500 kV Southwest Power Link. In less than 1 minute, two of IID's transformers in Coachella Valley had overloaded and disconnected. This caused severe low voltage on the IID system. Several minutes later, a third transformer tripped off, causing the bulk of the IID system to be disconnected from Southern California Edison to the north. This caused drastic voltage problems, which resulted in a loss of about half of IID's load as well as some generation.

Similar transformer overloads caused the Yuma area to be disconnected from the Western Area Power Administration-Lower Colorado (WALC) system. The only supply to Yuma at that point was a back feed from San Diego and Imperial Valley through the remainder of the 500 kV Southwest Power Link. One more transmission line, the last connection east of SONGS, tripped off between WALC to the north and SDG&E, the system of the Comisión Federal de Electricidad and the Yuma area to the south. What remained of the IID system had only one connection to the remnants of the 500 kV Southwest Power Link. This line overloaded as well. Instead of just cutting that line, the scheme commanded two generators in Mexico to go offline. This was intended to solve a problem that no longer existed; instead, it actually made the problem worse. The line did trip off and most of IID's remaining load was lost.

All power to San Diego; Baja California, Mexico; and Yuma was now being drawn from Southern California Edison through the SONGS switchyard. This draw was very high (around 170%) and a "safety-net" system built into the power plant operated and disconnected 230 kV lines going into San Diego. The SDG&E system, Comisión Federal de Electricidad's Baja California system, and Arizona Public Service's Yuma service area were now completely separated from the WI. This island had insufficient generation and rapidly spun down. Load shedding throughout the system operated rapidly, but some generation still was lost. Within seconds, San Diego, Baja California, and Yuma broke into three islands, all of which then collapsed. Both units at SONGS also shut down, although this had no effect.

---

[1] FERC/NERC. 2012. *Arizona-Southern California Outages on September 8, 2011*. Washington D.C. https://www.nerc.com/pa/rrm/ea/September%202011%20Southwest%20Blackout%20Event%20Document%20L/AZOutage_Report_01MAY12.pdf.

Eleven hours after the outage began, power was restored to 694,000 of the affected customers, and by 4:30 a.m. on September 9, power was restored to all customers, although the system was described as "still fragile." As a precaution, all public schools in San Diego County and the Capistrano Unified School District in southern Orange County were closed on September 9. Most major universities and community colleges, as well as all federal courts in San Diego, closed for the day as well.

The outage caused significant losses to restaurants and grocery stores, which were forced to discard quantities of spoiled food. Perishable food losses were estimated at $12–18 million. The outage also caused some sewage pumping stations to fail, resulting in contaminated beaches and potentially unsafe water supplies in several areas. As a precaution in some neighborhoods, residents were told to boil their water or use bottled water for several days after the outage. Because of the failure at the sewage pumping stations, five diesel generators were installed.

G.2 Cyberattack on Power Grid in Ukraine[2]

In a recent, well-publicized cyberattack, approximately 225,000 people in Ukraine were left without power for approximately 6 hours on December 23, 2015. The attackers gained access to internal networks of three utilities through spear-phishing schemes, malware, and manipulation of certain long-known Microsoft Office macro-vulnerabilities. Rather than try to engineer breaches through the firewall, the attackers patiently harvested the credentials needed to gain access to the supervisory control and data acquisition (SCADA) system and learned how to operate the SCADA software. The attackers executed a well-devised strategy, including the following:

- Creating virtual workstations inside SCADA systems that were trusted to issue system commands
- Co-opting remote terminal units within SCADA systems to issue "open" commands to specific breakers at substations
- Severing communications by targeting firmware in serial-to-Ethernet devices, making most unrecoverable
- Installing and running a modified KillDisk program that deleted information on what was occurring while making recovery reboots nearly impossible
- Shutting down uninterruptible power supplies at control centers
- Executing a large denial-of-service attack on utility call centers that prevented customers from reporting outages and reduced the utilities' understanding of the extent of outages.

These actions prevented operators from accessing the SCADA systems, left control centers without power, and left cyber monitoring and control systems inoperable. Service was restored by shutting off the SCADA system and resorting to manual operation. Although power was restored relatively quickly, control centers were not fully operational for months following the attack.

[2] Lee RM et al. 2016. *Analysis of the Cyber Attack on the Ukrainian Power Grid*. Electricity-Information Sharing and Analysis Center, Washington, D.C. https://ics.sans.org/media/E-ISAC_SANS_Ukraine_DUC_5.pdf.

NOTICE

Available electronically at OSTI.gov http:/www.osti.gov

Available for a processing fee to U.S. Department of Energy
and its contractors, in paper, from:

U.S. Department of Energy Office of Scientific and Technical Information
P.O. Box 62
Oak Ridge, TN 37831-0062
OSTI http://www.osti.gov
Phone: 865.576.8401
Fax: 865.576.5728
Email: reports@osti.gov

Available for sale to the public, in paper, from:

U.S. Department of Commerce
National Technical Information Service
5301 Shawnee Road
Alexandria, VA 22312
NTIS http://www.ntis.gov
Phone: 800.553.6847 or 703.605.6000
Fax: 703.605.6900
Email: orders@ntis.gov

How to cite this report: Somani, A.; Datta, S.; Kincic, S.; Chalishazar, V; Vyakaranam, B.; Samaan, N.; Colotelo, A., Zhang, Y.; Koritarov, V; McJunkin, T.; Mosier, T.; Novacheck, J.; Emmanuel, M.; Schwarz, M.; Markel, L.; and O'Reilley, C.; August 2021. Hydropower's Contributions to Grid Resilience. U.S. Department of Energy, Office of Energy Efficiency and Renewable Energy. Washington, D.C.

Hydro WIRES
U.S. DEPARTMENT OF ENERGY

Pacific Northwest NATIONAL LABORATORY

NREL NATIONAL RENEWABLE ENERGY LABORATORY

Argonne NATIONAL LABORATORY

INL Idaho National Laboratory

OAK RIDGE National Laboratory

https://www.energy.gov/hydrowires